STUDY ON SOLID ACID CATALYSTS PREPARED BY CHEMICAL VAPOR DEPOSITION

Satoshi Sato

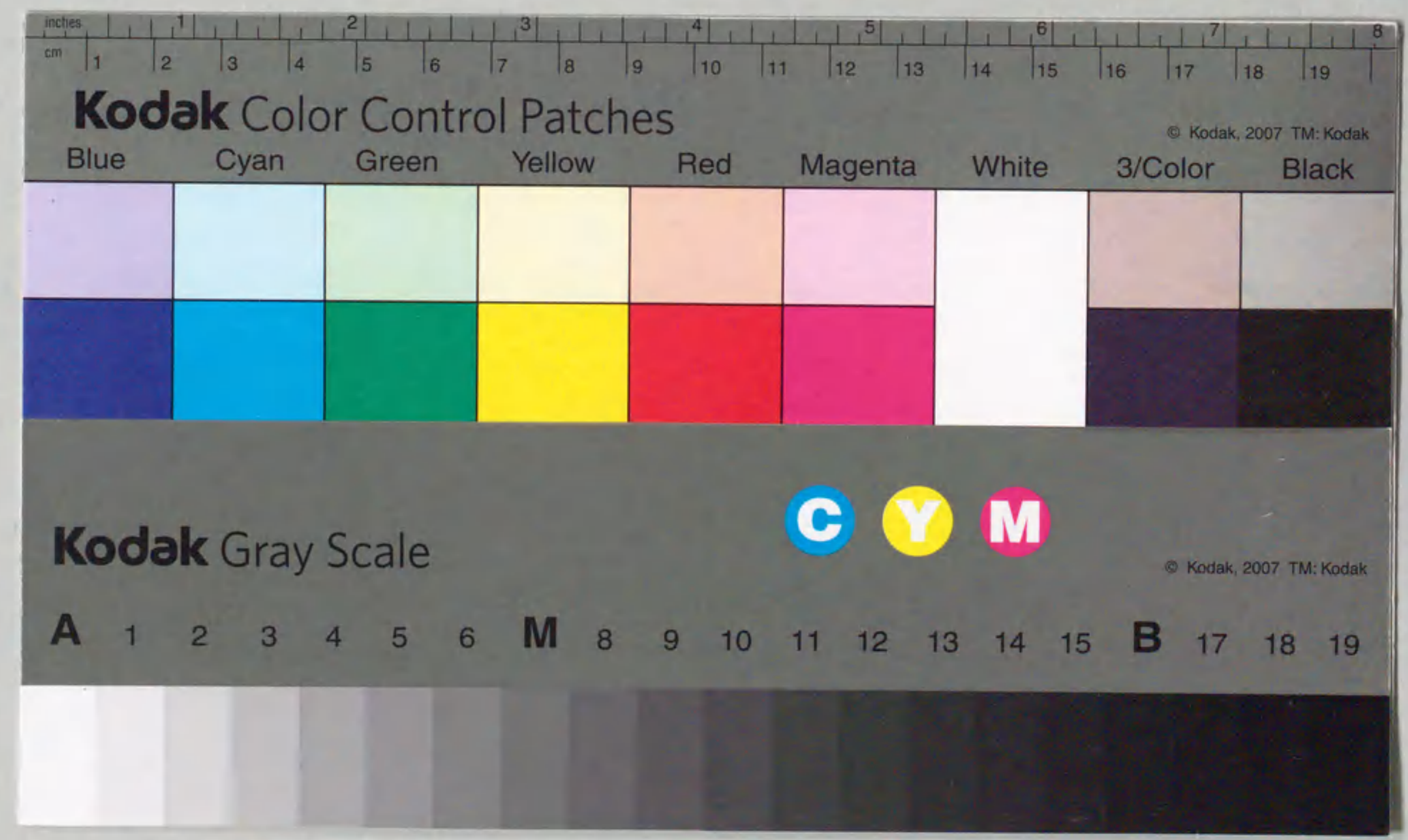

STUDY ON SOLID ACID CATALYSTS PREPARED BY CHEMICAL VAPOR DEPOSITION

Satoshi Sato

PREFACE

This thesis describes the author's studies on the catalyst design of a supported type of solid acids prepared by chemical vapor deposition of metal oxides. The studies have been carried out under the direction of Professor Yusuke Izumi at Department of Synthetic Chemistry, Faculty of Engineering, Nagoya University during 1982-1986, and have been continued under the suggestion of Professor Fumio Nozaki at Department of Applied Chemistry, Faculty of Engineering, Chiba University during 1986-1991.

A technique of chemical vapor deposition (CVD) have been greatly developed in the production of semiconductors and cutting tools. For example, silica thin films are now widely used for the protection of silicon devises, and TiC or TiN coating is convenient to enhance the hardness of W-TiC-Co cutting tools. Furthermore, the CVD technique has recently been used for the preparation of catalysts and the modification of microporous materials. In contrast to plain surfaces of silicon devises, catalyst supports are generally composed of three-dimensional pores with large surface areas. In the application of the CVD technique to catalyst preparation, active species must be deposited onto the walls of the pores inside the support. Fundamental investigations on the catalyst preparation by CVD technique are believed to contribute not only to the development of a new type of catalysts but also to the refinement of basic concepts in catalysis from the view point of surface science.

The main themes of the thesis are to estimate the effectiveness of the chemical vapor deposition for catalyst preparation of several supported types of solid acids, and to clarify the catalytic and acidic properties in connection with the geometrical structures of surface deposits.

The first chapter is an introduction of the general and basic aspects of solid acids, catalyst preparation, and CVD technique. The second chapter covers the application of CVD for supported boria catalysts. Chapter 3 covers the application of CVD for supported silica catalysts. Boron phosphate deposited on silica is dealt with in Chapter 4. Chapter 5 covers characteristic behaviors of the deposition of metal oxides onto porous catalyst support. In the last chapter, the application of CVD to the

preparation of solid acid catalysts is summarized.

The author would like to express his sincere gratitude to Professor Yusuke Izumi for his helpful suggestions, fruitful discussion, and continual encouragement throughout the work. The author is deeply grateful to Professor Fumio Nozaki and Associate Professor Toshiaki Sodesawa for helpful discussions and continual encouragement. The author heartily thanks Dr. Isamu Matsuda, Dr. Kazuo Urabe, and Dr. Makoto Onaka for their kind advice, instructive discussions, and continual encouragement.

Grateful acknowledgment is made to Professor Yuichi Murakami, Associate Professor Tadashi Hattori, and Associate Professor Miki Niwa for their helpful suggestions and encouragement. The author wishes to thank Professor Shigeharu Naka and Professor Kozo Sugiyama for their helpful suggestions from the view point of inorganic chemists. The author is grateful to Professor Takayoshi Uematsu and Dr. Shogo Shimazu for kind advice and encouragement.

The author would like to thank Dr. Hiroaki Sakurai and Mr. Shin Hasebe for their collaboration in Nagoya University. Thanks are also due to Mr. Masato Toita, Mrs. Yu-Qing Yu, Mr. Mitsuharu Hasegawa, Mr. Masahiro Hiratsuka, and Mr. Masahiro Tokumitsu for their collaboration in Chiba University. The author heartily thanks Dr. Akio Furuta, Dr. Hirofumi Ito and Mrs. S. Okamoto for measuring the differential heat of adsorption of ammonia. The author is also grateful to Mr. Hiroshi Shoji for measuring solid-state NMR and technical advice.

Finally, the author wishes to express his special thanks to Professor Yusuke Izumi, Professor Yuichi Murakami, Professor Kozo Sugiyama, Associate Professor Tadashi Hattori, and Associate Professor Miki Niwa for serving on his dissertation committee.

Satoshi Sato
October, 1991

Contents

Chapter 1. General Introduction

Solid Acid Catalyst

Catalytic reactions are usually classified into two types; homolytic (electronic, oxidation-reduction) and heterolytic (ionic, acid-base) reactions. Catalysts characteristic of the latter type are acids and bases; those of the former are metals and semiconductors. Restricted to acid-catalyzed reactions, liquid or soluble acids such as sulfuric acid and aluminum trichloride are used in the homogeneous phase. In contrast to the homogeneous processes where the used acid catalysts are usually deactivated by neutralization, heterogeneous processes have a great advantage with respect to product separation. Acidic solids are used as catalysts in the heterogeneous processes, both in the vapor phase and in the liquid phase, and they are called "solid acids".

Solid acids have been widely used as catalysts in chemical industry, particularly in the fields of refinery and petrochemistry. Many kinds of solid acids have been investigated; their catalytic behaviors, their acidic properties, and the structures of acid sites have been studied for the last 30 years, and those results have been reviewed by several workers.[1-7] Various types of solid acids are summarized in Table 1-1.[4,6] Solid acids are classified into two types; crystalline and amorphous solids. Natural clay minerals, synthetic zeolites, and heteropoly acids belong to a class of crystalline solid acids. The clays and zeolites mainly consist of silica and alumina. Various types of zeolites such as zeolites X, Y, and ZSM-5 have been synthesized, and their peculiar activities and selectivities for several catalytic reactions have been reported; an MTG (methanol to gasoline) process using ZSM-5 zeolite is a typical example.[8] On the other hand, amorphous solid acids are also sorted into several groups;

mounted acids, cation exchange resins, metal oxides, sulfates, phosphates, and mixed metal oxides. A well-known solid acid, amorphous SiO_2-Al_2O_3, is listed in the eighth group, which also includes the other various mixed oxides. Concerning acid strength of solid surface, binary mixed oxides such as SiO_2-Al_2O_3, TiO_2-ZrO_2, SiO_2-TiO_2, and SiO_2-ZrO_2 show high acidity ($H_o \leq -8.2$). In particular, SiO_2-Al_2O_3 and some zeolites have strong acid sites on their surface.[3,4] Furthermore, in the fourth and the fifth groups, strong solid acids such as Nafion H and sulfate-doped zirconia exhibit superacidity ($H_o \leq -11.9$).[5-7] Many of them have been found to show unique catalytic activities and selectivities.[1-8]

According to the definitions by Brønsted and Lewis, a solid acid shows a character to donate a proton or to accept an electron pair. The definitions are convenient for understanding of catalysis by solid acids. The mechanism of generation of acid sites on the binary mixed oxides belonging to the eighth group of Table 1-1 has been studied by several workers.[9-11] Tanabe *et al.* proposed a mechanism of the acidity generation which is associated with an excess of a negative or positive charge in a model structure of a binary oxide.[10] Recently, quantum mechanical calculations have been also carried out for model clusters of mixed oxides; the structures and the strengths of acid sites on the model clusters were investigated.[12-14]

Acidic properties of solid surface are characterized by various methods based on the neutralization of acid sites with basic molecules.[1,2,4] Both the strength and the number of acid sites are estimated by two types of methods such as amine titration in the liquid phase and gaseous base adsorption. The amine titration was usually performed by using an indicator in a non-aqueous solvent.[1,2] The gaseous base adsorption methods are subdivided into several types. Differential heat of adsorption (DHA), differential thermal analysis (DTA), thermogravimetry (TG), temperature-programmed desorption (TPD), infrared (IR), and nuclear magnetic resonance (NMR) belong to the gaseous base

adsorption methods.[1,4] In particular, the types of acid sites, Brønsted and Lewis, are distinguished by IR of pyridine and NMR of trimethylphosphine[15] adsorbed on acid sites. One must, therefore, thoroughly investigate on solid acidity, combining the several appropriate methods, in order to make global estimation of the strength, the number, and the type of acid sites.

Several solid acid catalysts have been practically used in very large-scale production of petrochemicals; amorphous silica-alumina and zeolites are used for fluidized catalytic cracking of naphtha and alkylation of benzene with propylene and ethylene, and supported phosphoric acid for ethylene hydration. In contrast to the very large-scale vapor-phase processes, many acid-catalyzed processes are operated still in the homogeneous phase using strong acids such as sulfuric acid, aluminum trichloride, boron trifluoride, and p-toluenesulfonic acid.[16,17] The homogeneous processes possess many problems as follows: (1) corrosion by strong acid, (2) side-reactions by strong acid, (3) difficult separation of products from catalyst, (4) difficult recovery and recycle use of catalyst, (5) coloring and degradation of product caused by residual catalyst, (6) treatment of waste water.

Table 1-2 summarizes some practical problems in various homogeneous acid-catalyzed processes.[16,17] Shifting to heterogeneous processes using effective solid acids has been desired to overcome the problems of these homogeneous processes. Despite many researches, however, it is not feasible to develop the solid acids with high activity and selectivity comparable to those of usual homogeneous processes. Solid acids which can clear these problems realize the replacement of homogeneous processes by heterogeneous processes, and can effect cost-saving because expensive corrosion-resistant materials are saved, and separating operation is simplified. The solid acids which can replace homogeneous acids must satisfy the following criteria: (1) sufficient activity and selectivity, especially high selectivity comparable to homogeneous systems, (2) long catalyst

life or ready regeneration when the catalyst showed a rapid decrease in activity, (3) no loss and sublimation of active species, (4) reasonable catalyst price.

Recent advances in organic synthesis using solid acids were reviewed by Izumi *et al.*.[18,19] Various heterogeneous processes, both in liquid and gas phases, have been studied to replace homogeneous processes. In particular, alkylation of aromatics with olefins has been focused.[20] For practical application, liquid-phase hydration of cyclohexene using high silica zeolites such as H-ZSM-5 and H-ZSM-11 has been realized to produce cyclohexanol selectively.[21] Therefore, it can be said that there is a plenty room of further improvement in the acid-catalyzed processes.

Chemical Vapor Deposition

The chemical vapor deposition (CVD) originates in the technique employed by the incandescent lamp industry. In the late of the past century, attempts were made to deposit pyrolitic carbon or metals in order to improve the fragile filaments; tungsten was deposited on carbon lamp filaments by hydrogen reducing WCl_6.[22] Since research activity on CVD coating increased drastically in the late 1950's, the CVD techniques have been remarkably developed.[23-31]

Excellent CVD coating materials have been widely used in a number of fields. For example, corrosion protection can be provided by CVD methods using deposits such as tantalum, BN, and SiC.[24] Hard coatings have also been applied to prepare various cutting tools; TiC or TiN coating improves the hardness of W-TiC-Co cutting tool.[26] Moreover, in the fields of electronic materials, CVD processes have been widely used for the formation and doping of epitaxial films such as silicon, germanium, and GaAs. Recently, hybrid CVD techniques such as reactive sputtering, photo-assisted CVD, and plasma-enhanced CVD have been developed as a key technology in polynary coatings for electronic

and optical devises, such as IC (integrated circuit), LSI (large-scale integration), LED (light emitting diode), OEIC (optoelectronic integrated circuit), LCD (liquid crystal display), and amorphous silicon solar battery.[29,31] The details in recent advanced CVD techniques are described in several books.[27-31]

Various types of chemical reactions such as thermal decomposition, reduction, oxidation, and hydrolysis are utilized in CVD processes.[28,31] Most of metals, oxides, nitrides, carbides, and silicides can be deposited through the CVD processes. Metal films are frequently produced by thermal decomposition of organometallic compounds or by reduction of metal halide or other simple inorganic compounds. In the production of metal oxide films, oxygen and water vapor are usually employed through oxidation and hydrolysis, respectively. For the deposition of nitrides and carbides, ammonia and hydrocarbon gases were used as reactant, respectively. Restricted to the deposition of oxides, Table 1-3 summarizes a number of examples which appear to be applicable for catalyst preparation.[28,31-48] Metal oxide films such as silica, titania, zirconia, and alumina can be prepared by using the respective metal alkoxides at relatively low temperatures. They will supply attractive materials as catalysts.

CVD process is defined to be the formation of a compound from gas phase onto a substrate where a solid deposit is produced through chemical reaction, in contrast to physical vapor deposition (PVD) which is the condensation of a reactant through mass transfer in vacuum without chemical reaction.[23,24] The PVD methods include sputtering, ion-plating, vacuum evaporation, and MBE (molecular beam epitaxy). The driving force of CVD is chemical potential difference between reactant and product whereas that of PVD is temperature difference between reactant vapor and substrate surface.

The total process of CVD generally consists of the following five steps: (a) transport of reactants to the substrate, (b)

adsorption of reactants onto the surface of substrate, (c) chemical reaction on the substrate surface, (d) desorption of product gases from the surface, and (e) transport of product gases away from the substrate.[24,25] The possible surface reactions are the steps (b), (c), and (d). These steps are collectively referred to as kinetic steps in the overall process. The steps (a) and (e) are mass transport processes. One mechanism of steps from (a) to (e) is usually the rate control step of deposition.

The effect of temperature upon deposition rate is shown qualitatively in Fig. 1-1.[24,25,28,30] Assuming the deposition has no thermodynamic limitation, deposition regions are divided into three types; A, limited by a reaction occurring at or near the surface of substrate (surface reaction limitation); B, limited by mass transport in the gas stream (diffusion limitation); and C, limited by homogeneous nucleation of product in the gas phase, respectively. When the deposition temperature is low, as shown in the region labeled A in Fig. 1-1, one of (b) to (d) processes becomes a rate determining step. At higher temperatures, in the region labeled B, nuclear growth of deposit is favorable rather than nucleation because of diffusion limitation of source reactants (process (a)). At further high temperatures, nucleation and nuclear growth take place in the gas phase to reduce the concentration of reactants vapor (in the region C).[25] Thus, the deposition rate in the region C decreased with increasing temperature. In addition, the deposition rate depends on the total pressure.[25,30] At low pressure, source reactants are readily diffuse onto the substrate surface. Uniformity of deposit increases with decreasing pressure at the same temperature, whereas the feed rate of reactants decreases.

A series of steps from (a) to (e) are quite similar to that of catalytic process. Only one difference between CVD and catalytic process is whether products remain on the surface of substrate as residuals. In contrast to the CVD process in which

the products remain on the surface as deposits, products are removed from the surface of catalyst in the catalytic reaction. When the reaction products are unfortunately remained on the catalyst surface, they will act as poisons. From this standpoint, a CVD process is also said to be "catalytic vapor deposition".

Several key aspects of CVD in the fields of thin film coating, such as deposit structure, control of process through thermodynamic aspects, and the basic features of the design of the equipment, are not dealt with in this section. The details in the CVD coating technologies are described in various reviews and books.[23-31]

Catalyst Preparation

Catalytic activities of solid catalysts are dependent not only on chemical component but also on preparation methods. This is caused by the facts that the physical properties of solid catalyst such as surface area, porosity, and particle structure are also influenced by the preparation methods. These properties are readily controlled by adjusting the preparation conditions.

Table 1-4 summarizes various catalyst preparation methods.[49-52] Solid catalysts are divided into two structure types; bulk type and supported type. The former is the entire solid material constituted the catalyst; it is produced through a liquid medium, and ordinarily prepared by such methods of precipitaion, hydrothermal synthesis, and melting. Many kinds of mixed metal oxides are prepared by precipitaion. Most of zeolites are synthesized by hydrothermal methods. The latter, a supported-type catalyst, includes the active species dispersed on a support having a large surface area, and is prepared by such ordinary methods as impregnation, ion-exchange, and immobilization of complex.

The supported-type catalyst is conveniently prepared by impregnation method. A catalyst carrier provides a large surface

area for a small amount of active components. The steps in the preparation of a catalyst impregnated on a support include the following sequences: contacting the support with the impregnating solution contained active components, removing the excess solution, drying, calcination and activation.[51] It is rememberable that a catalyst support influences not only physically but also chemically the resulting supported-type catalyst.

On the other hand, the bulk-type catalyst together with catalyst supports is usually prepared by precipitation method, including cogelation. The precipitation provides a method of obtaining a solid in a porous form. It consists of adding a precipitating agent to solution containing the desired components. Washing, drying, and usually calcination are subsequent steps in the process. The formation of a colloidal precipitate, gel, is included in the precipitation method. The steps in cogelation process are essentially the same as those in the usual precipitation procedure. In particular, catalysts containing silica and alumina are suitable for preparation by gel formation, since their precipitates are of a colloidal nature. Detailed techniques for producing catalysts through gel formation or ordinary precipitation are given in elsewhere.[49,50]

Another distinction is also drawn between liquid and vapor phases in which active species are formed (Table 1-4). Solid catalysts are usually prepared in liquid phase. The liquid-phase preparation is convenient and cheap for obtaining a large quantity of catalyst. In contrast to the liquid-phase preparation, a little application for catalyst preparation has been done in vapor phase. A bulk-type solid, a fine powder, is also produced by gas-phase reaction,[50] which occurs at high temperature where deposition is unfavorable in the region C in Fig. 1-1. The obtained fine powder, however, has a small surface area, and is applicable to inorganic materials such as pigment and ceramic powder rather than to catalyst. On the other hand, the supported-type catalyst can be made by CVD process.

CVD methods have been applied to surface modification[53-63] and catalyst preparation[64-74] for the last decade. Murakami *et al.* have reported that the size of the entry pore of zeolites such as mordenite and ZSM-5 can be narrowed by depositing SiO_2 by means of CVD using $Si(OCH_3)_4$ or $SiCl_4$. This modified mordenite showed higher selectivity to light hydrocarbons (C_1-C_3) when applied as a methanol conversion catalyst.[53-61] The other supported types of catalysts such as supported silica,[64-70] supported vanadium oxide,[71,72] supported niobia,[73] and supported metal[74] have been prepared through CVD techniques. In another vapor process, a microwave plasma has recently been used for the preparation of metal oxide powder.[75]

Several types of CVD reactors are applicable for catalyst preparation; fixed-bed reactor (Fig. 1-2),[76] rotary-type reactor in which the support material can be mixed by rotation (Fig. 1-3),[77] and fluidized-bed reactor are available. In this thesis, a fixed-bed reactor (Fig. 1-2) and a rotary-type reactor (Fig. 1-3) are used. Although fluidized-bed reactors are not dealt with in this thesis, they will have potential preparation by CVD method, particularly with respect to fine powder supports.

Volatile compounds, such as alkyl metal, metal carbonyl, hydride, acetylacetonate, and alkoxides, are practically used to obtain various metal oxide films. However, metal halides are not suitable for preparing catalyst because the unreacted residual halides are hardly removed. In general, metal alkoxides are convenient as the sources for CVD due to their feasible handling. Various alkoxides of Al, As, B, Ba, Ca, Ga, Ge, K, La, Li, Mg, Na, Nb, P, Sb, Si, Sn, Ta, Ti, V, W, Zn, and Zr are commercially supplied from Tri Chemical Laboratory Inc., (Phone: 0462-86-3000). Each of the alkoxides, except for alkali, alkali earth, lanthanum, and tungsten alkoxides, have a sufficient level of vapor pressure. Thus, the alkoxides can be preferably used as CVD source reactants. High vapor pressure alkoxides are listed in Table 1-5,[78] and some of them are used in this thesis. In addition, other alkoxides to be able to fill the demands for CVD

catalysts are summarized in Table 1-6.[78]

Research Background

Before the start of this research, the author had investigated on supported boria catalysts for the vapor-phase Beckmann rearrangement of cyclohexanone oxime. This rearrangement reaction is one of the important target reactions for catalyst chemists who aim at efficient, energy-saving and environmentally friendly catalysts to replace the present processes including some problems (Table 1-2).

The author examined the rearrangement reaction over supported boria catalysts by impregnation or kneading method using several supports with different acid-base properties, comparing with the results obtained by some typical solid acids (Table 1-7).[79] He found that the boria supported on a basic substance, hydroxyapatite, in a high boria loading was more active than boria-alumina and silica-alumina, although the boria-hydroxyapatite possessed a relatively small surface area (34 m^2/g). In particular, the boria-hydroxyapatite exhibited high selectivity for the product ε-caprolactam. Table 1-7 also indicates that strongly acidic silica-alumina and zeolite HX were both not necessarily suitable for this rearrangement reaction but even relatively weak acid, such as boria on hydroxyapatite, could work efficiently.

These results led the author to think that boria in high dispersion on a suitable support might show more uniform acid property pertinent to the selective catalysis in the rearrangement reaction. Based on this idea the author started his work from the design of supported boria catalyst by means of CVD technique which appeared to be the most appropriate method for obtaining catalysts with high boria loadings and uniform acid properties.

Throughout the study on CVD boria catalysts for the rearrangement reaction, the author was convinced that CVD

techniques were useful for the preparation of solid acids. Furthermore, he extended his work to the design of other various kinds of solid acids with high catalytic performance by incorporating uniform active species on supports with the aid of CVD technique.

Objective and Scope

As mentioned previously, CVD techniques have been developed greatly in the production of electronics and cutting tools. The coating thin films are required for the thickness in a order of micro-meter or lager. On the other hand, in consideration of catalyst surface, active species are usually required for dispersion as small as an order of nano-meter. The thin film encountered in the coating technologies will not be suited to the preparation of catalyst. A "super thin film" of deposit is expected to exhibit catalytic activities for various organic reactions, owing to various expectations such as high dispersion of deposits or formation of composite oxide phase on the surface of support.

CVD methods have recently been used for both the modification of microporous materials[53-63] and the preparation of catalysts.[64-74] In contrast to the plane surface of substrate such as silicon devise, porous materials as catalyst supports usually have large surface areas. For the preparation of catalyst, active catalyst species must be deposited on interior pore walls of the support material during the CVD process. Fundamental investigations on the catalyst preparation by using CVD techniques are believed to serve not only for development of a new type of catalyst but also for refinement of the basic concepts in catalysis from view the points of surface science.

The main themes of this thesis are to evaluate the possibility of CVD preparation method for various supported types (listed in Table 1-4) of solid acid catalysts, and to clarify the

correlation between the catalytic activities and the physicochemical structures of deposits (acidic character and geometric structure). With the background aforementioned, the author has carried out the following studies.

In chapter 2, the author introduces a method of catalyst preparation which involved the CVD of boria onto silica and alumina using boron triethoxide to produce silica-supported boria and alumina-supported boria catalysts, which belong to the fourth and eighth groups in Table 1-1, respectively. A boria component has been reported to be active for the vapor-phase Beckmann rearrangement of cyclohexanone oxime; the catalytic activity, especially lactam selectivity, have been known to be remarkably affected by the method of catalyst preparation. Thus, the author attempted to prepare silica-supported boria (section 2-1) and alumina-supported boria (section 2-2), and investigated their catalytic activities for the vapor-phase Beckmann rearrangement of cyclohexanone oxime. The physical and chemical properties of the resulting CVD catalysts were examined to clarify the correlation to catalytic activities. In particular, both uniformity of boria deposit and acidic character of the resulting CVD catalysts were examined in detail. Moreover, the influences of support materials upon the catalytic activities were discussed.

In chapter 3, silica-alumina catalyst, one of the representative amorphous solid acids, was taken up as a subject of investigation. A supported type of silica-alumina was prepared by depositing silica on alumina surface using tetraethoxysilane in the section 3-1. Both the influences of silica deposition conditions and the catalytic activities of the resulting silica-alumina for various organic reactions were studied. In section 3-2, the acidic properties of the silica-alumina catalyst prepared in section 3-1 were characterized by several measurements such as solid-state magic-angle spinning (MAS) NMR measurement and temperature-programmed desorption (TPD) of adsorbed dimethylpyridine. The ^{31}P MAS NMR of

trimethylphosphine chemisorbed on solid surface was employed to elucidate the intrinsic nature of acid sites, concerning the type of Brønsted or Lewis acid. Furthermore, the measurement of TPD of adsorbed dimethylpyridine was performed to clarify the acidic properties, *i.e.* strength, amount, and type of acid sites. The author established a TPD method to characterize the acidic properties of CVD silica-alumina catalysts. Correlations between the catalytic activities and the acidic properties of the CVD catalysts were discussed in detail. In section 3-3, structural characteristics of the CVD silica-alumina catalyst were carefully investigated by solid-state MAS NMR. The ^{29}Si MAS NMR of silica deposited on alumina surface revealed the microstructures of silica.

In section 3-4, deposition of silica on amorphous silica-alumina was attempted to newly generate Brønsted acid sites on the surface of the original silica-alumina. The original silica-alumina used as a support had both Brønsted and Lewis acid sites. The Lewis acid sites were allowed to convert to Brønsted acid sites by the deposition of silica. Their catalytic activities for the cracking of cumene and the isomerization of 1-butene were examined. The acidic character of the catalyst was also clarified by means of TPD of adsorbed 2,6-dimethylpyridine.

In chapter 4, the author attempted to prepare several composite surface compounds by depositing binary mixed components onto inert supports. As a representative example, boron phosphate was deposited on a silica support. A silica-supported boron phosphate catalyst was prepared by CVD using a mixture of boron triethoxide and phosphoryl trimethoxide. Various CVD conditions were applied to deposit boron phosphate with a desired P/B ratio. The micro-structures of deposit boron phosphate were characterized by means of ^{31}P NMR. The catalytic activity of 1-butene isomerization was also investigated, comparing with a catalyst prepared by a usual method of impregnation.

In chapter 5, deposition behaviors in the preparation of various solid acids were summarized. The correlation between the

kind of support material and the nature of the acid sites generated were discussed in consideration of the difference in deposition rate. Moreover, the effect of the type of CVD reactor on catalyst preparation was also described.

In chapter 6, the conclusions obtained in this thesis were summarized.

References

1. K. Tanabe, "*Solid Acids and Bases, Their Catalytic Properties.*" Tokyo Kodansha, Academic Press, New York, 1970.
2. H. A. Benesi and B. H. C. Winquist, *Adv. Catal.*, 27 (1978) 97.
3. I. M. Campbell, "*Catalysis at Surfaces*", Chapman and Hall, London, 1988.
4. K. Tanabe, M. Misono, Y, Ono, and H. Hattori, *Stud. Surf. Sci. Catal.*, 51 (1989) 1.
5. K. Tanabe, *Shokubai (Catalyst)*, 27 (1985) 198.
6. K. Arata, *Adv. Catal.*, 37 (1990) 165.
7. T. Yamaguchi, *Appl. Catal.*, 61 (1990) 1.
8. C. D. Chang, *Catal. Rev. Sci. Eng.*, 25 (1983) 1.
9. C. L. Thomas, *Ind. Eng. Chem.*, 41 (1949) 2564.
10. K. Tanabe, T. Sumiyoshi, K. Shibata, T. Kiyoura, and J. Kitagawa, *Bull. Chem. Soc. Jpn.*, 47 (1974) 1064.
11. T. Seiyama, "*Metal Oxides and their Catalytic Actions*", Kodansha, Tokyo, 1978.
12. G. M. Zhidomirov and V. B. Kazansky, *Adv. Catal.*, 34 (1986) 131.
13. S. Yoshida and H. Kawakami, *Hyomen (Surface)*, 21 (1983) 737.
14. H. Kawakami, S. Yoshida and T. Yonezawa, *J. Chem. Soc., Faraday Trans. 2*, 80 (1984) 205.
15. J. H. Lunsford, W. P. Rothwell, and W. Shen, *J. Am. Chem. Soc.*, 107 (1985) 1540.
16. Reported by Catalysis Society of Japan, Committee of Solid Acids Processing, *Shokubai (Catalyst)*, 23 (1981) 223.
17. K. Tanabe, *ibid.*, 25 (1983) 78.
18. Y. Izumi, K. Urabe, and M. Onaka, *ibid.*, 27 (1985) 27.
19. Y. Izumi, *ibid.*, 30 (1988) 583.

20. T. Takase, *ibid.*, 21 (1979) 183.
21. M. Kono, Y. Fukuoka, O. Mitsui, and H. Ishida, *Nippon Kagaku Kaishi*, 1989, 521.
22. A. de Lodyguine, *U. S. Pat.*, 575,002 (1897) and 575,668 (1897).
23. C. F. Powell, J. H. Oxley, and J. M. Blocher, Jr., "*Vapor Deposition*", John Wiley & Sons, Inc., New York, 1966
24. W. A. Bryant, *J. Mater. Sci.*, 12, (1977) 1285.
25. K. Sugiyama, *Zairyou Kagaku*, 15 (1978) 9.
26. K. Sugiyama, *Ceramics*, 16 (1981) 155.
27. S. Hayakawa and K. Wasa, "*Hakumakuka Gijutsu*", Kyoritsu Shuppan, Tokyo, 1982.
28. "*Thin Film Handbook*", ed. by Japan Society for the Promotion of Science, 131st Committee (Thin Film), Ohmsha, Tokyo, 1983.
29. "*Hikari Hakumaku Gijutsu Manual*", Optronics, Tokyo, 1989.
30. S. Yoshida, "*Hakumaku (Thin Film), Oyobutsurigaku Sensho 3*", Baifukan, Tokyo, 1990.
31. "*CVD Handbook*", ed. by the Society of Chemical Engineers, Japan, Asakura Shoten, Tokyo, 1991.
32. S. Rojas, A. Modelli, and W. S. Wu, *J. Vac. Sci. Technol. B*, 8 (1990) 1177.
33. S. Hayashi and T. Hirai, *J. Crystal Growth*, 36 (1976) 157.
34. S. Hayashi and T. Hirai, *ibid.*, 41 (1977) 41.
35. E. T. Fitzgibbons, K. J. Sladek and W. H. Hartwig, *J. Electrochem. Soc.*, 119 (1972) 735.
36. Y. Shimogaki and H. Komiyama, *Chem. Lett.*, 1986 267.
37. R. N. Ghoshtagore, *J. Electrochem. Soc.*, 117 (1970) 529.
38. M. Yokozawa and H. Iwasa, *Jpn. J. Appl. Phys.*, 7 (1968) 96.
39. M. Balog, M. Schieber, S. Patai, and M. Michman, *J. Crystal Growth*, 17 (1972) 298.
40. Y. Takahashi, H. Suzuki, and M. Nasu, *J. Chem. Soc., Faraday Trans. 1*, 81 (1985) 3117.
41. Y. Takahashi, K. Tsuda, K. Sugiyama, H. Minoura, D. Makino, and M. Tsuiki, *ibid.*, 77 (1981) 1051.
42. N. Tauber, A. C. Dumbri, and R. E. Caffrey, *J. Electrochem. Soc.*, 118 (1971) 747.

43. J. Melsheimer and D. Ziegler, *Thin Solid Films*, **109** (1983) 71.
44. J. A. Aboaf, V. C. Marcotte, and N. J. Chou, *J. Electrochem. Soc.*, **120** (1973) 701.
45. R. Colmet, R. Naslain, and P. Hagenmuller, *ibid.*, **129** (1982) 1367.
46. J. Kim, C. Park, and J. S. Chun, *Thin Solid Films*, **97** (1982) 97.
47. J. A. Aboaf, *J. Electrochem. Soc.*, **114** (1967) 948.
48. J. Saraie, J. Kwon, and Y. Yodogawa, *ibid.*, **132** (1985) 890.
49. T. Shirasaki and N. Todo, "*Shokubai Chosei (Catalyst Preparation)*", Kodansya, Tokyo, 1974.
50. A. Ozaki, "*Shokubai Chosei Kagaku (Catalyst Preparation Chemistry)*", Kodansya, Tokyo, 1980.
51. J. M. Smith, "*Chemical Engineering Kinetics*", McGraw-Hill, 1981.
52. "Shokubai Koza 5, Shokubai Sekkei", ed. by Catalysis Society of Japan, Kodansha Scientific, Tokyo, 1985.
53. M. Niwa, S. Kato, S. Morimoto, T. Hattori, and Y. Murakami, *Shokubai (Catalyst)*, **25** (1983) 371.
54. M. Niwa, M. Kato, T. Hattori and Y. Murakami, *ibid.*, **27** (1985) 76.
55. T. Hibino, Y. Kawashima, M. Niwa, and Y. Murakami, *ibid.*, **29** (1989) 414.
56. M. Niwa, S. Kato, T. Hattori, and Y. Murakami, *J. Chem. Soc., Faraday Trans. 1*, **80** (1984) 3135.
57. M. Niwa, Y. Kawashima, and Y. Murakami, *ibid.*, **81** (1985) 2757.
58. M. Niwa, M. Kato, T. Hattori, and Y. Murakami, *J. Phys. Chem.*, **90** (1986) 6233.
59. T. Hibino, M. Niwa, T. Hattori, and Y. Murakami, *Appl. Catal.*, **44** (1988) 95.
60. M. Niwa and Y. Murakami, *Nippon Kagaku Kaishi*, **1989**, 410.
61. M. Sawa, K. Kato, K. Hirota, M. Niwa, and Y. Murakami, *Appl. Catal.*, **64** (1990) 297.
62. H. Itoh, S. Okamoto, and A. Furuta, *Nippon Kagaku Kaishi*, **1989**, 420.
63. Y. Teraoka, K. Kunitake, S. Kagawa and M. Iwamoto, *ibid.*, **1989**, 424.
64. T. Okuhara and J. M. White, *Appl. Surf. Sci.*, **29** (1987) 223.
65. T. Okuhara, T. Jin, and J. M. White, *Shokubai (Catalyst)*, **30** (1988) 384.
66. Y. Imizu, A. Tada, and I. Toyoshima, *ibid.*, **30** (1988) 388.
67. S. Sato, M. Toita, T. Sodesawa, and F. Nozaki, *ibid.*, 31 (1989) 124.
68. M. Niwa, T. Hibino, H. Murata, N. Katada, and Y. Murakami, *J. Chem. Soc., Chem. Commun.*, **1989**, 289.
69. Y. Imizu and A. Tada, *Chem. Lett.*, **1989**, 1793.
70. N. Katada, M. Niwa, and Y. Murakami, *Shokubai (Catalyst)*, **32** (1990) 59.
71. M. Matsuda, K. Suzuki, A. Miyamoto, T. Hattori, and Y. Murakami, *ibid.*, **26** (1984) 138.
72. K. Inumaru, T. Okuhara, and M. Misono, *ibid.*, **32** (1990) 51.
73. K. Asakura, Y. Iwasawa, and H. Kuroda, *ibid.*, **27** (1985) 371.
74. H. Miura, K. Oki, H. Ochiai, and J. Kimura, *ibid.*, **31** (1989) 417.
75. K. Sugiyama, H. Aoki, Y. Yokota, and T. Matsuda, *ibid.*, **31** (1989) 457.
76. S. Sato, K. Urabe, and Y. Izumi, *J. Catal.*, **102** (1986) 99.
77. S. Sato, M. Toita, T. Sodesawa, and F. Nozaki, *Appl. Catal.*, **62** (1990) 73.
78. D. C. Bradley, R. C. Mehrotra and D. P. Gaur, "*Metal Alkoxides*", Academic Press, 1978.
79. Y. Izumi, S. Sato, and K. Urabe, *Chem. Lett.*, **1983**, 1649.

Table 1-1. Solid acids.

Crystalline solids

1. Natural clay minerals:
   kaolinite, montmorillonite, beidellite, hectorite, saponite,
   cation exchanged clays
2. Synthetic zeolites:
   zeolite (X, Y, A, H-ZSM etc.), cation exchanged zeolites
3. Heteropoly acids:
   silicotungstic acid, phosphomolybdic acid, phosphotungstic acid

Amorphous solids

4. Mounted acids:
   H_2SO_4, H_3PO_4, H_3BO_3, $AlCl_3$, SbF_5, NbF_5 mounted on silica or alumina,
   sulfate-doped metal oxides
5. Cation exchange resins:
   Amberlite, Amberlyst (resin sulfonic acid),
   Nafion H (perfluorinated resin sulfonic acid)
6. Metal salts:
   $MgSO_4$, $BaSO_4$, $CuSO_4$, $ZnSO_4$, $Al_2(SO_4)_3$, $FeSO_4$, $Fe_2(SO_4)_3$, $CoSO_4$, $NiSO_4$,
   BPO_4, $AlPO_4$, $CrPO_4$, $FePO_4$, $Mg_3(PO_4)_2$, $Ti_3(PO_4)_4$, $Ti(HPO_4)_2$, $Zr_3(PO_4)_4$,
   $Zr(HPO_4)_2$, $Ni_3(PO_4)_2$,
7. Metal oxides:
   ZnO, Al_2O_3, CeO_2, ThO_2, TiO_2, ZrO_2, V_2O_5, Nb_2O_5, Ta_2O_5, Cr_2O_3, MoO_3, WO_3
8. Mixed oxides:
   SiO_2-Al_2O_3, SiO_2-TiO_2, SiO_2-ZrO_2, SiO_2-Ga_2O_3, SiO_2-Y_2O_3, SiO_2-La_2O_3,
   SiO_2-ZnO, SiO_2-MoO_3, SiO_2-BeO, SiO_2-MgO, SiO_2-CaO,
   Al_2O_3-B_2O_3, Al_2O_3-TiO_2, Al_2O_3-ZrO_2, Al_2O_3-MoO_3,
   TiO_2-ZrO_2, TiO_2-ZnO, TiO_2-CdO, TiO_2-SnO_2, TiO_2-CuO

Table 1-2. Practical problems for homogeneous acid-catalyzed processes.

Reaction reactant	product	Catalyst	Reaction temp.(°C)	Problems
Beckmann rearrangement		H_2SO_4-SO_3	100-150	by-product ammonium sulfate,
cyclohexanone oxime	ε-caprolactam			corrosion
Esterification		H_2SO_4	100-120	side-reaction, treatment of
phthalic acid		p-TsOH*		waste water, corrosion,
salicylic acid				coloring of product,
acrylic acid				recovery of catalyst
Hydrolysis		H_2SO_4	80-100	side-reaction, corrosion,
acetone cyanohydrin				recovery of catalyst,
acetonitrile				waste water
Hydration		H_2SO_4	120-150	recovery of catalyst,
1-butene	2-butanol	BF_3		corrosion
Alkylation				
isobutane+isobutene		H_2SO_4	2-10	treatment of waste water
p-cresol+isobutene		H_2SO_4	60-80	side reaction, corrosion
benzene		$AlCl_3$,	50-200	
		BF_3, HF		
Prins reaction		H_2SO_4	30-60	by-product, recovery of
isobutene+HCHO				catalyst from HCHO
Polymerization				
isobutene		$AlCl_3$	ca.100	corrosion, deactivation and
1-olefin		BF_3		removal of catalyst
β-pinene		$AlCl_3$	-	cat. required eq. reactant
THF	PTMG**	H_2SO_4+SO_3	-	deactivation and separation
		FSO_3H		of catalyst
Isomerization				
m-xylene	o-,p-xylene	HF-BF_3	<100	corrosion, toxicity of HF
α-pinene	paramethadiene	H_2SO_4		treatment of waste water

* p-toluenesulfonic acid, ** polyoxytetramethylene glycol.

Table 1-3. Oxide thin files prepared by CVD.

Oxide	Ref.	Reactant system	CVD Temp. (^{o}C)	Comments
SiO_2	31	SiH_4-N_2O	700-850	$SiH_4 + 2N_2O = SiO_2 + 2H_2 + 2N_2$
	28,31	SiH_4-O_2	300-500	$SiH_4 + O_2 = SiO_2 + 2H_2$
	28,31	$Si(OEt)_4$	700-800	$Si(OEt)_4 = SiO_2 + 4C_2H_4 + 2H_2O$
	32	$Si(OEt)_4$-O_2	650-780	0.4 - 0.8 Torr
TiO_2	33,34	$TiCl_4$-H_2O	100-900	rutile and/or anatase
	35	$Ti(OPr^i)_4$-H_2O	150	anatase (350 ^{o}C)
	36	$Ti(OPr^i)_4$	350	amorphous
	37	$TiCl_4$-O_2	400-1050	$TiCl_4 + O_2 = TiO_2$(rutile) + Cl_2
	38,39	$Ti(OPr^i)_4$-O_2	220-700	anatase
	40	$Ti(OPr^i)_4$-O_2	450-500	rutile (rapid deposition)
	41	$Ti(OEt)_4$-O_2	445-490	rutile
ZrO_2	42	$ZrCl_2$-H_2-CO_2	800-1000	$H_2 + CO_2 = CO + H_2O$
	39	$Zr(acac)_4$-O_2	450-700	
	31	$Zr(OBu^i)_4$	300-700	maximized at 450 ^{o}C
SnO_2	43	$SnBu_2Ac_2$-H_2O	430-450	
	44	$SnCl_4$-H_2O	380-600	polycrystalline
Al_2O_3	45,46	$AlCl_3$-H_2-CO_2	900-1150	α-alumina
	47	$Al(OPr^i)_3$-O_2	420	γ-alumina (800 ^{o}C)
	48	$Al(OPr^i)_3$	250-420	

Et, ethyl; Pr^i, isopropyl; Bu^i, isobuthyl; acac, acetylacetonate; $SnBu_2Ac_2$, dibutyltin diacetate.

Table 1-4. Catalyst preparation methods.

Classification	Method	Application
Liquid phase process		
Bulk type		
Precipitation	Coprecipitaion	Mixed metal oxides
	Cogelation	
	Kneading	
Hydrothermal synthesis		Zeolites
Melting		Alloys
Supported type		
Impregnation	Equilibrium adsorption	Supported metal
	Pore-filling	
	Incipient wetness	
	Evaporation to dryness	
Ion-exchange		Supported metal
Immobilization of complex		
Vapor phase process		
Bulk type		
Fine powder synthesis		Metal oxides
Supported type		
Chemical vapor deposition (CVD)		Supported metal and oxide

Table 1-5. Boiling point of volatile metal alkoxides.[76]

R in alkoxide	Boiling point (°C)			
	$B(OR)_3$	$P(OR)_3$	$PO(OR)_3$	$Si(OR)_4$
Me	68.7	117	197	121
Et	117.4	159	215	166
Pr^i	140	-	206	226

Me, methyl; Et, ethyl; Pr^i, isopropyl.

Table 1-6. Boiling point of metal alkoxides.[76]

R in alkoxide	Boiling point (°C/mmHg)						
	$Fe(OR)_3$	$Al(OR)_3$	$Ti(OR)_4$	$Zr(OR)_4$	$Hf(OR)_4$	$Nb(OR)_5$	$Ta(OR)_5$
Et	155/0.1	169/1.5	103/0.1	180/0.1	180-200/0.1	156/0.05	146/0.15
Pr^n	162/0.1	205/1.0	-	-	-	166/0.05	184/0.15
Pr^i	149/0.1	106/1.5	49/0.1	160/0.1	170/0.35	60-70/0.1	122/0.1
			91/5.0	204/5.0			
Bu^n	171/0.1	242/0.7	142/0.1	243/0.1	-	197/0.15	217/0.15
Bu^t	136/0.1	151/1.3	94/5.0	89/5.0	90/6.5	110-20/0.3	96/0.1

Et, ethyl; Pr^n, n-propyl; Pr^i, isopropyl; Bu^n, n-butyl; Bu^t, *tert*-butyl.

Table 1-7. Vapor-phase catalytic Beckmann rearrangement of cyclohexanone oxime.[a]

Catalyst	Conversion of oxime[b] (%)	Selectivity to caprolactam (mol%)
Boria(40 wt%)-hydroxyapatite[c]	67.1	97.1
Boria(25 wt%)-alumina[d]	63.3	89.1
Boria(14 wt%)-silica gel[d]	53.5	85.7
Silica-alumina[e]	71.6	73.3
Zeolite (HX)[f]	27.0	84.6

a) 300 °C, W/F=2.0 g-cat·h/mol, oxime/benzene/nitrogen=1/13/16 (mole ratio).
b) Average initial conversion at 2-3 h after the feed was initiated.
c) Prepared by kneading wet gel of hydroxyapatite in boric acid solution.
d) Prepared by impregnating β-alumina or silica gel with boric acid.
e) A reference catalyst of The Catalysis Society of Japan (SAH-1 containing 28.61 wt% of alumina).
f) Obtained by calcining NH_4-exchanged X-type zeolite at 350 °C for 40 h.

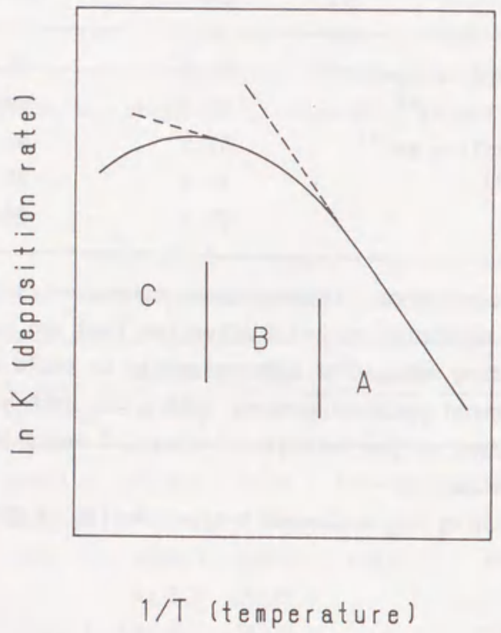

Fig. 1-1. The effect of temperature on deposition rate.

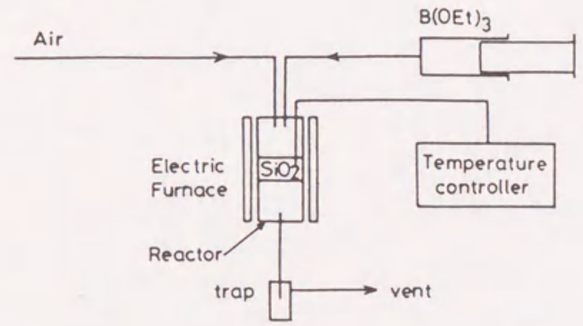

Fig. 1-2. A CVD apparatus for the catalyst preparation with fixed-bed reactor.

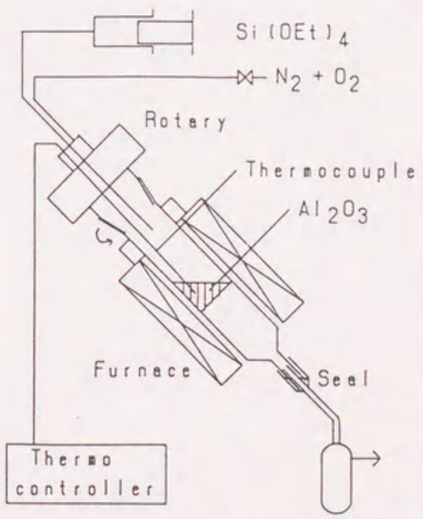

Fig. 1-3. A CVD apparatus for the catalyst preparation with rotary-type CVD reactor (Et=ethyl).

Chapter 2. Deposition of Boria

2-1 Silica-Supported Boria Catalyst

Abstract

A CVD method was introduced to catalyst preparation which involved the deposition of triethylborate onto silica gel to produce a silica-supported boria (CVD B_2O_3/SiO_2). A CVD B_2O_3/SiO_2 catalyst showed high catalytic efficiency for the vapor-phase Beckmann rearrangement of cyclohexanone oxime at 250 ^oC (oxime conversion: 98 %, ε-caprolactam selectivity: 96 mol%, at B_2O_3 content of 34 wt%). The CVD B_2O_3/SiO_2 was more active and selective at any B_2O_3 content than the B_2O_3/SiO_2 obtained by the ordinary impregnation method using H_3BO_3. The amounts of the acid sites whose acid strengths exceeded 80 kJ/mol in terms of the differential heat of adsorption of ammonia (DHA) were 0.7 and 0.4 mmol/g for the most active CVD B_2O_3/SiO_2 and the most active impregnation B_2O_3/SiO_2, respectively. The CVD effected uniform deposition of B_2O_3 on SiO_2, and produced a solid acid with relatively uniform distribution of acid strength. It is suggested that the acid strength (H_o) of an effective catalyst pertinent to the vapor-phase Beckmann rearrangement should be less than -5.6 which approximately corresponds to a DHA value of more than 80 kJ/mol.

Introduction

The vapor-phase Beckmann rearrangement of cyclohexanone oxime has been studied in order to replace sulfuric acid with solid acids for the manufacture of ε-caprolactam.[1-16] A number of solid acid catalysts, such as mixed boron oxide,[1-6] amorphous silica-alumina,[7-9] and modified zeolites,[10-16] have been

proposed. Strong acid sites on an HY zeolite catalyze the rearrangement of ketoxime at 120 ^{o}C, but the produced lactam is strongly adsorbed on the zeolite surface.[17] Since the adsorbed lactam needs energy to desorb from catalyst, the rearrangement reactions are ordinarily carried out at temperatures higher than 300 ^{o}C. These solid acid catalysts were accompanied by undesirable catalytic side reactions, such as decomposition of the reactant oxime and polymerization of the product lactam, and deactivated by rapid carbon deposit. Recently, an modified H-ZSM-5 zeolite has been reported as a high selective catalyst; neutral hydroxyl groups are claimed to be effective for the rearrangement after the strong protonic acid sites had reacted with trimethylsilyl chloride.[14]

The chemical vapor deposition of metal alkoxides or halides onto several inorganic materials has recently been applied to catalyst preparation as well as to modification of catalytic property of zeolites. Murakami *et al.* have reported that the size of the entry pore of mordenite can be narrowed by depositing SiO_2 by means of vapor decomposition using $Si(OCH_3)_4$ or $SiCl_4$. This modified mordenite showed higher selectivity of light hydrocarbons (C_1 - C_3) when applied as a methanol conversion catalyst.[18,19]

In this section, the silica-supported boria catalysts prepared by the CVD method using $B(OEt)_3$ will be characterized in detail with respect to the acid property and the catalytic efficiency for the vapor-phase Beckmann rearrangement of cyclohexanone oxime, in comparison with the boria catalysts obtained by the ordinary impregnation method. The reason for selecting the Beckmann rearrangement as a test reaction is that supported boria catalysts such as boria-alumina[1-4] have long been known as favorable catalysts for this reaction but there is still plenty of room for improvement, particularly in the selectivity to ε-caprolactam as well as in catalyst life in view of practical application.

Experimental

Catalysts. An apparatus for the catalyst preparation through CVD technique is shown in Fig. 1-2. A specific silica support having a surface area of 281 m^2/g and a pore volume of 1.35 ml/g (Fuji Davison Chemical, ID type) was employed in all experiments, except for a case of the examination on the effects of physical property of silica support. Silica gel (0.5 - 1.0 g, 24 - 60 mesh granules) was placed in a Pyrex glass reactor, and $B(OEt)_3$ vapor was brought into contact with the silica support at 250 - 400 ^{o}C for 0.1 - 6.0 h in a stream of air. The flow rates of $B(OEt)_3$ and air were 3.5 mmol/h and 115 ml/min, respectively. There was observed no carbon left on the resulting catalysts. The B_2O_3 content of catalyst was determined from the weight increase of SiO_2 after the CVD treatment; the data obtained by this method agreed closely with those by the alkalimetric titration of the H_3BO_3 extracted from catalyst with hot water.

The impregnation catalyst was prepared by impregnating the same silica support with aqueous H_3BO_3 followed by calcination at 350 ^{o}C for 3 h.

Catalytic tests. The vapor-phase Beckmann rearrangement of cyclohexanone oxime was carried out using a fixed-bed continuous flow apparatus under atmospheric pressure. The reaction temperature, which was measured by a thermocouple placed in the catalyst bed, was maintained at 250 ^{o}C. A mixture of the oxime, benzene as a diluent and N_2 was passed in a mole ratio of 1:13:16 through the catalyst bed (0.2 g) packed in a 15 mm-i.d. Pyrex glass reactor at a WHSV of 0.81 h^{-1} in terms of the oxime. The reactor effluent was collected in a trap and analyzed by GLC using a PEG 20M column (1 m). The major by-products included cyclohexanone and hex-5-enenitrile.

Analysis. The desorption spectra of pyridine on B_2O_3/SiO_2 catalysts were measured by use of a conventional TPD apparatus combined with thermal conductivity detector. A catalyst sample (30 mg) was preheated in a TPD cell at 400 ^{o}C for 1 h in a stream

of He (115 ml/min). Pyridine (10 μl) was injected at 300 ^{o}C, and the cell was cooled rapidly to 25 ^{o}C. The TPD measurement was done from 25 ^{o}C at a heating rate of 10 ^{o}C/min.

The differential heat of adsorption of ammonia was measured by use of a multipurpose calorimeter (Tokyo RIKO, Model MPC-11). The sample was preheated at 400 ^{o}C for 1 h.

The scanning electron microscopy for the examination of catalyst surface was performed using a JEOL JSM-T20 instrument.

Results

Figure 2-1 shows the change in catalytic activity for the Beckmann rearrangement with the time on stream at 300 and 250 ^{o}C. When the reaction was performed at 300 ^{o}C, the catalytic activity of impregnation B_2O_3/SiO_2 gradually decreased with the time on stream owing to coking, but little change in activity was observed with CVD B_2O_3/SiO_2 up to 5 h of the run. In the present study, however, the reaction data were taken at 250 ^{o}C in order to compare the catalytic efficiency of CVD B_2O_3/SiO_2 with that of impregnation B_2O_3/SiO_2, because the oxime conversion at 300 ^{o}C were too high to discuss the difference in catalytic efficiency between those two catalysts in detail. At 250 ^{o}C, however, the oxime conversion decreased more rapidly with the time on stream than at 300 ^{o}C owing to faster coke formation which was caused probably by slower desorption of high boiling point products. Hence, the average oxime conversion and lactam selectivity obtained between 3 and 4 h after the reactant feed were taken as the standard data; mass balance was not completed during initial 3 h of each run at this reaction temperature.

Effects of CVD conditions

Figure 2-2 shows the influence of CVD temperature on the catalytic activity of the resulting B_2O_3/SiO_2. The rate of B_2O_3 deposition on SiO_2 surface was greatly influenced by CVD temperature. The B_2O_3 content increased with increasing

temperature, and the maximum B_2O_3 content was attained at 350 ^{o}C. The oxime conversion was correlated well to the B_2O_3 content, but the lactam selectivity decreased markedly at above 350 ^{o}C.

Figure 2-3 gives the influence of CVD time at a constant rate of $B(OEt)_3$ feed. The B_2O_3 content increased monotonously up to 3 h, and then leveled off. The oxime conversion depended on the B_2O_3 content, but when the CVD time exceeded 3 h, the lactam selectivity decreased rapidly. Thus the B_2O_3 content could be adjusted by changing either CVD temperature or time. The best B_2O_3/SiO_2 catalyst containing 34 wt% of B_2O_3 was obtained under the condition of 350 ^{o}C for 3 h at a $B(OEt)_3$ feed rate of 3.5 mmol/h. This catalyst showed an oxime conversion of 98 % with a lactam selectivity of 96 % at a reaction temperature of 250 ^{o}C.

Figure 2-4 illustrates the change in catalytic performance with B_2O_3 content, comparing CVD B_2O_3/SiO_2 with impregnation B_2O_3/SiO_2. Both the oxime conversion and the lactam selectivity increased with the B_2O_3 content, but the oxime conversion over impregnation B_2O_3/SiO_2 began to decrease at a B_2O_3 content above 20 wt%. It is obvious that CVD B_2O_3/SiO_2 excelled impregnation B_2O_3/SiO_2 in the catalytic efficiency for the Beckmann rearrangement.

When N_2 was employed as a carrier gas in place of air in the CVD operation, only a little deposition of B_2O_3 (0.8 wt%) was attained under the conditions of 350 ^{o}C for 3 h at a $B(OEt)_3$ feed rate of 3.5 mmol/h. The resulting B_2O_3/SiO_2 was as inactive as SiO_2 support itself for the Beckmann rearrangement. On the other hand, when steam was used in place of air in the CVD operation, a B_2O_3/SiO_2 having a B_2O_3 content of 29 wt% was obtained. But in this case B_2O_3 was deposited exclusively on the upper side of the SiO_2 bed packed in the reactor for CVD, because $B(OEt)_3$ had already changed into B_2O_3 or H_3BO_3 through hydrolysis in the gas phase before $B(OEt)_3$ reached the surface of SiO_2 particles. The B_2O_3/SiO_2 prepared by the CVD using H_2O showed lower catalytic activity (oxime conversion: 82 %, lactam selectivity: 93 mol%, at 250 ^{o}C) than the B_2O_3/SiO_2 prepared by use of air. It is,

therefore, necessary for uniform B_2O_3 deposition to decompose $B(OEt)_3$ with O_2 not with H_2O.

Effects of physical property of SiO_2 support

Table 2-1 summarizes the influences of physical property of SiO_2 support on the efficiency of CVD catalyst. The amount of the B_2O_3 deposited on SiO_2 depended neither on the surface area nor on the average pore diameter, but depended on the pore volume. The larger the pore volume of support was, the more B_2O_3 could be deposited to give more active catalysts.

Table 2-2 represents the effect of pretreatment of SiO_2 support on the catalytic activity of the resulting B_2O_3/SiO_2. When the calcination temperature was below 600 ^oC, no appreciable influences were observed both on the B_2O_3 content and on the catalytic activity. However, when SiO_2 support was treated at 800 ^oC, the catalyst obtained became less active because of the decrease in surface area, although its B_2O_3 content was as much as 30 wt%. Probably, when calcined at 800 ^oC, the surface hydroxy groups of SiO_2 were irreversibly dehydrated to reduce its surface area.[20]

The pore size distribution of CVD B_2O_3/SiO_2 was measured to study the process of B_2O_3 position on the internal surface of SiO_2 (Fig. 2-5). SiO_2 support had a sharp peak at about 66 Å in addition to a broad peak at between 200 and 500 Å in the pore size distribution. When the B_2O_3 content increased, the broad peak in a larger pore size region got smaller and the sharp peak at 66 Å shifted to a larger size of about 100 Å. At the same time, the pore volume was changed from 1.25 to 0.68 ml/g. Similar tendency of the change in pore size distribution was observed with the impregnation B_2O_3/SiO_2.

Characterization of CVD B_2O_3/SiO_2

Figure 2-6 shows the change in BET surface area of B_2O_3/SiO_2 catalyst with B_2O_3 content. The surface area decreased with increasing B_2O_3 content with respect to both CVD and impregnation

catalysts. The surface area of impregnation B_2O_3/SiO_2 was larger than that of CVD B_2O_3/SiO_2 at any B_2O_3 content. This result implies that there remained more parts of the SiO_2 surface free from B_2O_3 deposition in the case of impregnation catalyst.

Figures 2-7a and b show the SEM images of the external surfaces of impregnation and CVD catalysts, respectively. Large B_2O_3 crystallites (ca. 50 μm) were deposited on the surface of impregnation catalyst. On the other hand, such large B_2O_3 crystallites were hardly observed on the surface of CVD catalyst; the surface was as smooth as that of SiO_2 support itself.

Figure 2-8 illustrates the TPD profiles of the pyridine adsorbed on CVD B_2O_3/SiO_2 catalysts having different B_2O_3 contents. The TPD profile of SiO_2 support showed only a single sharp peak at 100 ^oC, and all the pyridine adsorbed was removed below 150 ^oC. In contrast, the TPD profiles of B_2O_3/SiO_2 catalysts had the desorption maxima between 150 and 250 ^oC. The amount of pyridine desorbed above 250 ^oC increased with B_2O_3 content. These results obviously tell that B_2O_3/SiO_2 catalyst is more acidic than SiO_2 support, and that the amount of strongly acidic sites whose acid strengths correspond to pyridine desorption temperatures above 150 ^oC increased with B_2O_3 content.

The TPD profiles shown in Fig. 2-9 demonstrate the difference in acid property between CVD and impregnation B_2O_3/SiO_2 whose B_2O_3 contents are similar. Compared with the spectra of impregnation catalysts, each pyridine desorption peak on CVD catalyst slightly shifted to the higher temperature side.

Figure 2-10 shows the changes in the differential heat of adsorption of ammonia (DHA) on the most active CVD and impregnation catalysts, together with the data of SiO_2 support. The level of DHA corresponds to the acid strength of B_2O_3/SiO_2 and the adsorbed amount of ammonia means the number of acid sites. The initial value of DHA obtained with SiO_2 support was less than 80 kJ/mol, and the DHA decreased with increasing amount of adsorbed ammonia. The acid strength to catalyze the Beckmann rearrangement is thought to be at least 80 kJ/mol, because SiO_2

support alone had little activity for this reaction. The initial value of DHA on the impregnation catalyst was 110 kJ/mol, and the amount of adsorbed ammonia in the region where the DHA level exceeded 80 kJ/mol was 0.4 mmol/g. As to CVD catalyst, the DHA change was similar to that of impregnation catalyst up to 0.2 mmol/g of adsorbed ammonia, but the total amount of the effective acid sites having DHA values more than 80 kJ/mol was as much as 0.7 mmol/g. Moreover, it should be noted that the DHA curve observed with the CVD catalyst became flat in the range of adsorbed ammonia from 0.3 to 0.6 mmol/g.

Discussion

Deposition of B_2O_3 on SiO_2 through CVD

On the basis of the above experimental observations, the following two schemes in which O_2 participates can be suggested to explain the deposition of B_2O_3 on SiO_2 surface in the process of CVD:

scheme 1 : $B(OEt)_3 \xrightarrow{O_2} B_2O_3 \xrightarrow{SiO_2} B_2O_3/SiO_2$

scheme 2 : $B(OEt)_3 \xrightarrow{SiO_2} \xrightarrow{O_2} B_2O_3/SiO_2$

According to the scheme 1, B_2O_3 is formed by the combustion of $B(OEt)_3$ in the gas phase to be directly deposited on the SiO_2 surface. In the scheme 2, first $B(OEt)_3$ reacts with the hydroxyl groups of SiO_2 surface forming Si-O-B bonds, and then the residual ethoxy groups on boron are oxidized to form surface B-OH groups; B_2O_3 can be deposited on SiO_2 surface through repetition of these surface reactions. If the CVD process proceeds via the scheme 1, a certain B_2O_3 deposition should be observed also on the internal wall of the reactor. The deposition of B_2O_3, however, was never observed on the reactor wall around the SiO_2 bed, and in contrast with the case of CVD using H_2O, no preferential B_2O_3 deposition occurred on the upper side of the

SiO_2 bed. Moreover, it was confirmed that only a trace amount of B_2O_3 (0.8 wt%) was deposited by the CVD of $B(OEt)_3$ in a stream of N_2, but a certain amount of B_2O_3 (4.0 wt%) could be introduced through repetition (18 times) of a pulse procedure which involved the CVD of $B(OEt)_3$ in a stream of N_2 followed by the combustion with air at 350 ^oC. These results suggest that the CVD with O_2 in the present study proceeds substantially via the scheme 2.

When the CVD was performed at 400 ^oC, more B_2O_3 was deposited on the upper side than on the lower side of the SiO_2 bed. This undesirable phenomenon was probably due to an increase in the rate of B_2O_3 deposition at higher temperature. In addition, the SiO_2 particles were adhered each other with B_2O_3 melt at 400 ^oC. At higher temperatures, the reaction via the scheme 1 is possibly predominant.

Catalytic feature of CVD B_2O_3/SiO_2

It is obvious that CVD B_2O_3/SiO_2 is more active and selective than impregnation B_2O_3/SiO_2 (Fig. 2-4). The most active catalyst for the Beckmann rearrangement was obtained through CVD performed at 350 ^oC for 3 h at a $B(OEt)_3$ feed rate of 3.5 mmol/h. The lactam selectivity, however, was dropped when CVD was carried out either at 400 ^oC for 3 h (Fig. 2-2) or at 350 ^oC for more than 3 h (Fig. 2-3). The selectivity drop may be due to the change in acid property of catalyst through high-temperature or long-time operation of CVD which causes melting of a part of B_2O_3 crystallites. In fact, at 400 ^oC, the SiO_2 particles were adhered each other with glassy B_2O_3. In this context, it was confirmed experimentally that B_2O_3 alone without support was quite inactive for the rearrangement reaction (oxime conversion: 4.0 %, lactam selectivity: 26.4 mol% at 300 ^oC), and that after the reaction B_2O_3 particles changed into a glassy melt with a very small surface area. This fact suggests that melting of B_2O_3 is also probably responsible for the decreases both in activity and in selectivity.

The change in BET surface area with B_2O_3 content (Fig. 2-6)

as well as the comparative SEM images of B_2O_3/SiO_2 (Fig. 2-7) clearly suggest that the SiO_2 surface is uniformly covered with B_2O_3 by means of CVD. On the other hand, the present impregnation method involves a step of calcination of the supported H_3BO_3, so that H_3BO_3 is prone to aggregate into large B_2O_3 particles in the course of dehydration leaving the SiO_2 surface free from the accumulation of B_2O_3. Since SiO_2 itself is inactive for the rearrangement reaction and furthermore the exposure of SiO_2 surface is not preferable to enhancement of the lactam selectivity (Fig. 2-4), it is necessary for obtaining an efficient B_2O_3/SiO_2 catalyst to cover the SiO_2 surface with B_2O_3 uniformly and completely as exemplified by a CVD catalyst having a B_2O_3 content of 34 wt%. According to the study on the CVD of B_2O_3 onto alumina using $B(OEt)_3$,[21] a B_2O_3 content between 20 and 25 wt% was enough to cover the alumina surface to give the most active rearrangement catalyst, because the surface area of the alumina was smaller (160 m^2/g) than that of the SiO_2 used in the present study (281 m^2/g).

The result of the measurement of DHA (Fig. 2-10) indicates that the most active CVD B_2O_3/SiO_2 possesses much more effective acid sites whose DHA values are at least 80 kJ/mol, compared with the most active impregnation B_2O_3/SiO_2. Since the maximum DHA values are almost the same for both catalysts, the average acid strength of the CVD catalyst must be greater than that of the impregnation catalyst. This reasoning is in good harmony with a result obtained in the TPD measurement that the pyridine desorption peaks observed with CVD catalysts shifted to the higher temperature side compared with those observed with impregnation catalysts (Fig. 2-9).

It has previously been reported that a DHA value of 76 kJ/mol corresponds to a pKa value of -5.6.[22] According to qualitative measurement of acid strength by use of the Hammett indicators, both CVD and impregnation B_2O_3/SiO_2 could change Benzalacetophenone (pKa = -5.6) into its acidic color, but SiO_2 could change only Dimethyl Yellow (pKa = +3.3). Since SiO_2

support itself (DHA < 80 kJ/mol) is inactive for the Beckmann rearrangement, it can be deduced that the acid sites of B_2O_3/SiO_2 whose acid strengths are less than -5.6 in terms of H_o should be responsible for catalyzing the rearrangement reaction. In addition, the acid strength of CVD B_2O_3/SiO_2 was found reasonably uniform, judging from the flatness of DHA curve.

In conclusion, higher catalytic activity and selectivity of CVD B_2O_3/SiO_2 for the Beckmann rearrangement in comparison with impregnation B_2O_3/SiO_2 should be attributed to a larger amount of effective acid sites in addition to more uniform acid strength. Such favorable acid property was obtained through uniform deposition of B_2O_3 by means of CVD.

References

1. W. Davydoff, *Chem. Tech.*, **7** (1955) 647.
2. L. Werke, *East German P.*, 10920 (1955).
3. BASF, *Ger. P.*, 1227028 (1967).
4. Bayer, *Japan Kokai*, 1978-37686.
5. Bayer, *Fr. P.*, 1547240 (1968).
6. Y. Izumi, S. Sato, and K. Urabe, *Chem. Lett.*, **1983**, 1649.
7. British Petroleum, *Brit. P.*, 881927 (1961).
8. T. Yashima, S. Horie, S. Saito, and N. Hara, *Nippon Kagaku Kaishi*, **1977**, 77.
9. Y. Murakami, Y. Seki, and K. Ito, *Nippon Kagaku Kaishi*, **1978**, 21.
10. P. S. Landis and P. B. Venuto, *J. Catal.*, **6**, (1966) 245.
11. Mobil Oil Corp., *Neth. Appl.*, 6514009 (1966).
12. A. Aucejo, M. C. Burguet, A. Corma, and V. Fornes, *Appl. Catal.*, **22**, (1986) 187.
13. H. Sato, N. Ishii, K. Hirose, and S. Nakamura, *Stud. Surf. Sci. Catal.*, **28**, (1986) 755.
14. H. Sato, K. Hirose, M. Kitamura, and S. Nakamura, *Stud. Surf. Sci. Catal.*, **49**, (1989) 1213.
15. H. Sato, K. Hirose, and M. Kitamura, *Nippon Kagaku Kaishi*, **1989**, 548.
16. T. Takahashi, K. Ueno, and T. Kai, *Shokubai (Catalyst)*, **31**, (1989) 365.

17. J. D. Butler and T. C. Poles, *J. Chem. Soc., Perkin Trans. 2*, **1973**, 41.
18. C. V. Hidalgo, M. Kato, T. Hattori, M. Niwa, and Y. Murakami, *Zeolite*, **4** (1984) 175.
19. M. Niwa, S. Kato, T. Hattori, and Y. Murakami, *J. Chem. Soc., Faraday Trans. 1*, **80** (1984) 3135.
20. G. J. Young, *J. Colloid Sci.*, **13** (1958) 67.
21. H. Sakurai, S. Sato, K. Urabe, and Y. Izumi, *Chem. Lett.*, **1985**, 1783.
22. H. Taniguchi, T. Masuda, K. Tsutsumi, and H. Takahashi, *Bull. Chem. Soc. Jpn.*, **51** (1978) 1970.

Table 2-1

The effect of physical property of SiO_2 support

Physical property of SiO_2			CVD B_2O_3/SiO_2		
SA (m^2/g)	PD (Å)	PV (ml/g)	B_2O_3 content (wt%)	oxime conversion (%)	lactam selectivity (mol%)
281	192	1.35	34	98.6	96.4
70	583	1.02	32	66.3	94.0
585	51	0.86	15	69.6	91.0
115	223	0.64	29	47.1	95.0
347	93	0.81	41	37.7	97.1
649	36	0.59	7.2	22.3	58.5
166	140	0.58	2.0	11.1	35.6

SA, specific surface area; PD, average pore diameter;
PV, pore volume; these values were given by the suppliers.
CVD conditions: $B(OEt)_3$, 3.5 mmol/h; air, 115 ml/min; at 350 ^oC for 3 h. Average conversion of 3 - 4 h at 250 ^oC.

Table 2-2

The effect of calcination of SiO_2 support

Calcination temperature of SiO_2[a] (^oC)	CVD B_2O_3/SiO_2 catalyst			
	B_2O_3 content[c] (wt%)	BET surface area (m^2/g)	oxime conversion (%)	lactam selectivity (mol%)
350[b]	34	135	98.6	96.4
450	30	-	94.9	95.4
600	28	-	95.8	97.0
800	30	85.4	72.4	96.8

a, Calcination 3h; b, calcination 1h;

c, CVD conditions: $B(OEt)_3$ feed, 3.5mmol/h; air, 115ml/min; at 350 ^oC for 3 h.

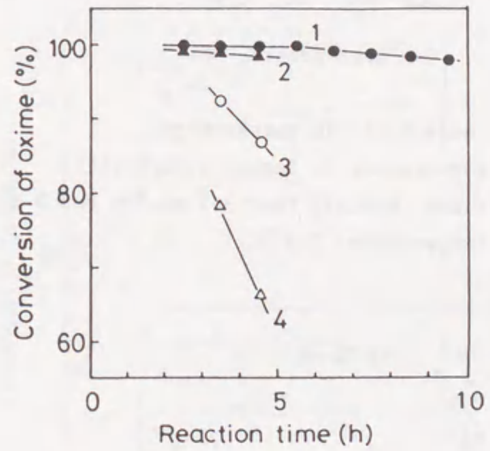

Fig. 2-1. The change in catalytic activity of B_2O_3/SiO_2 with the time on stream.
1, CVD B_2O_3/SiO_2 (B_2O_3 32 wt%); 2, impregnation B_2O_3/SiO_2 (B_2O_3 26 wt%); reaction temperature, 300 ^oC;
3, CVD B_2O_3/SiO_2 (B_2O_3 25 wt%); 4, impregnation B_2O_3/SiO_2 (B_2O_3 19 wt%); reaction temperature, 250 ^oC.

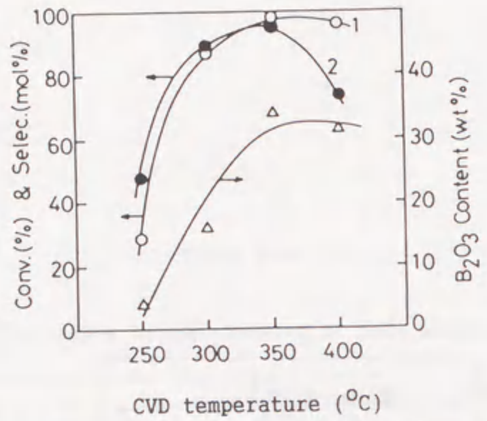

Fig. 2-2. The effect of CVD temperature.
1, oxime conversion; 2, lactam selectivity;
CVD conditions, $B(OEt)_3$ feed 3.5 mmol/h for 3 h;
reaction temperature, 250 ^oC.

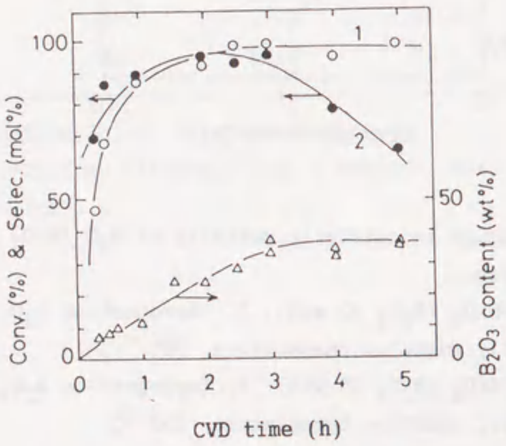

Fig. 2-3. The effect of CVD time.
1, oxime conversion; 2, lactam selectivity;
CVD temperature, 350 ^oC; $B(OEt)_3$ feed rate, 3.5 mmol/h;
reaction temperature, 250 ^oC.

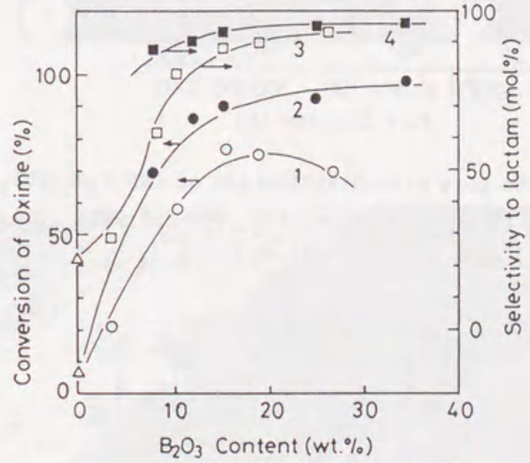

Fig. 2-4. The effect of B_2O_3 content at 250 ^oC.
1, oxime conversion of impregnation B_2O_3/SiO_2;
2, oxime conversion of CVD B_2O_3/SiO_2;
3, lactam selectivity of impregnation B_2O_3/SiO_2;
4, lactam selectivity of CVD B_2O_3/SiO_2.

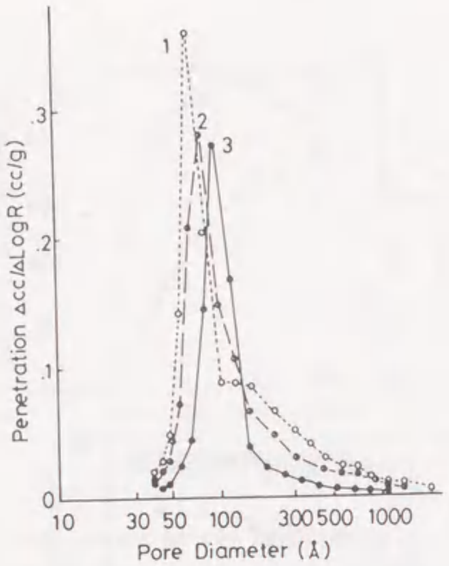

Fig. 2-5. The pore size distribution of CVD B_2O_3/SiO_2.
1, SiO_2 support; 2, B_2O_3/SiO_2 (B_2O_3 15 wt%);
3, B_2O_3/SiO_2 (B_2O_3 34 wt%).

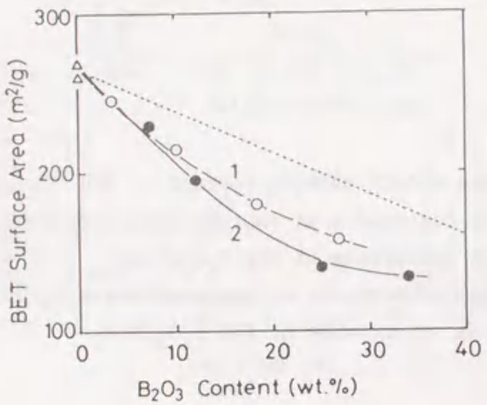

Fig. 2-6. The change in BET surface area.
1, impregnation B_2O_3/SiO_2; 2, CVD B_2O_3/SiO_2;
Dotted line denotes the surface area of SiO_2 alone calculated from the amount of silica support in a unit weight of catalyst.

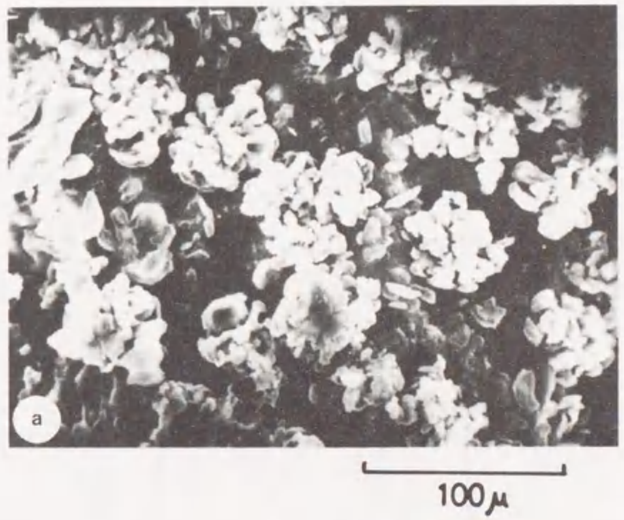

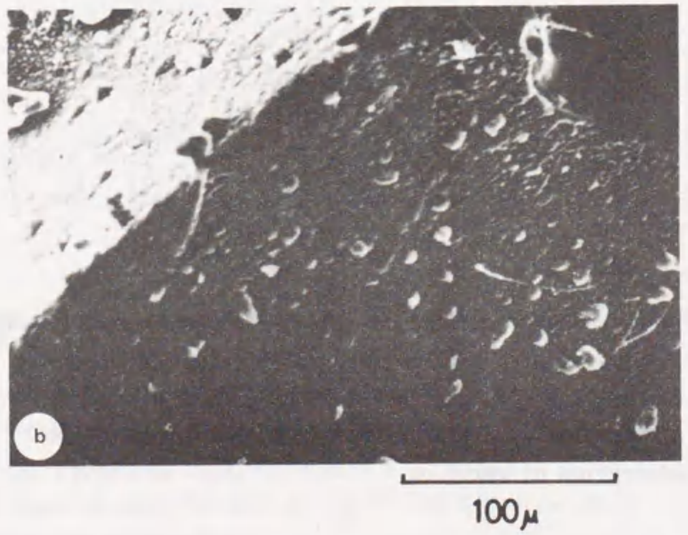

Fig. 2-7. The SEM images of B_2O_3/SiO_2 external surfaces.
a, impregnation B_2O_3/SiO_2 (B_2O_3 19 wt%);
b, CVD B_2O_3/SiO_2 (B_2O_3 34 wt%).

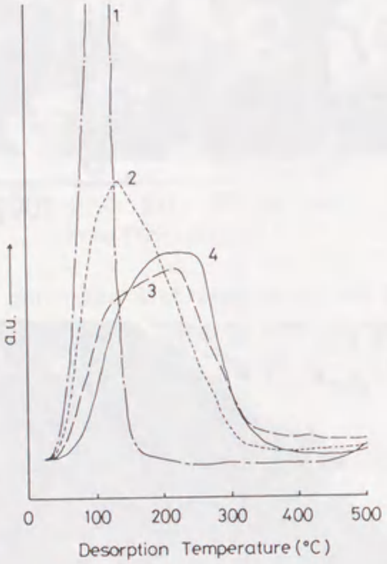

Fig. 2-8. The TPD profiles of pyridine adsorbed on CVD B_2O_3/SiO_2.
1, SiO_2 support; 2, B_2O_3/SiO_2 (B_2O_3 10 wt%);
3, B_2O_3/SiO_2 (B_2O_3 22 wt%); 4, B_2O_3/SiO_2 (B_2O_3 33 wt%);
all samples were treated at 400 ^{o}C for 1 h prior to
adsorption of pyridine.

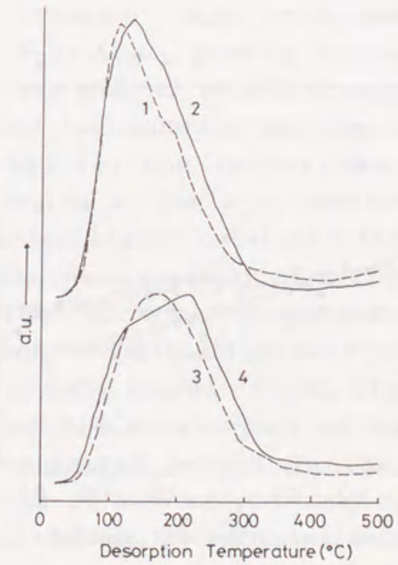

Fig. 2-9. Comparative TPD profiles of CVD and impregnation B_2O_3/SiO_2.
1, impregnation B_2O_3/SiO_2 (B_2O_3 8.0 wt%);
2, CVD B_2O_3/SiO_2 (B_2O_3 10 wt%);
3, impregnation B_2O_3/SiO_2 (B_2O_3 27 wt%);
4, CVD B_2O_3/SiO_2 (B_2O_3 22 wt%);
all samples were treated at 400 ^{o}C for 1 h prior to
adsorption of pyridine.

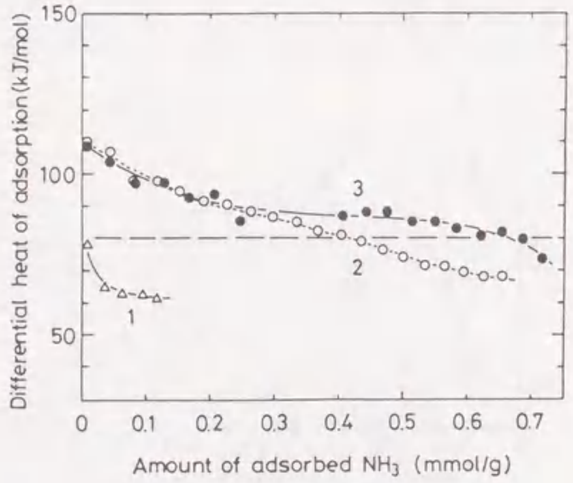

Fig. 2-10. The change in the differential heat of adsorption of ammonia.
1, SiO_2 support; 2, impregnation B_2O_3/SiO_2 (B_2O_3 17 wt%); 3, CVD B_2O_3/SiO_2 (B_2O_3 34 wt%); all samples were treated at 400 ^oC for 1 h prior to adsorption of ammonia.

2-2 Alumina-Supported Boria Catalyst

Abstract

Alumina-supported boria (B_2O_3/Al_2O_3) catalysts were prepared by CVD technique using ethyl borate in the presence of oxygen under atmospheric pressure. Both acidic and catalytic properties of the resulting B_2O_3/Al_2O_3 greatly changed with B_2O_3 content. At B_2O_3 contents less than 12 wt%, both boria-alumina ($H_o \geq -8.2$) obtained by CVD and impregnation methods showed almost the same catalytic activity for the isomerization of m-xylene. In contrast to the region at low B_2O_3 content, the CVD B_2O_3/Al_2O_3 ($H_o \geq -3.0$) exhibited higher catalytic efficiency, e.g. for the vapor-phase Beckmann rearrangement of cyclohexanone oxime at B_2O_3 contents higher than 15 wt%. In particular, complete oxime conversion and high ε-caprolactam selectivity (95 - 98 mol%) were obtained at a B_2O_3 content of 25 wt% at 300 ^oC. The CVD B_2O_3/Al_2O_3 excelled the counterpart obtained by means of the conventional impregnation method in the selectivity to the lactam. The results of microscopic observation and surface area measurement suggested that the high lactam selectivity of the CVD catalyst was probably due to uniform dispersion of B_2O_3 onto alumina which was effected by a procedure of CVD.

Introduction

The author has attempted to prepare solid acid catalysts by loading silica with acidic metal oxides through CVD technique. Such an attempt is based on an idea that CVD may produce more uniform load of oxide species on support than the conventional impregnation method and may yield more active and selective solid acid catalysts. In the previous section, it was illustrated that the silica-supported boria obtained by bringing ethyl borate

vapor into contact with silica gel in the presence of oxygen exhibited higher catalytic efficiency for the vapor-phase Beckmann rearrangement of cyclohexanone oxime, in comparison with the counterparts prepared by means of impregnation of boric acid.[1,2] In this connection, effective solid acids for this rearrangement reaction have long been expected to be developed in order to replace the conventional sulfuric acid process by a catalytic process.

Boria-alumina is also well known to be a solid acid which catalyzes the Beckmann rearrangement of cyclohexanone oxime[3-5] and the hydrocarbon conversion reactions such as toluene disproportionation and xylene isomerization.[6] Boria-alumina is usually obtained by impregnating an alumina with aqueous boric acid followed by calcination. For the vapor-phase Beckmann rearrangement, there is still plenty of room for improvement particularly in the selectivity to ε-caprolactam.

This section deals with the alumina-supported boria prepared through CVD technique. The preparative conditions for CVD B_2O_3/Al_2O_3 and its catalytic efficiency both for the isomerization of m-xylene and for the vapor-phase Beckmann rearrangement of cyclohexanone oxime were examined in detail in comparison with the boria-alumina obtained by the conventional impregnation method.

Experimental

Catalysts. The CVD boria-alumina (abbreviated as CVD B_2O_3/Al_2O_3(1)) was prepared in a 15 mm-i.d. fixed-bed reactor, as shown in Fig. 1-2. It was prepared by bringing triethylborate ($B(OEt)_3$) vapor into contact with an alumina (JRC,[7] ALO-1, 0.5 g, surface area 160 m^2/g, pore volume 0.67 ml/g, 24 - 60 mesh granules) at 300 °C for 0.5 - 5.0 h in the presence of air; the flow rates of $B(OEt)_3$ and air were 3.5 mmol/h and 113 ml/min, respectively.

The CVD B_2O_3/Al_2O_3(2) catalyst was prepared by rotary CVD

reactor, as shown in Fig. 1-3. An alumina (Shokubai Kasei, ACBM, 1.0 g, surface area 210 m^2/g, pore volume 1.0 ml/g, 24 - 60 mesh granules) was placed in a 27 mm-i.d. Pyrex glass reactor which inclined by 45° from the vertical. $B(OEt)_3$ vapor was brought into contact with the support at a constant temperature between 200 and 350 °C for 1 - 10 h in a stream of dry air under atmospheric pressure while the reactor was rotated at revolution rate of 80 rpm. The flow rates of $B(OEt)_3$ and air were 3.5 mmol/h and 115 ml/min, respectively.

The impregnation (IMP) catalyst was obtained by the conventional impregnation method; the respective alumina support was immersed in aqueous boric acid then followed by calcination at 300 or 350 °C for 3 h. The B_2O_3 content of catalyst was determined by the alkalimetric titration of the boric acid that was extracted from catalyst with hot water using mannitol. The IMP boria-alumina catalyst was calcined at 300 °C for 2 h prior to the use in the Beckmann rearrangement of cyclohexanone oxime, and both CVD and IMP boria-aluminas were pretreated at 500 °C for 3 h in the isomerization of m-xylene.

Catalytic tests. The isomerization of m-xylene was performed at 450 °C in a flow apparatus, which was equipped with a 15 mm-i.d. Pyrex glass reactor containing 0.2 g of catalyst, at a WHSV of 2.6 h^{-1} in terms of the m-xylene fed. The reactor effluent was collected in a trap and analyzed by GLC using a column of Bentone 34 + DNP (4 m). An activity declining owing to coking was observed for every catalyst tested, and hence the catalytic efficiency was evaluated on the basis of the initial average conversion and selectivity at 0 - 2 h after the feed of reactant was initiated.

The vapor-phase Beckmann rearrangement of cyclohexanone oxime was carried out under atmospheric pressure in an ordinary flow system. A mixture of the oxime, benzene as a diluent and N_2 was passed through the catalyst bed in a mole ratio of 1:13:16 at a WHSV of 0.81 h^{-1} based on the oxime fed. The reactor effluent was analyzed by off-line GLC using a PEG 20M column (1 m). In

order to evaluate the catalytic efficiency, some of the reaction runs for the vapor-phase Beckmann rearrangement were performed at a relatively lower temperature of 250 ^{o}C to keep the oxime conversion level below 50 %. Since the oxime conversion decreased with the time on stream owing to coke formation, the average values of oxime conversion and lactam selectivity obtained at 250 ^{o}C between 3 - 4 h after the reactant feed were taken as the standard data: mass balance was not completed during the initial 3 h of each run at this reaction temperature. The major by-products included hex-5-enenitrile and cyclohexanone.

Sample characterization. The desorption spectra of the pyridine adsorbed on boria-alumina catalysts were measured by use of a conventional TPD apparatus combined with a thermal conductivity detector. A catalyst sample (30 mg) was preheated in a TPD cell at 400 ^{o}C for 1 h in a stream of helium. Pyridine (10 μl) was injected at 300 ^{o}C, and the cell was cooled rapidly to 25 ^{o}C. The TPD measurement was done at a heating rate of 10 ^{o}C/min using helium as a carrier gas (115 ml/min).

The microscopic examination on the supported B_2O_3 was performed by use of a JEOL JSM-T20 instrument. The sample was used for the measurement without further heat treatment.

Results and Discussion

Effect of CVD conditions on the B_2O_3 content of catalyst

With respect to the catalyst preparation using a rotary-type CVD reactor, the amount of B_2O_3 to be supported greatly depended on both CVD temperature and time (Figs. 2-11 and 2-12). The B_2O_3 content increased with increasing CVD temperature until 250 ^{o}C, and then leveled off at 25 wt% which signified that 76 % of the total feed of $B(OEt)_3$ was supported as B_2O_3. The amount of B_2O_3 deposited on alumina, however, increased monotonously with CVD time at 250 ^{o}C, and a higher B_2O_3 content of 35 wt% attained for 7 h (Fig. 2-12). At a low temperature of 225 ^{o}C, the B_2O_3 content also increased with CVD time.

The deposition of B_2O_3 on alumina presumably proceeds via a surface reaction between $B(OEt)_3$ and the hydroxy groups of alumina followed by the combustion of the organic moieties of the immobilized borate with oxygen, not via the simple accumulation of the B_2O_3 liberated beforehand through oxidation or hydrolysis of $B(OEt)_3$ in the gas phase above the support zone, because such liberated B_2O_3 neither deposited on the wall near the support bed nor accumulated among the catalyst particles obtained.

Meager loading of B_2O_3 observed at a CVD temperatures below 250 ^{o}C indicates that such low CVD temperatures are insufficient to activate the surface reaction between $B(OEt)_3$ and the hydroxy groups of alumina. Even at a low temperature of 225 ^{o}C, however, a B_2O_3 content of 25 wt% could be attained through CVD of longer operation such as 10 h, although only 30 % of the borate fed converted into B_2O_3. Thus the B_2O_3 content can be adjusted to a required level either by regulating CVD temperature from 200 to 250 ^{o}C or by changing the CVD time. When CVD temperature exceeded 325 ^{o}C, the resulting catalyst turned dark owing to coke formation probably through undesirable conversion of the organic moieties of borate, and its particles became to adhere each other owing to partial melting of the supported B_2O_3. Preferable CVD temperature, therefore, lies between 225 and 300 ^{o}C.

The deposition behavior in the fixed-bed CVD reactor resembles that in the rotary-type CVD reactor. The differences will be discussed in detail in chapter 5.

Catalytic efficiency for the isomerization of m-xylene

Figure 2-13 illustrates the catalytic performance of CVD B_2O_3/Al_2O_3(1) in the isomerization of m-xylene. A maximum conversion was attained at a B_2O_3 content of 12 wt% for both CVD and IMP boria-alumina. Furthermore, both CVD and IMP boria-alumina were almost the same in catalytic efficiency at a B_2O_3 content of less than 12 wt%: conversion of m-xylene, selectivity to xylene isomers (85 - 93 mol%) and ratio of product p-/o-xylene (1.1 - 1.3).

The same catalytic behavior of CVD and IMP boria-alumina observed in the isomerization reaction can reasonably be explained by assuming that, until B_2O_3 content does not exceed 12 wt%, all of the B_2O_3 introduced form a surface compound by reacting with alumina independent of the preparation method to develop the strong Brønsted acid sites which can effectively catalyze the isomerization.[6,8] The isomerization of xylene which needs strong acidity was catalyzed most efficiently by a B_2O_3/Al_2O_3 having a B_2O_3 content of 12 wt% whose maximum acid strength (H_o) lay between -5.6 and -8.2.

Catalytic efficiency for the Beckmann rearrangement

In contrast to m-xylene isomerization, the Beckmann rearrangement of cyclohexanone oxime was effectively catalyzed at higher B_2O_3 content (Figs. 2-14 and 2-15). For an alumina support (ALO-1), the CVD B_2O_3/Al_2O_3(1) exhibited higher efficiency than the IMP B_2O_3/Al_2O_3 in catalyzing the Beckmann rearrangement at B_2O_3 content of more than 15 wt% (Fig. 2-14). Furthermore, for another alumina support (ACBM), Fig. 2-15 denotes the effect of B_2O_3 content on the oxime conversion and the lactam selectivity for the CVD B_2O_3/Al_2O_3(2) catalysts prepared in the rotary-type CVD reactor. The levels of oxime conversion obtained with both CVD and IMP boria-alumina were almost similar, and each maximum conversion appeared at a B_2O_3 content between 20 and 25 wt%. It should, however, be noted that the CVD catalyst unambiguously showed higher lactam selectivity than the impregnation catalyst at a B_2O_3 content above 15 wt%.

This difference in lactam selectivity (ca. 10 %) is really significant from the practical viewpoint. Similar tendency of the changes in conversion and selectivity with B_2O_3 content was observed also with other CVD and IMP boria-alumina prepared from different alumina supports (JRC,[7] ALO-1, and ALO-3) which had smaller surface areas (160 and 123 m^2/g, respectively), except for their lower oxime conversions than those of the present support (ACBM, 210 m^2/g) given in Fig. 2-15. In addition, for a

silica support with high surface area (281 m^2/g) described in section 2-1, much larger B_2O_3 content (34 wt%) was needed to catalyze effectively the rearrangement reaction. In each case of the above four supports, an effective B_2O_3 surface density is in a region between 1.6 and 2.0 mg/m^2, which corresponds to the number of surface boron atom from 28 to 35 nm^{-2}. The order in the catalytic activity for the rearrangement reaction is proportional to the surface area of support.

In contrast to the region of low B_2O_3 content, at a B_2O_3 content of more than 15 wt%, the acid sites of free B_2O_3 which can selectively catalyze the rearrangement reaction become to dominate over the strong Brønsted acid sites, and the optimum B_2O_3 content to effect the most active and selective Beckmann rearrangement occurred between 20 and 25 wt% at which the maximum acid strength (H_o) became as low as -3.0 which represents the acid strength inherent to B_2O_3. It was confirmed by XRD measurement that the characteristic diffraction lines of B_2O_3 appeared at $2\theta = 14.5^o$ and 28.0^o when B_2O_3 content exceeded about 20 wt%. The acid property of B_2O_3/Al_2O_3 remarkably changed with B_2O_3 content.

These results obviously suggest that B_2O_3 itself, not a surface mixed oxide of alumina-boria formed at lower B_2O_3 loading, is responsible for catalyzing the selective rearrangement reaction. CVD B_2O_3/Al_2O_3 showed quite the same catalytic behavior as IMP boria-alumina so long as B_2O_3 content remained below 12 wt%, because at such lower B_2O_3 loading the surface mixed oxide of alumina-boria with strong acidity were first formed in the similar manner with respect to both IMP and CVD catalysts. Such strong acid sites accelerate the conversion of the lactam into hex-5-enenitrile as well as the decomposition of the oxime into cyclohexanone. On the other hand, at higher B_2O_3 loading the surface mixed oxide species become to be covered with free B_2O_3 which is responsible for selective reaction, and both the oxime conversion and the lactam selectivity increase. In this region including high B_2O_3 content, the CVD technique can

effect more uniform deposition of B_2O_3 to produce more selective catalysts (vide infra), leaving less amount of the undesirable strong acid sites.

In contrast to the CVD technique, IMP method was inadequate to give the boria-alumina having a high B_2O_3 content of more than 15 wt%, because large crystals of boric acid were deposited on the surface of alumina in the process of impregnation. This is caused by the poor solubility of boric acid in water.

Effect of reaction temperature on catalytic efficiency

In order to enhance oxime conversion, the rearrangement reaction was performed at higher temperatures over a CVD catalyst having a B_2O_3 content of 28 wt% (Fig. 2-16). The conversion increased with increasing reaction temperature and the complete conversion was attained at 350 ^oC still holding a high selectivity of 95 mol%. The lactam selectivity, however, began to decrease above 350 ^oC. Since the heat treatment of catalyst up to 500 ^oC prior to use for the reaction caused neither the decline in selectivity nor the vaporization of B_2O_3 from the support, the rapid decrease in lactam selectivity observed above 350 ^oC is not due to the change in acid property of catalyst but undoubtedly due to the rise of the side reactions.

Change in catalytic efficiency with time on stream

Figure 2-17 illustrates the changes in oxime conversion and lactam selectivity with the time on stream at 300 ^oC over the most active CVD and IMP boria-alumina having the same B_2O_3 content of 25 wt%. The CVD $B_2O_3/Al_2O_3(2)$ served for this experiment was prepared through CVD at 225 ^oC for 10 h followed by calcination at 300 ^oC for 3 h.

For the IMP boria-alumina catalyst, the oxime conversion already began to decline owing to coke formation at a time on stream of 3 h. On the other hand, over the CVD $B_2O_3/Al_2O_3(2)$ the complete oxime conversion was maintained until 6 h. Concerning the lactam selectivity, it should be noted that the CVD

B_2O_3/Al_2O_3 always exhibited higher levels by 5 to 10 % than the IMP boria-alumina during 10 h on-stream.

According to a preliminary examination on the regeneration of the used catalyst by burning off the coke with air at 500 ^oC for 3 h, it was confirmed that the oxime conversion was completely recovered but the lactam selectivity remained at the level prior to regeneration as to both CVD and IMP boria-alumina. Since the coke could not be completely removed under the present regeneration condition, an optimum condition should be further explored. In addition, it was found that the regeneration temperature should be below 600 ^oC, because about 20 % of the supported B_2O_3 was lost through vaporization during the regeneration operated above 600 ^oC.

Characterization of CVD boria-alumina catalyst

The higher lactam selectivity observed over the CVD boria-alumina strongly suggests that the morphology of the active species B_2O_3 supported on alumina may be considerably different between CVD and IMP boria-alumina. Indeed, the SEM images of both catalysts shown in Fig. 2-18 represent that the B_2O_3 of IMP catalyst is supported as large crystallites of about 10 μm size in average at a B_2O_3 content of 25 wt%, while such aggregation of B_2O_3 is scarcely observed on the surface of the CVD catalyst at the same B_2O_3 content: the appearance of the surface of the CVD catalyst was quite similar to that of alumina support itself without aggregation of B_2O_3. The result of the SEM observation clearly indicates that B_2O_3 could be uniformly supported on the surface of alumina through CVD technique. The XRD patterns of both CVD and IMP boria-alumina showed two distinct diffraction lines (2θ = 14^o and 28^o) assigned to B_2O_3 crystal, provided its content exceeded 20 wt%. This result of XRD is consistent with the above mentioned suggestion that the effective catalyst species should be the supported B_2O_3 crystallites, because the maximum oxime conversion and the highest lactam selectivity were actually obtainable at a B_2O_3 content above 20 wt% (Fig. 2-15).

Figure 2-19 illustrates the change in BET surface area of catalyst with B_2O_3 content. In both cases of CVD and IMP boria-alumina, the surface area decreased monotonously with increasing B_2O_3 content because of plugging of the micropores of alumina with B_2O_3 in addition to the relative decrease in alumina content of catalyst (dotted line). It should, however, be pointed out that the surface area of CVD B_2O_3/Al_2O_3(2) decreased more rapidly. Probably the micropores of alumina were filled up with B_2O_3 much more uniformly than in the case of IMP boria-alumina in which B_2O_3 the result of surface area measurement endorses uniform dispersion of B_2O_3 by CVD technique.

In order to examine the difference in acid property between CVD and impregnation catalysts, the desorption spectra of adsorbed pyridine were measured. The TPD spectra obtained with both catalysts were quite similar, each showing a single desorption maximum at around 230 ^{o}C. In addition, no appreciable difference in acid amount was observed between them.

It is, therefore, concluded that the higher lactam selectivity obtained over CVD catalyst is probably due to the uniformity in acid strength produced by uniform dispersion of B_2O_3 onto alumina support.

References

1. S. Sato, H. Sakurai, K. Urabe and Y. Izumi, *Chem. Lett.*, **1985**, 277.
2. S. Sato, K. Urabe, and Y. Izumi, *J. Catal.*, **102**, 99 (1986).
3. V. Davydoff, *Chem. Tech.*, **7**, 647 (1955); C.A., 50:10678d (1956).
4. L. Werke, *East German P.*, 10920 (1955).
5. BASF, *Ger. Patent*, 1,227,028 (1967).
6. Y. Izumi and T. Shiba, *Bull. Chem. Soc. Jpn.*, **37** (1964) 1797.
7. A reference catalyst of the Catalysis Society of Japan (JRC).
8. T. Kaji, N. Yamazoe, and T. Shimizu, *Nippon Kagaku Zasshi*, **1974**, 320.

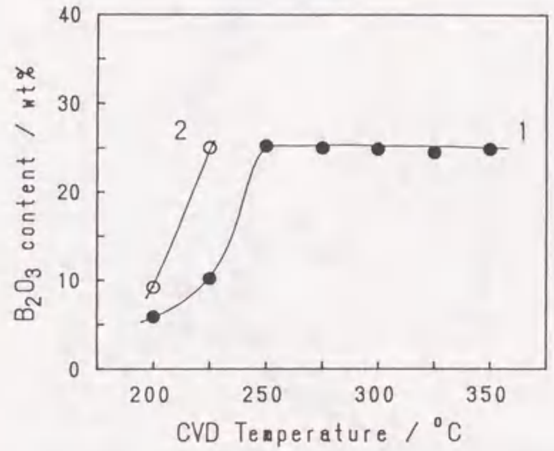

Fig. 2-11. Effect of CVD temperature on B_2O_3 content; Flow rate of $B(OEt)_3$, 3.5 mmol/h; air, 115 ml/min; CVD time: 1, 4 h; 2, 10 h.

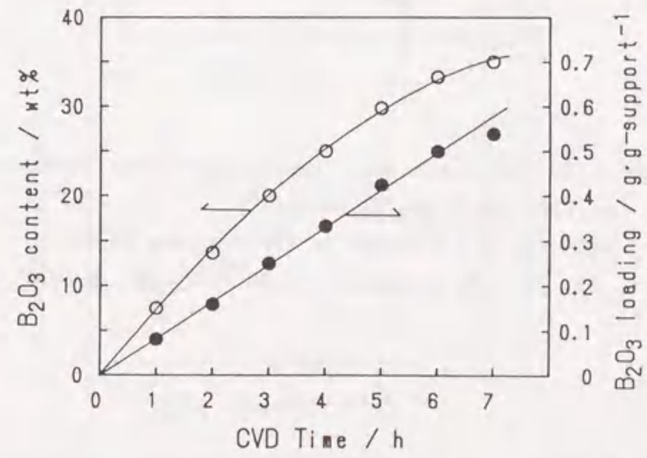

Fig. 2-12. Effect of CVD time on B_2O_3 content at 250 ^{o}C; Flow rate of $B(OEt)_3$, 3.5 mmol/h; air, 115 ml/min.

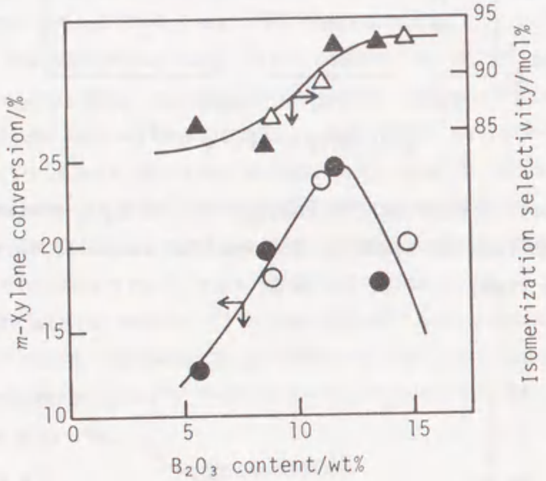

Fig. 2-13. Catalytic activities for m-Xylene isomerization of CVD B_2O_3/Al_2O_3(1) at 450 ^{o}C.
WHSV = 2.6 h^{-1} (based on the m-xylene fed);
○, △: CVD (prepared at 300 ^{o}C); ●, ▲: IMP.

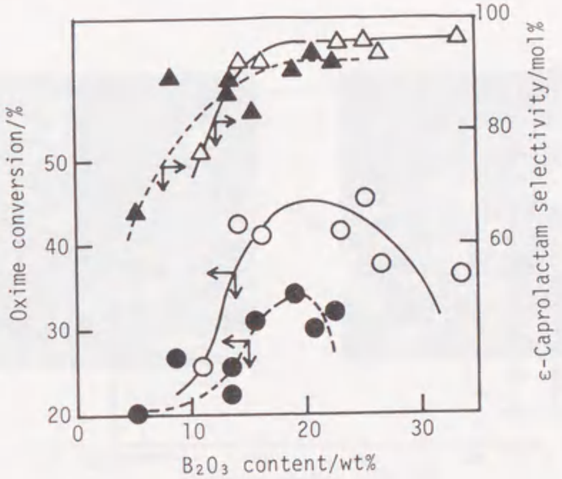

Fig. 2-14. Catalytic activities for Beckmann rearrangement of CVD B_2O_3/Al_2O_3(1) at 250 ^{o}C. oxime:benzene:nitrogen = 1:13:16;
WHSV = 0.81 h^{-1} (based on the oxime fed);
Symbols as those in Fig. 2-13.

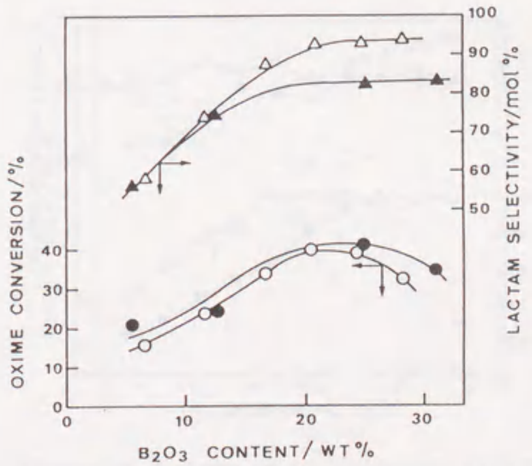

Fig. 2-15. Catalytic activities for Beckmann rearrangement of CVD B_2O_3/Al_2O_3(2) at 250 ^{o}C.
Symbols as those in Fig. 2-13.

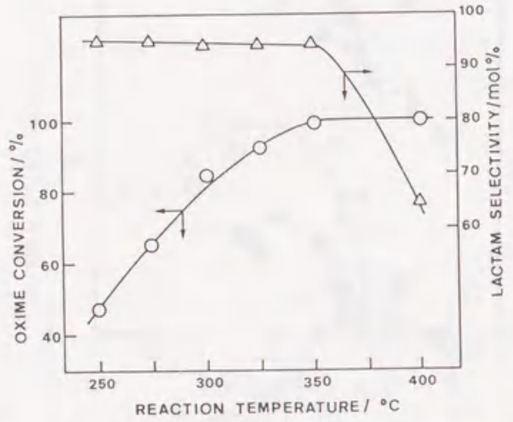

Fig. 2-16. Effect of reaction temperature on catalytic efficiency over CVD B_2O_3/Al_2O_3(2) (B_2O_3 28 wt%, CVD temperature 300 ^{o}C).

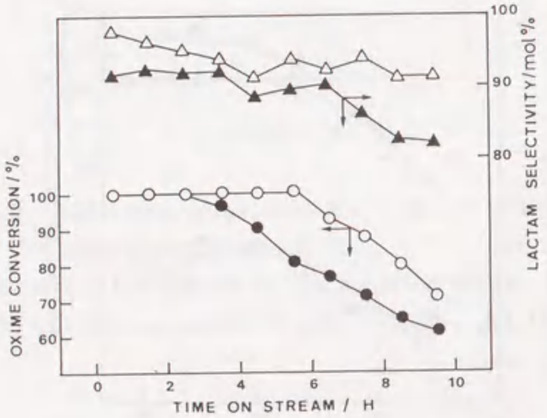

Fig. 2-17. Change in catalytic efficiency with time on stream over CVD B_2O_3/Al_2O_3(2) and IMP boria-alumina (B_2O_3 25 wt%).
Reaction temperature, 300 ^{o}C.
Symbols as those in Fig. 2-13.

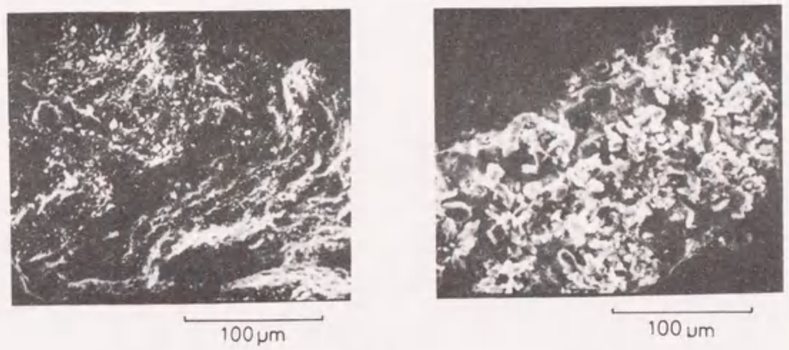

CVD B_2O_3/Al_2O_3 IMP B_2O_3/Al_2O_3

Fig. 2-18. SEM images of CVD and IMP boria-alumina catalysts. B_2O_3 content, 25 wt%; a, CVD B_2O_3/Al_2O_3(2) prepared at 225 ^{o}C for 10 h; b, IMP boria-alumina.

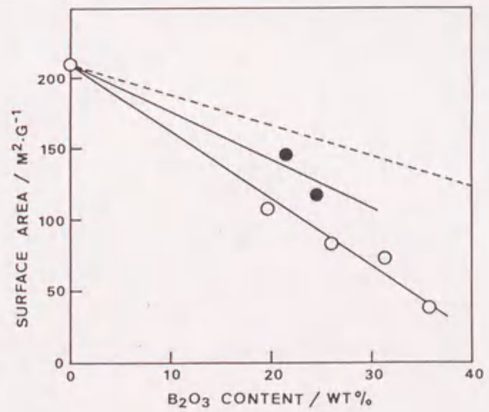

Fig. 2-19. Change in surface area of catalyst with B_2O_3 content. ○, CVD B_2O_3/Al_2O_3(2) (CVD 250 ^{o}C); ●, IMP catalyst; ---, change in surface area with relative decrease in alumina content.

Chapter 3. Deposition of Silica

3-1 Alumina-Supported Silica Catalyst

Abstract

Attempts were made to prepare a supported type of silica-alumina by depositing silica on an alumina surface by chemical vapor deposition (CVD). Silica loading was affected by CVD temperature, time, and reaction atmosphere. Silica was effectively and uniformly deposited on alumina using tetraethoxysilane at 240 ^{o}C in the presence of oxygen. The resulting silica-alumina (CVD SiO_2/Al_2O_3) exhibited high catalytic activities for several types of organic reactions such as 2-butanol dehydration, m-xylene isomerization, 1-butene isomerization, cumene cracking, and n-heptane cracking. The catalytic activities of CVD SiO_2/Al_2O_3 varied with silica loading, attaining maximum conversions for the respective reactions at different silica loadings. They were comparable to those of commercial silica-alumina catalysts; particularly, for the isomerization of 1-butene, the catalytic activity of CVD SiO_2/Al_2O_3 was four times higher than that of the commercial silica-alumina. In addition, the catalytic activities of CVD SiO_2/Al_2O_3 prepared under different conditions differed from each other even at the same silica content.

Introduction

The chemical vapor deposition (CVD) of metal oxides on various inorganic substrates using metal alkoxides has recently been applied to preparation of catalyst and to control of the pore-opening size of zeolites. Niwa and co-workers[1,2] reported that the pore-opening sizes of mordenite and ZSM-5 zeolite were

finely controlled through a CVD process using tetramethoxysilane. These modified zeolites, when used as catalysts, caused a shift to smaller molecules in the hydrocarbon product distribution in methanol conversion. Okuhara and White[3] prepared a thin film of silica on oxide substrates such as ZrO_2, TiO_2, MgO, SiO_2, and Al_2O_3 using tetraethoxysilane under reduced pressure. In the previous chapter, the author described that silica-supported boria catalyst prepared by CVD using boron triethoxide in the presence of oxygen exhibited excellent catalytic efficiencies for the vapor-phase Beckmann rearrangement of cyclohexanone oxime.[4,5]

Amorphous silica-aluminas have usually been prepared by wet methods such as cogelation, coprecipitation,[6] impregnation,[7] and ion-exchange.[8] The author attempted to prepare a supported type of silica-alumina by depositing silica on alumina. In this section, the CVD conditions in the preparation of silica-alumina were investigated in detail, and the catalytic properties of the resulting CVD SiO_2/Al_2O_3 catalysts were examined for various organic reactions such as 2-butanol dehydration, m-xylene isomerization, 1-butene isomerization, cumene cracking, and n-heptane cracking, comparing with commercial silica-alumina catalysts.

Experimental

Catalysts. CVD apparatus for catalyst preparation is shown in Fig. 1-3. The CVD reactor consisted of a Pyrex glass column rotating in an electrical furnace inclined at 45°. An alumina support with a specific surface area of 203 m^2/g, a pore volume of 0.72 ml/g, and a granule size of 24-60 mesh was supplied by Dia Catalyst & Chemicals Ltd. (DC-2282). The alumina support (1.0 g) was placed on a bed fixed with a glass-wool and glass beads in a CVD reactor. After the alumina had been pretreated under the same temperature as in the CVD process for 1 h, tetraethoxysilane vapor was brought into contact with the alumina

support at 200 - 340 °C for a prescribed time in a stream of air or nitrogen. The flow-rates of tetraethoxysilane and carrier gas were 2.7 and 400 mmol/h, respectively. A small amount of residual carbon on the resulting catalysts was observed, and was removed by calcining the catalyst in air at 500 °C for 3 h. The silica loading of the catalyst was determined by measuring the weight increase of the alumina support after the CVD operation and the subsequent calcination.

Commercial silica-aluminas prepared by co-gelation (N631-L and N631-H, supplied by Nikki Chemical Co. Ltd.) were used as reference catalysts. They are used industrially for the production of bulk chemicals such as p-xylene and alkylbenzenes.

K^+ ion-exchange was performed by immersing a sample in 2 mol/l potassium chloride solution at room temperature for 2 h.

Pore characteristics and surface area. A BET surface area and pore characteristic were calculated from nitrogen physisorption at -196 °C. The pore volume distribution was calculated using the method of Cranston and Inkley[9] and the desorption isotherm of nitrogen.

Catalytic tests. The dehydration of 2-butanol was performed at between 170 and 200 °C using a fixed-bed reactor at a W/F of 15 g-cat.h/mol in a stream of nitrogen as a carrier gas; where W is the catalyst weight (g) and F is the flow-rate of reactant (mol/h). The reaction products were analyzed by on-line gas-liquid chromatography (GLC) using a PEG 1500 column (2 m), and the butene isomers produced were analyzed by an off-line GLC using a VZ-7 column (5 m).

The isomerization of m-xylene was carried out at 520 °C in a flow system at a W/F of 44 g-cat.h/mol. The products were analyzed by off-line GLC using a column of Bentone 34 + dinonyl phthalate (DNP).

The cracking of n-heptane was carried out at 500 °C in a flow system at a W/F of 120 g-cat.h/mol, and the products was analyzed by on-line GLC using a column of Porapack Q (2 m).

The cracking of cumene was performed at 468 °C in a stream

of hydrogen using a micropulse reactor. A cumene pulse (2 μl) was passed over 0.1 g of catalyst and the products were directly analyzed by a column of Bentone 34 + DNP.

The isomerization of 1-butene was carried out in a closed circulation system (reactor volume, 200 ml; catalyst, 0.05 g) under the conditions of a 1-butene initial pressure of 19 kPa at 0 ^{o}C. Prior to the reaction, the catalyst was preheated at 500 ^{o}C under reduced pressure (0.1 Pa). The products was analyzed by on-line GLC using a column of VZ-7 (4.5 m). The catalytic activity was evaluated in terms of the first-order rate constant during the initial reaction period.

Results and Discussion

Deposition of silica onto alumina

Figure 3-1 shows the relation between silica loading and CVD temperature. The silica loading increased with increasing CVD temperature both in air and in nitrogen. Much large amounts of silica were deposited on the alumina support in air than in nitrogen. Under CVD conditions in nitrogen, a temperature of about 50 degree higher was needed to attain the same silica loading as that obtained in air. The broken line in Fig. 3-1 expresses the maximum loading of silica for 2 h. At temperatures above 280 ^{o}C in air, the deposition of silica was limited by the supply of tetraethoxysilane because almost all of the latter fed was deposited on alumina. As CVD was effectively operated at a temperature at which the rapid deposition was attained and the supply of feed was not limited, the optimum CVD temperatures in air and in nitrogen were ca. 240 and 300 ^{o}C, respectively. Figure 3-2 shows the relation between silica loading and CVD time. The broken line in Fig. 3-2 expresses the maximum loading of silica for each CVD time. When CVD was operated at 240 ^{o}C in air in addition to 300 ^{o}C in nitrogen, the silica loading increased linearly with CVD time. On the other hand, the silica loading was not more than 14 wt% at 240 ^{o}C for 4 h in nitrogen,

and even prolonged CVD did not effect any increase in silica loading. However, repetitive increases in silica loading were attainted even at 240 ^{o}C in nitrogen after the sample had been in contact with air at 240 ^{o}C for 1 h. Oxygen thus accelerated the deposition of silica in the temperature range 200 - 300 ^{o}C in a similar manner as that of boria on silica at 350 ^{o}C. In subsequent work, CVD SiO_2/Al_2O_3 catalysts prepared at 240 ^{o}C in air were mainly used for the catalytic tests.

Physical properties of CVD SiO_2/Al_2O_3

The changes in the specific surface areas of CVD SiO_2/Al_2O_3 catalysts with silica loading are shown in Fig. 3-3. The surface area based on unit weight of catalyst decreased monotonously with increasing silica loading because the content of the alumina support in the bulk of catalyst decreased with increasing silica loading. The surface area with respect to unit weight of the alumina support, however, did not change with increase in silica loading. The pore-size distribution of CVD SiO_2/Al_2O_3 together with the alumina support are shown in Fig. 3-4. The alumina support had a maximum pore volume at a diameter of 16.5 nm. For CVD SiO_2(16.9 wt%)/Al_2O_3, the maximum pore volume and the pore size distribution were slightly shifted to smaller values with a 17.2 % decrease in total pore volume. On the other hand, silica would be non-uniformly deposited on alumina by impregnation method, because impregnating alumina with 20.8 wt% of silica elicited 37.5 % decrease of pore volume.[7] These results indicated that the unevenness of the alumina surface was maintained after the deposition of silica, as silica was uniformly deposited on the alumina surface without aggregation.

Catalytic activities

Figure 3-5 shows the catalytic activities of CVD SiO_2/Al_2O_3 for several types of reactions. In all reactions, the CVD SiO_2/Al_2O_3 catalysts showed high catalytic efficiency, although alumina support itself had little activity. The deposition of

silica on alumina thus induced a change in the acidic properties of alumina. The catalytic activity of CVD SiO_2/Al_2O_3 were greatly affected by the silica loading. The maximum conversions for the respective reactions are summarized in Table 3-1 together with the physical and catalytic properties of commercial silica-aluminas. For the dehydration of 2-butanol, the maximum conversion (92 %) appeared at a silica loading of 23 wt%, but for the other reactions such as m-xylene isomerization, cumene cracking, and n-heptane cracking, the maximum conversions (24, 62, and 4.7 %) appeared at lower silica loadings of 19, 16, and 9.6 wt%, respectively. Commercial silica-aluminas were also active for the reactions. The catalytic activities of CVD SiO_2/Al_2O_3 were comparable to those of N631-H containing 27 wt% alumina in spite of its lower surface area and smaller amount of acid. Although N631-L containing 13 wt% alumina was more active than CVD SiO_2/Al_2O_3 under the same W/F conditions, the activities of N631-L based on a surface area is probably comparable to those of the CVD SiO_2/Al_2O_3 catalyst.

For the isomerization of 1-butene, the catalytic activity was also changed with silica loading (Fig. 3-6), and was maximized at a silica loading of 12 wt%. The catalytic activity of CVD SiO_2/Al_2O_3 was four times higher than that of a commercial silica-alumina catalyst, N631-L (Table 3-1). Moreover, the CVD SiO_2/Al_2O_3 catalyst has a cation exchange ability, and that will be described in the section 3-2. An exchange of a proton with the K^+ ion suppressed the catalytic activity for 1-butene isomerization (Fig. 3-6b). In addition, a CVD SiO_2/Al_2O_3 catalyst prepared at 300 ^oC in nitrogen was less active than that prepared at 240 ^oC in air (Fig. 3-6c).

Figure 3-7 shows the influence of the CVD conditions on the catalytic activity for 2-butanol dehydration. The CVD SiO_2/Al_2O_3 catalysts prepared in air showed higher catalytic efficiencies than those prepared in nitrogen. Interestingly, the catalytic efficiency for 2-butanol dehydration over the CVD SiO_2/Al_2O_3 was greatly enhanced by treatment of steam at 500 ^oC. Figure 3-8

shows the product distribution of 2-butanol dehydration. The equilibrium composition of n-butene isomers at 170 ^oC is 7.6:30.6:61.8 for 1-, cis-2-, and trans-2-butenes. The fraction of 1-butene was beyond the equilibrium composition and decreased slightly with increase in silica loading. The cis-to-trans ratio of the product 2-butene monotonously decreased with increasing silica loading, regardless of the CVD conditions and the conversion level. On the other hand, in the dehydration of 2-butanol over the alumina support itself at a reaction temperature of 200 ^oC, the product distribution was 32.4:59.7:7.7 for 1-, cis-2-, and trans-2-butenes at a conversion of 7 %.

The mechanism for 2-butanol dehydration had been discussed previously with regard to product distribution.[10] The dehydration of 2-butanol catalyzed by a Brønsted acid site proceeds through an intermediate such as the alkoxonium ion $C_4H_9OH_2^+$ and the carbonium ion $C_4H_9^+$ (E1 mechanism), and the product distribution approaches the equilibrium value. In the case of alumina which has both Lewis acidity and basicity, however, the dehydration proceeds via acid-base concerted mechanism, where H^+ and OH^- are eliminated simultaneously for cis-elimination (E2 mechanism), to give high 1-/2-butenes and cis-/trans-2-butenes ratios. The great difference in the product distribution found between CVD SiO_2/Al_2O_3 catalyst and the alumina support appears to be mainly due to the differences in their acidic properties, which include the type of acid site (Lewis or Brønsted acid) and the acid strength.

Figures 3-9 and 3-10 show influence of the CVD conditions on the catalytic activities for the cracking of cumene and the isomerization of 1-butene, respectively. For both the reactions, interestingly, the catalytic activities were influenced by the conditions of catalyst preparation. The catalysts prepared at 240 ^oC in air were more active than those prepared at 300 ^oC in nitrogen at the same silica loading, although a comparable rate of silica deposition was attained both at 300 ^oC in nitrogen and at 240 ^oC in air. A similar tendency in catalytic activity has

been observed for the dehydration of 2-butanol. In addition, other CVD catalysts, which were prepared at 240 ^{o}C by repetitive deposition carried out in nitrogen followed intervals of oxidation at 240 ^{o}C in air, were as active as those prepared at 240 ^{o}C in air (Fig. 3-10). Thus, the catalytic activity is influenced by the preparation conditions, in particular by CVD temperature.

For the isomerization of 1-butene, a cis/trans ratio of the produced 2-butene was varied with silica loading (Fig. 3-11). For the CVD catalysts prepared at 240 ^{o}C in air, the cis/trans ratio decreased with increasing silica loading up to a silica loading of 12 wt%, and became constant above this loading. At this loading where a trend of change in the cis/trans ratio was altered, the maximum catalytic activity for 1-butene isomerization was obtained, as shown in Fig. 3-10. This fact suggests that the acid properties, especially acid strength and acid type, varied with silica loading below 12 wt%, and became constant with further silica deposition. The activity drop above this critical loading is caused by a decrease in the number of acid sites. For the catalysts prepared at 300 ^{o}C in nitrogen, however, the cis/trans ratio rather monotonically decreased with increasing silica loading. This indicates that the microstructure of the deposited silica was affected by changes in CVD conditions.

Acidic properties, which are directly concerned with the above-mentioned catalytic properties, are discussed in the following section.

References

1. M. Niwa, M. Kato, T. Hattori, and Y. Murakami, *J. Phys. Chem.*, **90** (1986) 6233.
2. T. Hibino, M. Niwa, A. Hattori, and Y. Murakami, *Appl. Catal.*, **44** (1988) 95.
3. T. Okuhara and J. M. White, *Appl. Surf. Sci.*, **29** (1987) 223.
4. S. Sato, K. Urabe, and Y. Izumi, *J. Catal.*, **102** (1986) 99.
5. S. Sato, S. Hasebe, H. Sakurai, K. Urabe, and Y. Izumi, *Appl. Catal.*, **29** (1987) 107.
6. V. C. F. Holm, G. C. Bailey, and A. Clark, *J. Phys. Chem.*, **63** (1959) 129.
7. J. C. Yori, J. C. Luy, and J. M. Parera, *Appl. Catal.*, **41** (1988) 1.
8. J. H. D. Boer and W. J. Visseren, *Catal. Rev.*, **5** (1972) 55.
9. R. W. Cranston and F. A. Inkley, *Adv. Catal.*, **9** (1957) 143.
10. T. Yamaguchi and K. Tanabe, *Bull. Chem. Soc. Jpn.*, **47** (1974) 424.

Table 3-1. Physical and catalytic properties of CVD SiO_2/Al_2O_3 and commercial silica-aluminas.

Catalyst	CVD SiO_2/Al_2O_3	N631-H	N631-L
SiO_2 content (wt%)	9.6 - 23	73	87
Surface area (m^2/g)	156 - 183	360	430
Amount of acid (mmol/g)[a]	0.07 - 0.09	0.25	0.20
Conversion (mol%)			
2-Butanol dehydration	92 (23)[b]	91	-
m-Xylene isomerization	24 (19)[b]	38	53
Cumene cracking	62 (16)[b]	68	99
n-Heptane cracking	4.7 (9.6)[b]	4.3	5.7
Rate constant ($g^{-1}min^{-1}$)			
1-butene isomerization	1.2[c] (12)[b]	-	0.27[d]

[a] The amount of acid was determined by measuring the amount of ammonia adsorbed at 300°C after a sample had been evacuated at 500°C.

[b] The numbers in parentheses show the silica content (wt%) at which the maximum conversion for the respective reactions appeared.

[c] Reacted at 0 °C.

[d] Reacted at 50 °C.

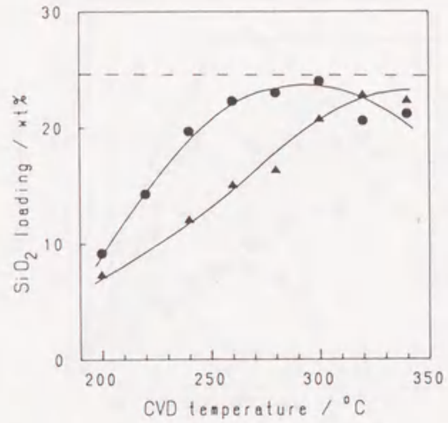

Fig. 3-1. Effect of CVD temperature.
CVD was operated for 2h, (●) in air and (▲) in nitrogen.

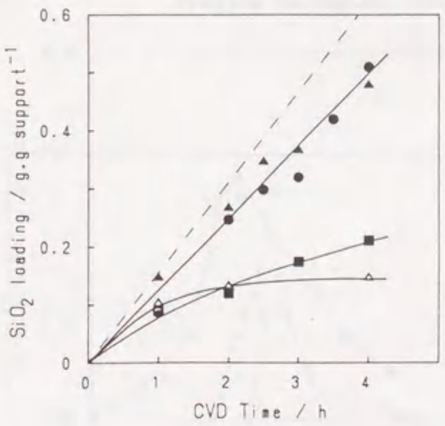

Fig. 3-2. Effect of CVD time.
CVD was operated (▲) at 300 °C in nitrogen, (●) at 240 °C in air and (△) at 240 °C in nitrogen; (■) repetitive CVD carried out at 240 °C in nitrogen for 1h followed intervals of oxidation at 240 °C in air for 1h.

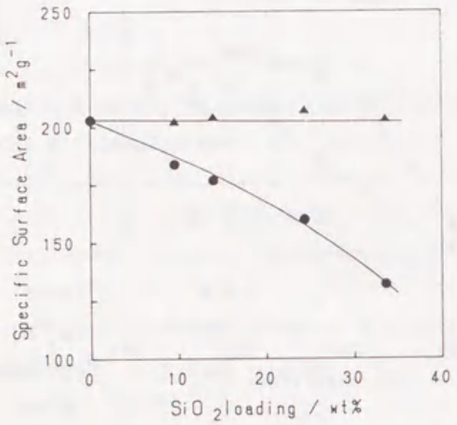

Fig. 3-3. Change in specific surface area with silica loading.
● , based on unit weight of catalyst;
▲ , based on unit weight of support.

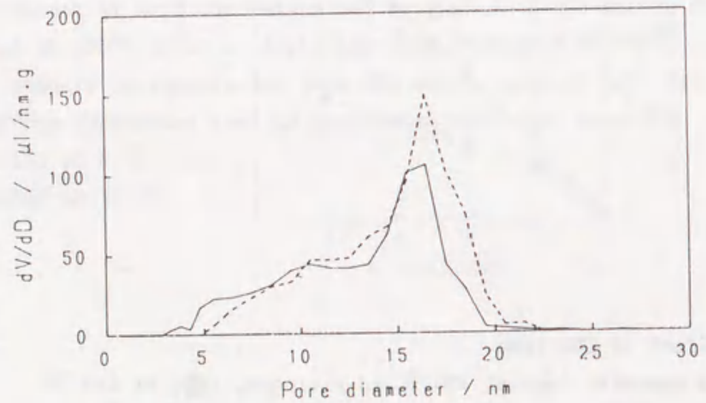

Fig. 3-4. Pore size distribution of catalyst.
Dashed line, alumina; solid line, CVD SiO_2(16.9 wt%)/Al_2O_3.

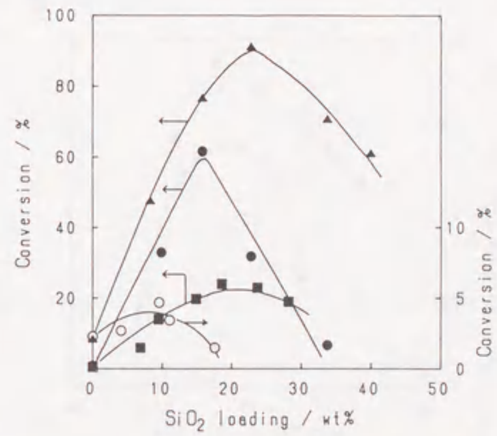

Fig. 3-5. Catalytic activities of CVD SiO_2/Al_2O_3.
●, cumene cracking at 468°C; ○, n-heptane cracking at 500 °C;
▲, 2-butanol dehydration at 200 °C; ■, m-xylene isomerization at 520°C.

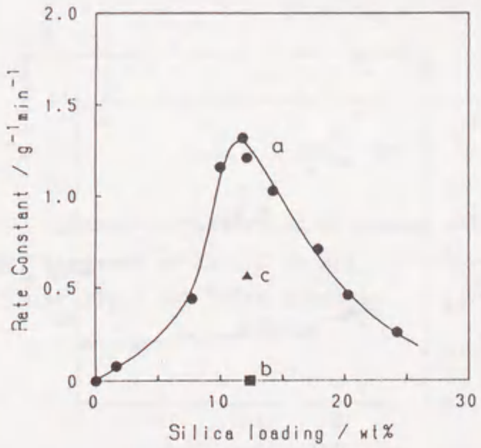

Fig. 3-6. Change in the initial rate constant for 1-butene isomerization.
a, CVD SiO_2/Al_2O_3 prepared at 240 °C in air;
b, CVD SiO_2(12.4wt%)/Al_2O_3 exchanged with 0.11 mmol/g of K^+ ion;
c, CVD SiO_2(12.2wt%)/Al_2O_3 prepared at 300 °C in nitrogen.

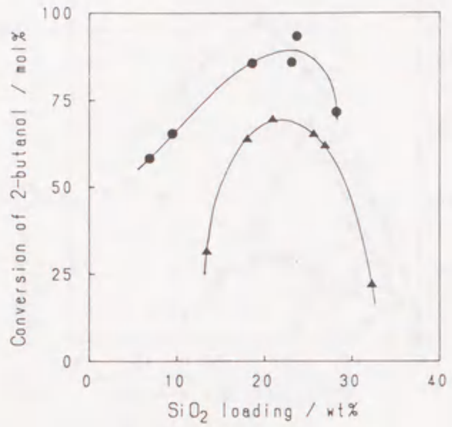

Fig. 3-7. 2-Butanol dehydration (170 ^{o}C) over steam-treated CVD SiO_2/Al_2O_3.
Prepared (●) in air at 240 ^{o}C and (▲) in nitrogen at 280 - 300 ^{o}C.

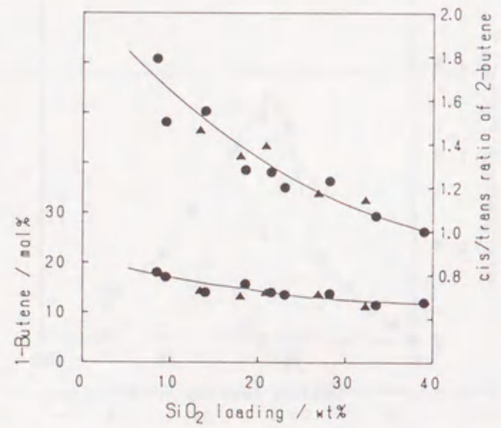

Fig. 3-8. Product distribution of 2-butanol dehydration.
Symbols as those in Fig. 3-7.

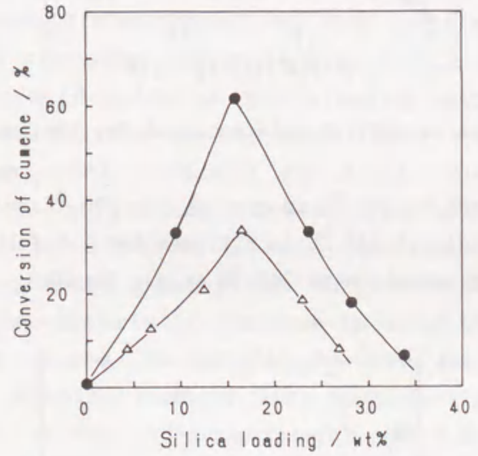

Fig. 3-9. Change in conversion of cumene with silica loading.
●, Prepared at 240 ^{o}C in air;
△, at 280 - 300 ^{o}C in nitrogen.

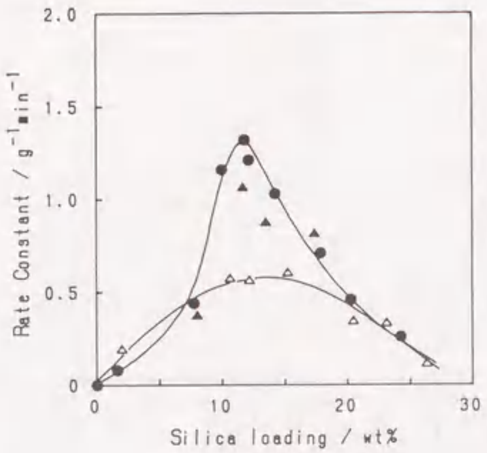

Fig. 3-10. Change in initial rate constant for the isomerization of 1-butene.
●, Deposited at 240 °C in air; △, at 300 °C in nitrogen; ▲, repeatedly at 240 °C in nitrogen for 1 h followed intervals of oxidation at 240 °C in air for 1h.

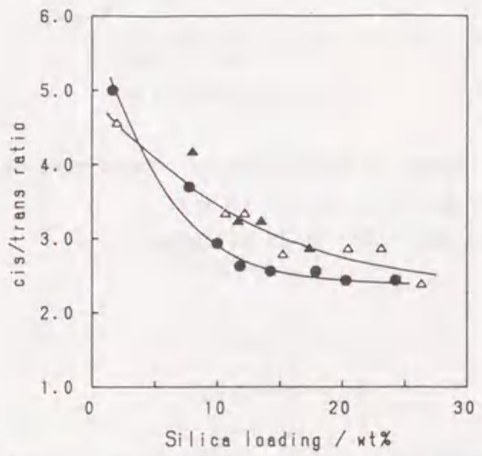

Fig. 3-11. Change in cis/trans ratio of produced 2-butene at 10 % conversion of 1-butene. Symbols as those in Fig. 3-10.

3-2 Acidic Properties of Silica Deposited on Alumina

Abstract

Acidic properties of silica-alumina catalyst prepared by depositing silica on an alumina (SiO_2/Al_2O_3) were characterized by several measurements, such as solid-state magic-angle spinning (MAS) NMR measurement and temperature-programmed desorption (TPD) of adsorbed dimethylpyridine. The ^{31}P MAS NMR of trimethylphosphine chemisorbed on the catalyst elucidated the change in acid property (Brønsted or Lewis type) with silica loading. Lewis acid sites on the alumina surface were converted into Brønsted acid sites by the deposition of silica. At lower silica loadings, both Brønsted and Lewis acid sites existed. Above 12 wt% silica loading, Lewis acid sites disappeared and only Brønsted acid sites were observed. Furthermore, a temperature-programmed desorption of adsorbed dimethylpyridine clarified the characteristic changes in acid type, acid strength, and acid amount of the CVD SiO_2/Al_2O_3 catalyst. Lewis acid sites of the support alumina changed into Brønsted acid sites together with a change in the acid strength with increasing silica deposition. The catalytic activities of CVD SiO_2/Al_2O_3 described in the previous section were correlated with the amount of Brønsted acid sites generated by silica deposition.

Introduction

Acidic property is one of the most important characteristics of solid catalyst, and is evaluated by various methods such as titration, temperature-programmed desorption (TPD), and infrared spectroscopy.[1] Infrared spectroscopy of adsorbed pyridine reveals acid type (Brønsted acid or Lewis acid), and TPD measurement of adsorbed ammonia elucidates both acid strength and

acid amount. The conventional TPD measurement, however, unfortunately gives us no information about acid type because ammonia adsorbs non-selectively on both Brønsted and Lewis acid sites. One must, therefore, apply several different methods in order to evaluate acid property of solid surface. On one hand, 2,6-dimethylpyridine (2,6-DMP) is known to selectively adsorb on Brønsted acid sites because of the steric hindrance arising from the two methyl groups, each of which is located adjacent to the nitrogen atom, whereas non-hindered 3,5-DMP is capable of adsorbing on both Lewis and Brønsted acid sites.[2-5] Although titration methods using DMP are reported to obtain reasonable results, it appears to be rather tedious.[4,5] As a facile method to be able to examine the amount, strength, and type of solid acid, the author propose here a TPD technique of the DMP adsorbed on solid acids such as alumina and silica-alumina.

Recently, a solid-state NMR spectroscopy has been used for structural studies of inorganic materials.[6-12] In addition to the characterization of bulk solid, adsorbed species have been observed on the surface of solid acids.[13-15] A ^{31}P NMR of trimethylphosphine adsorbed on acid sites elucidates the acidic nature of solid acids because the ^{31}P chemical shifts of trimethylphosphine chemisorbed on Brønsted acid sites is quite distinct from those on Lewis acid sites. The acid properties of HY zeolite[13,14] and amorphous silica-alumina[15] are thus characterized by ^{31}P NMR measurement.

In the previous section, a supported type of silica-alumina prepared by depositing silica on an alumina surface was described. Silica was effectively deposited on alumina using tetraethoxysilane in the presence of oxygen at 240 ^{o}C, and silica loading was readily controlled by the CVD time. The resulting silica-alumina (CVD SiO_2/Al_2O_3) exhibited catalytic activities for several types of organic reactions such as 2-butanol dehydration, m-xylene isomerization, 1-butene isomerization, cumene cracking, and heptane cracking.

In this section, the acid properties, acid type (Brønsted or

Lewis), acid strength, and acid amount, were clarified. A ^{31}P magic-angle spinning (MAS) NMR experiment of trimethylphosphine chemisorbed on the catalysts was carried out in order to elucidate the acid types, Brønsted and Lewis. A temperature-programmed desorption (TPD) of dimethylpyridine (DMP) adsorbed on a CVD SiO_2/Al_2O_3 catalyst using a conductivity cell immersed in a dilute H_2SO_4 solution was carried out in order to evaluate the entire acid property, including acid type (Brønsted or Lewis), acid strength, and acid amount. In addition, the amount of ammonia adsorbed was measured, and the amount of Brønsted acid was determined from the extent of the liberated proton in the phase of an aqueous solution.

Experimental

Catalysts. Alumina supplied by Dia Catalyst & Chemicals Ltd. (DC-2282: specific surface area, 203 m^2/g; pore volume, 0.72 ml/g; granule size, 24-60 mesh.) was used as a support. A CVD SiO_2/Al_2O_3 catalyst was prepared by contacting tetraethoxysilane vapor with the alumina support in a CVD reactor (Fig. 1-3) which comprised a glass column rotating in an electrical furnace inclined at 45^{o} at 240 and 300 ^{o}C for a prescribed time in a stream of air and nitrogen, respectively; the flow rates of tetraethoxysilane and carrier gas were 2.7 and 400 mmol/h, respectively. The silica loading was determined by measuring the weight increase of the alumina support after CVD operation followed by calcination at 550 ^{o}C for 3 h.

A commercial silica-alumina (Nikki Chemical Co. Ltd., N631-L) was used as a reference catalyst.

A K^+ ion-exchanged sample was prepared by immersing a sample in 2 mol/l potassium chloride solution at room temperature for 2 h followed by drying at 110 ^{o}C.

Adsorption of ammonia. The total amount of acid was determined by the volumetric measurement of ammonia chemisorbed at an elevated temperature. Prior to ammonia adsorption, 0.5 g of

catalyst sample was evacuated at 500 ^{o}C for 1 h. The total amount of physisorbed and chemisorbed ammonia was measured either at 300 ^{o}C or 400 ^{o}C for 1 h. After the physisorbed ammonia had been desorbed by evacuating the sample at the same temperature as the first adsorption for 1 h, the physisorbed ammonia was measured with the second ammonia adsorption. The total amount of acid was calculated as the difference between the first and second adsorptions of ammonia.

Liberation of proton in aqueous solution. The amount of proton exchanged with potassium ion was measured to establish the proton-liberating ability of the catalyst in aqueous solution. A catalyst sample (0.5 g) was immersed in 0.5 mol/l potassium chloride solution at room temperature for 20 h. The amount of the proton liberated from the catalyst was determined with alkalimetric titration of the supernatant solution.

NMR measurement. The ^{31}P magic angle spinning (MAS) NMR spectra were recorded on a Bruker AM-400 multinuclear spectrometer, according to the procedure outlined by Lunsford *et al.*[13] The ^{31}P MAS NMR measurement of the trimethylphosphine chemisorbed on catalyst was performed at 161.98 MHz at a spinning rate of 4 kHz, while H_3PO_4 was used as a external standard. Radio-frequency pulses of 2.7 μs and residence times of 2 s were used, and 2000 FID were accumulated. About 0.04 ml of catalyst sample was filled in a Pyrex tube (5 mm-o.d.) and the tube was attached to a vacuum line with a greaseless joint. After evacuation at 500 ^{o}C for 2 h, trimethylphosphine was adsorbed at 25 ^{o}C for 1 h, followed by evacuation at 80 ^{o}C for 1 h. The sample tube was then sealed to a length of 17 mm. The sealed tube attached to the spinning holder was supplied for the NMR measurement.

Temperature-programmed desorption of adsorded dimethylpyridine. After a sample (50 mg) placed in a quartz tube (4 mm-i.d.) with quartz wool had been evacuated at 500 ^{o}C for 1 h, excess DMP was injected via a microsyringe at 200 ^{o}C, and then evacuated at 200 ^{o}C for 1 h. A TPD measurement was carried out from 100 to 600 ^{o}C at a heating rate of 5 ^{o}C/min in a nitrogen flow of 30 ml/min.

The desorbed DMP was monitored by a conductivity cell immersed in aqueous sulfuric acid (1/2000 mol/l). A cumulative amount of desorbed DMP as a function of the desorption temperature was recorded, then differentiated to give the acid strength distribution. Independently, desorbed molecules were collected at -196 ^{o}C, then analyzed by GLC.

Results and Discussion

Ammonia chemisorption and liberation of proton

The amount of chemisorbed ammonia was measured to examine the acidic properties of CVD SiO_2/Al_2O_3 catalyst. After a catalyst sample had been evacuated at 300 ^{o}C, only 6 μmol/g of ammonia was chemisorbed on alumina at 300 ^{o}C. With respect to the CVD SiO_2/Al_2O_3 catalysts, however, considerable amounts (46 - 47 μmol/g) of chemisorbed ammonia were observed, independent on the silica loading. The change in the amount of ammonia chemisorbed at 300 ^{o}C after evacuation at 500 ^{o}C is shown in Fig. 3-12. The alumina support was highly dehydrated and became more acidic (104 μmol/g). The amount of acid sites on the alumina surface thus treated decreased slightly with increasing silica loading. The surface acidity was thus greatly influenced by the degree of dehydration. Yori *et al.* reported on the surface acidity of silica-alumina prepared by impregnation;[16] the total amount of acid, which was evaluated by the amount of ammonia desorbed in the range 250 - 550 ^{o}C, decreased with increasing silica loading and the fraction of strong acid sites, which was defined as a ratio of the amounts of desorbed ammonia in the ranges 400 - 550 ^{o}C and 250 - 550 ^{o}C, was increased with increasing silica loading. In order to evaluate the strong acid sites, the amount of chemisorbed ammonia was measured at a high temperature of 400 ^{o}C. The amount of ammonia chemisorbed at 400 ^{o}C decreased with increasing silica loading in a similar manner as the ammonia chemisorption at 300 ^{o}C (Fig. 3-12). Hence the fraction of strong acid sites, defined as a ratio of the amounts

of ammonia chemisorbed at 400 ^{o}C and 300 ^{o}C, decreased slightly with increasing silica loading. For example, the fractions for alumina and CVD SiO_2(20 wt%)/Al_2O_3 were 0.69 and 0.61, respectively. The results of the ammonia chemisorption study unexpectedly indicated that the total amount of acid sites decreased slightly with increasing silica loading with a small change in acid strength.

As the changes in catalytic activity with silica loading shown in Figs. 3-5 and 3-6 could not be clearly explained by the results of ammonia chemisorption, alternatively the proton-liberating ability of the catalyst was examined by measuring the amount of proton exchanged with potassium ion in aqueous potassium chloride solution (Fig. 3-12). For the CVD SiO_2/Al_2O_3 catalysts, proton liberation was observed even in an aqueous solution, whereas no protons were liberated from alumina. The amount of protons liberated from CVD SiO_2/Al_2O_3 increased with increasing silica loading, and eventually reached a maximum. In addition, the active commercial silica-alumina (N631-L) showed a large amount of liberated proton (152 μmol/g), 2.5 times larger than that of CVD SiO_2(20 wt%)/Al_2O_3 based on unit weight of catalyst.

Holm *et al.*[17] investigated the relationship between the acidity of silica-alumina prepared by coprecipitation and its catalytic activity, concluding that propylene polymerization was correlated with the amount of protonic acid measured in an aqueous solution of ammonium acetate rather than with the total acid amount determined by non-aqueous butylamine titration. Also in this work, the catalytic activity for a water-producing reaction of 2-butanol dehydration (Fig. 3-7) correlated well to the amount of protonic acid of CVD SiO_2/Al_2O_3. In contrast to alumina, CVD SiO_2/Al_2O_3 catalysts were thus acidic enough to liberate protons even in an aqueous medium. The other hydrocarbon conversion reactions shown in Fig. 3-5 appeared to be also activated by the protonic acids, although their maximum conversions were obtained at relatively lower silica loadings and

not at a silica loading of ca. 23 wt% which gave the maximum of protonic acid. Compared with 2-butanol dehydration, these hydrocarbon conversions require higher protonic acid strengths to be activated. The protonic acid strength of CVD SiO_2/Al_2O_3 hence appears to be higher at lower silica loadings. In addition, compared with the CVD SiO_2/Al_2O_3 catalysts prepared in air, those prepared in nitrogen had smaller amounts of protonic acid sites, and this result was consistent with their lower catalytic activities shown in Fig. 3-7.

^{31}P NMR spectra of the trimethylphosphine chemisorbed

The ^{31}P chemical shifts of trimethylphosphine chemisorbed on solid acids were studied by Lunsford *et al.*.[13] They showed that an alumina and HY zeolites calcined at higher temperatures of 600 and 700 ^{o}C exhibited chemical shifts of the chemisorbed trimethylphosphine in the region from -32 to -58 ppm, which were assigned to the trimethylphosphine chemisorbed on Lewis acid sites, and that a chemical shift of the trimethylphosphine chemisorbed on Brønsted acid sites of HY zeolite calcined at 400 ^{o}C was observed at -3 ppm.

To elucidate the acidic nature of CVD SiO_2/Al_2O_3 catalyst without deterioration of sample, ^{31}P MAS NMR measurement of chemisorbed trimethylphosphine was examined. The ^{31}P MAS NMR spectrum of the trimethylphosphine chemisorbed on the alumina support was dominated by a resonance at -47.8 ppm with a small chemical shift at 3.7 ppm (Fig. 3-13a). When the alumina support was evacuated at 600 ^{o}C, the chemical shift at -47 ppm was predominated, and the chemical shift at 4 ppm almost disappeared. The former chemical shift is due to trimethylphosphine chemisorbed on Lewis acid sites. The latter is probably attributable to trimethylphosphine chemisorbed on weak Brønsted acid sites which may correspond to the surface hydroxyl groups attached to aluminum atoms.

In contrast, the spectrum of the trimethylphosphine chemisorbed on CVD SiO_2(15.9 wt%)/Al_2O_3 catalyst had a single

chemical shift at -1.7 ppm (Fig. 3-13b), which was identical with that of the trimethylphosphine chemisorbed on Brønsted acid sites observed on an HY zeolite calcined at 400 ^{o}C.[13] In addition, the active commercial silica-alumina (N631-L) had both Lewis and Brønsted acid sites confirmed by the chemical shifts of chemisorbed trimethylphosphine at -47.0 and -3.1 ppm, respectively, with both the unknown sharp shift at 22.5 ppm and the broad spinning side bands at 22.5 and -31.7 ppm (Fig. 3-13c).

The ^{31}P NMR spectra of the trimethylphosphine chemisorbed on the CVD SiO_2/Al_2O_3 catalysts prepared at 240 ^{o}C in air are illustrated in Fig. 3-14. The ^{31}P chemical shift of the trimethylphosphine chemisorbed on alumina support itself was dominated by Lewis acid sites (-47 ppm in Fig. 3-14a). Silica deposition induced strong Brønsted acid sites (-2 ppm in Fig. 3-14b). With increasing silica loading, the number of Brønsted acid sites (-2 ppm) was increased while the number of Lewis acid sites (-47 ppm) and that of weak Brønsted acid sites (4 ppm) were decreased. The Lewis acid sites almost disappeared at a silica loading of 12 wt% (Fig. 3-14c). In addition to these chemical shifts, an unknown sharp chemical shift appeared at 23 ppm (Fig. 3-14b,c), which was not a spinning side band and also observed with protonated Y-type zeolites[13] and a commercial silica-alumina (Fig. 3-13c). Moreover, all the ^{31}P chemical shifts disappeared at a silica loading of 39 wt%. The ^{31}P NMR studies thus indicates that the Lewis acid sites on alumina decreased and other Brønsted acid sites were newly generated with increasing silica loading, and that the Lewis acid sites were completely converted into Brønsted acid sites.

Figure 3-15 compares the ^{31}P MAS NMR spectra of two different catalysts prepared at 240 ^{o}C in air and 300 ^{o}C in nitrogen. The catalyst prepared at 240 ^{o}C in air exhibited only Brønsted acid sites (-2 ppm) at a silica loading of 12 wt%. In contrast, the catalyst prepared at 300 ^{o}C in nitrogen had both Brønsted (-2 ppm) and Lewis (-50 ppm) acid sites at the same silica loading. This observation on ^{31}P MAS NMR is consistent

with the ^{29}Si NMR results (Figs. 3-14 and 3-15). Since the catalyst prepared at 300 ^{o}C in nitrogen showed a ^{29}Si chemical shift at around -110 ppm, much more silica had aggregated to form multilayers, thereby exposing alumina surface which exhibits Lewis acidity; this is discussed in section 3-3. The catalytic behavior is thus well explained by the newly generated Brønsted acidity. Another aspect concerning about the amount of acid sites are discussed later.

Temperature-programmed desorption of adsorded dimethylpyridine

Decomposition of DMP was preliminarily examined. In the TPD process above 500 ^{o}C, about 30 % of the 3,5-DMP desorbed from the alumina was decomposed into 3-methylpyridine and pyridine. The desorbed amines were detected by the change in the conductivity of a cell solution in which protons are neutralized with them. The conductivity detector was sensitive to such amines as pyridine and DMP, but insensitive to desorbed water as well as to such neutral molecules as benzene and ethanol. In addition, the sensitivity for DMP was almost the same as those for methylpyridine and pyridine. The conductivity detector, therefore, is convenient for the TPD measurement of adsorbed DMP.

Figure 3-16 shows the cumulative amounts of DMP desorbed from the catalysts. For the alumina support, itself, the cumulative amounts of desorbed DMP were 106 and 14 μmol/g for 3,5- and 2,6-DMP, respectively. For the CVD SiO_2(12 wt%)/Al_2O_3 prepared at 240 ^{o}C in air, they were 85 and 77 μmol/g for 3,5- and 2,6-DMP, respectively. 2,6-DMP is known to selectively adsorb on Brønsted acid sites because of the steric hindrance arising from the two methyl groups, each of which is located adjacent to the nitrogen atom, whereas non-hindered 3,5-DMP is capable of adsorbing on both Lewis and Brønsted acid sites.[2,4,5] The adsorption of 2,6-DMP on the alumina was seriously restricted, compared to that of 3,5-DMP. The acid amounts measured by 3,5-DMP were also comparable to the amount measured by pyridine.

Figures 3-17 and 3-18 show the acid strength distribution of the catalysts. The alumina had a large desorption peak of 3,5-DMP at 300 ^{o}C with a shoulder at 570 ^{o}C, whereas two small desorption peaks of 2,6-DMP appeared at 300 and 560 ^{o}C (Fig. 3-17). The small peak of 2,6-DMP at 300 ^{o}C (Fig. 3-17b) appears to be caused by desorption from weak Brønsted acid sites. The small peak at 560 ^{o}C (Fig. 3-17b), however, seems to be attributable not to strong Brønsted acid sites, but to strong Lewis acid sites, since alumina has no strong Brønsted acid sites.[1] Additionally, IR spectroscopic observations have revealed that 2,6-di-*tert*-butylpyridine is strongly adsorbed on alumina,[3] and that 2,6-DMP adsorb on Lewis acid sites together with weak Brønsted acid sites,[18] whereas they have not dealt with the quantitative aspects. Although the TPD of adsorbed 2,6-DMP tends to overestimate the Brønsted acid sites, the large difference between the distribution curves for 3,5- and 2,6-DMP indicates clearly that the acid sites of the alumina are predominantly composed of the Lewis type. On the other hand, the CVD SiO_2(12 wt%)/Al_2O_3 had a wide distribution at a peak top of 250 and 275 ^{o}C for 3,5- and 2,6-DMP, respectively (Fig. 3-18). Since there is no significant difference between two distribution curves for 3,5- and 2,6-DMP, the CVD SiO_2/Al_2O_3 catalyst has a large amount of Brønsted acid sites together with a small amount of strong Lewis acid sites.

Figure 3-19 shows the change in the acid strength distribution measured by the desorption of 2,6-DMP for CVD catalysts prepared at 240 ^{o}C in air. When a small amount of silica (5 wt%) was deposited on alumina, the amount of 2,6-DMP desorbed near 250 ^{o}C was drastically increased (Fig. 3-19b). A further increase in silica deposition induced an increase in the strong acid sites represented by desorption around 400 ^{o}C; both the highest acid strength and the maximum amount of desorbed 2,6-DMP were attained at a silica loading of 12 wt% (Fig. 3-19c). Above 12 wt%, the amount was decreased with increasing silica loading, together with a small change in the acid strength (Fig. 3-19d). On the other hand, the desorption behavior of 3,5-DMP was similar to that of alumina, as is shown in Figs. 3-17a and 3-18a.

Figure 3-20 shows changes in the amount of desorbed DMP with silica loading. The amount of desorbed 3,5-DMP was almost unchanged up to about 10 wt% of silica; above this loading it slightly decreased with increasing silica loading. In contrast, the amount of desorbed 2,6-DMP exhibited a maximum at a silica loading of 12 wt%. According to a ^{31}P magic-angle spinning NMR experiment of chemisorbed trimethylphosphine, the alumina had predominately Lewis acid sites, and Brønsted acid sites were generated on the CVD SiO_2/Al_2O_3, accompanying the disappearance of the Lewis acid sites in the ^{31}P NMR results. The TPD results are consistent with the ^{31}P NMR results, and are allowed to characterize the strength of Brønsted acid sites of the CVD SiO_2/Al_2O_3 catalysts.

For the isomerization of 1-butene, the catalytic activity was changed with silica loading (Fig. 3-6), and was maximized at a silica loading of 12 wt%, at which both the acid strength and amount measured by 2,6-DMP desorption showed maxima. In addition, the CVD SiO_2/Al_2O_3 catalyst has a cation exchange ability (Fig. 3-12), and an exchange of a proton with the K^+ ion suppressed the catalytic activity for 1-butene isomerization (Fig. 3-6b). The K^+ ion-exchange decreased both the acid strength and the amount (Fig. 3-21b), and the amount of desorbed 2,6-DMP drastically decreased at temperatures higher than 400 ^{o}C. Moreover, a CVD SiO_2/Al_2O_3 catalyst prepared at 300 ^{o}C in nitrogen, which had a smaller amount of desorbed 2,6-DMP (Fig. 3-21c), was less active than that prepared at 240 ^{o}C in air (Fig. 3-6c). The catalytic behavior are well correlated with the Brønsted acidity measured by 2,6-DMP desorption.

References

1. K. Tanabe, M. Misono, Y. Ono, and H. Hattori, *Stud. Surf. Sci. Catal.*, 51

(1989) 82.
2. H. A. Benesi, *J. Catal.*, **28** (1973) 176.
3. J. Dewing, G. T. Monks, and B. Youll, *J. Catal.*, **44** (1976) 226.
4. S. L. Soled, G. B. McVicker, L. L. Murrell, L. G. Sherman, N. C. Dispenziere, Jr., S. L. Hsu, and D. Waldman, *J. Catal.*, 111 (1988) 286.
5. L. L. Murrell, and N. C. Dispenziere, Jr., *J. Catal.*, **117** (1989) 275.
6. M. Mägi, E. Lippmaa, A. Samoson, G. Engelhardt, and A. R. Grimmer, *J. Phys. Chem.*, **88** (1984) 1518.
7. E. Lippmaa, M. Mägi, A. Samoson, G. Engelhardt, and A. R. Grimmer, *J. Am. Chem. Soc.*, **102** (1980) 4889.
8. J. M. Thomas and J. Klinowski, *Adv. Catal.*, **33** (1985) 199.
9. S. Komarneni, R. Roy, C. A. Fyfe, G. J. Kennedy, and H. Strobl, *J. Am. Ceram. Soc.*, **69** (1986) C42.
10. D. Müller, P. Starke, M. Jank, K. P. Wendlandt, H. Bremer, and G. Scheler, *Z. Anorg. Allg. Chem.*, **517** (1984) 167.
11. L. B. Welsh, J. P. Gilson, and M. J. Gattuso, *Appl. Catal.*, 15 (1985) 327.
12. K. Segawa, Y. Nakajima, S. Nakata, S. Asaoka, and H. Takahashi, *J. Catal.*, **101**, (1986) 81.
13. J. H. Lunsford, W. P. Rothwell, and W. Shen, *J. Am. Chem. Soc.*, **107** (1985) 1540.
14. J. H. Lunsford, P. N. Tutunjian, P. Chu, E. B. Yeh, and D. J. Zalewski, *J. Phys. Chem.*, **93** (1989) 2590.
15. L. Baltusis, J. S. Frye, and G. E. Maciel, *J. Am. Chem. Soc.*, **109** (1987) 40.
16. J. C. Yori, J. C. Luy, and J. M. Parera, *Appl. Catal.*, **41** (1988) 1.
17. V. C. F. Holm, G. C. Bailey, and A. Clark, *J. Phys. Chem.*, **63** (1959) 129.
18. A. Corma, C. Rodellas, and V. Fornes, *J. Catal.*, **88** (1984) 374.

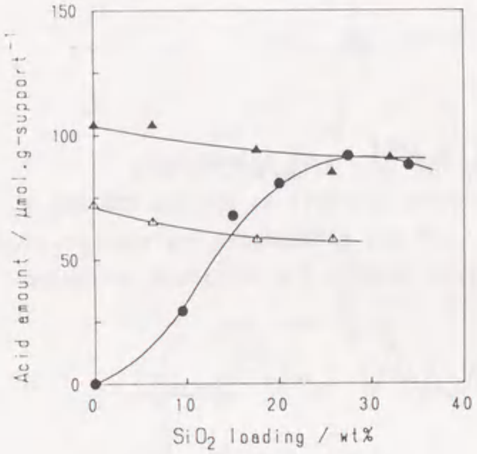

Fig. 3-12. Change in amount of acid with silica loading.
▲, Amount of ammonia adsorbed at 300 °C; △, at 400 °C;
●, Amount of liberated proton in KCl solution.

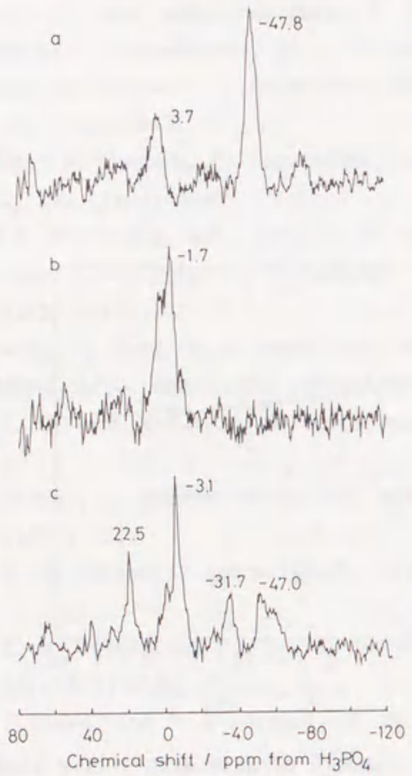

Fig. 3-13. ^{31}P NMR spectra of chemisorbed trimethylphosphine. (a) Alumina; (b) CVD SiO_2(15.9 wt%)/Al_2O_3; (c) N631-L.

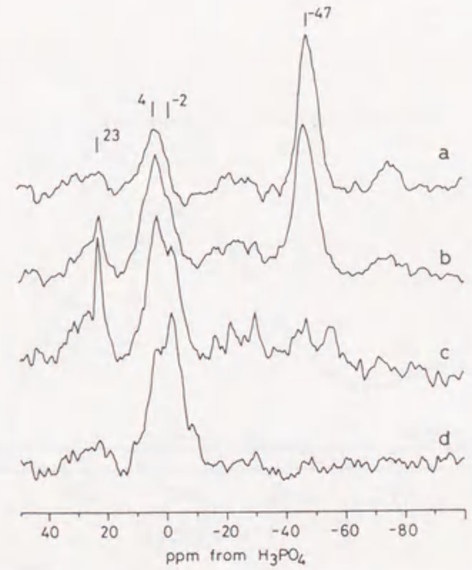

Fig. 3-14. ^{31}P MAS NMR spectra of trimethylphosphine chemisorbed on CVD SiO_2/Al_2O_3 catalyst prepared at 240 ^oC. Silica loading: a, 0 wt%; b, 4.5 wt%; c, 12.3 wt%; d, 15.7 wt%.

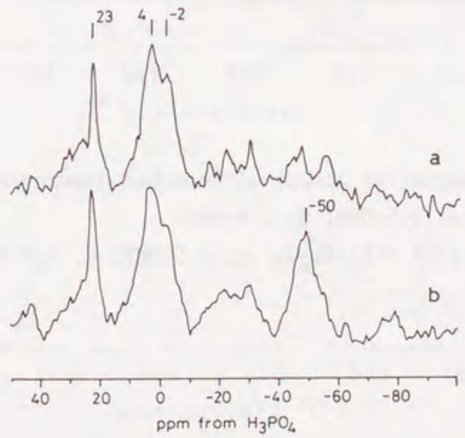

Fig. 3-15. Difference in ^{31}P MAS NMR spectra between the catalyst prepared at 240 ^oC and 300 ^oC at the same silica loading of 12 wt%. a, Prepared at 240 ^oC in air; b, at 300 ^oC in nitrogen.

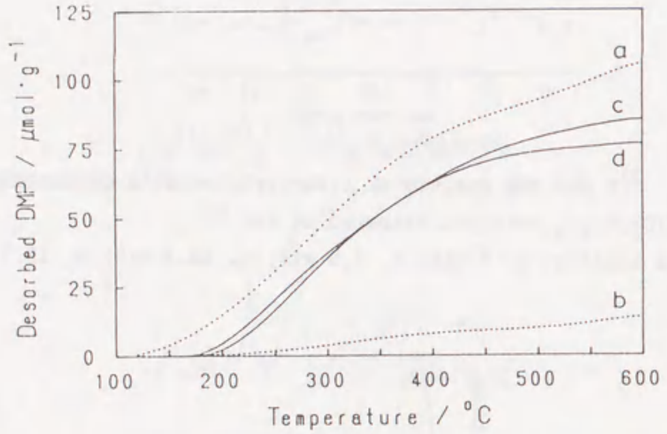

Fig. 3-16. Cumulative amount of desorbed dimethylpyridine (DMP).
Alumina: a, 3,5-DMP; b, 2,6-DMP;
CVD SiO_2(12.4 wt%)/Al_2O_3: c, 3,5-DMP; d, 2,6-DMP.

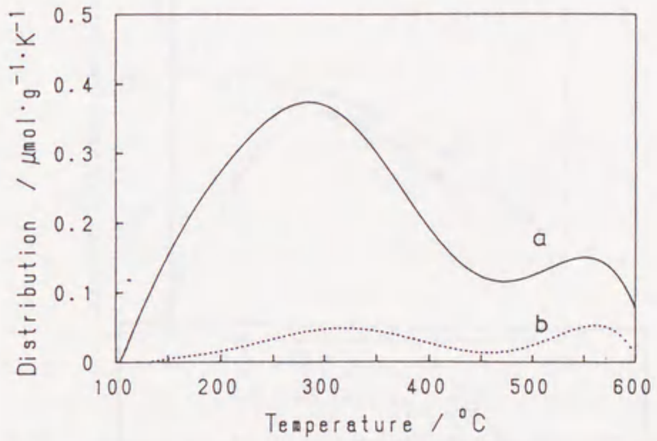

Fig. 3-17. TPD profiles of DMP desorbed on alumina.
a, 3,5-DMP; b, 2,6-DMP.

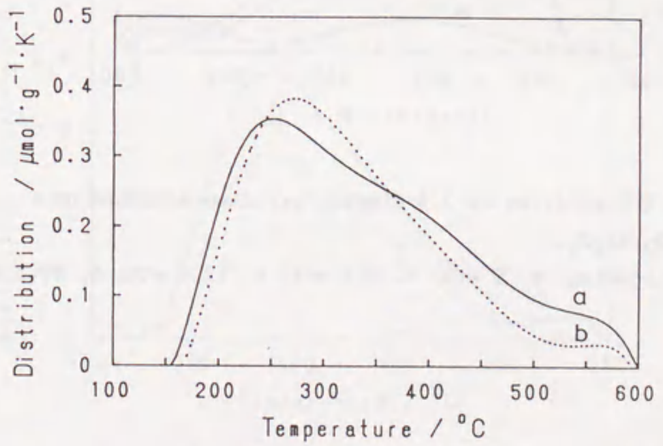

Fig. 3-18. TPD profiles of CVD SiO_2(12.4 wt%)/Al_2O_3.
a, 3,5-DMP; b, 2,6-DMP.

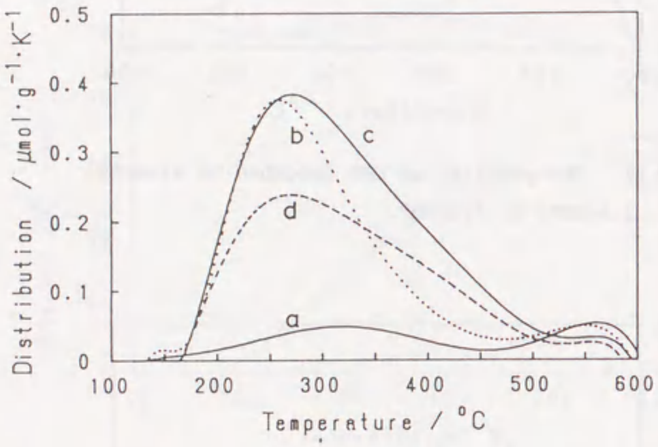

Fig. 3-19. TPD profiles of 2,6-dimethylpyridine adsorbed on CVD SiO_2/Al_2O_3.
Silica loading: a, 0 wt%; b, 5.1 wt%; c, 12.4 wt%; d, 20.3 wt%.

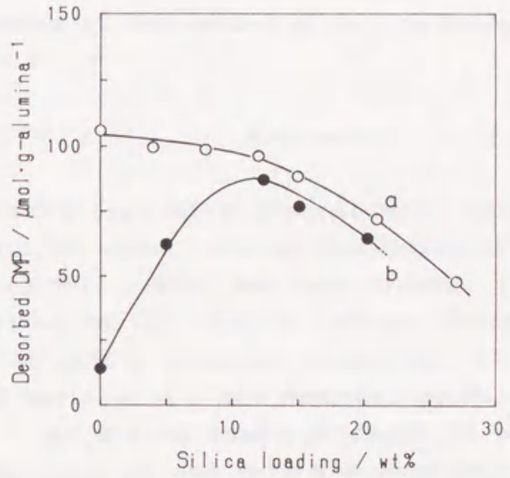

Fig. 3-20. Change in the total amount of desorbed DMP with silica loading.
a, 3,5-DMP; b, 2,6-DMP.

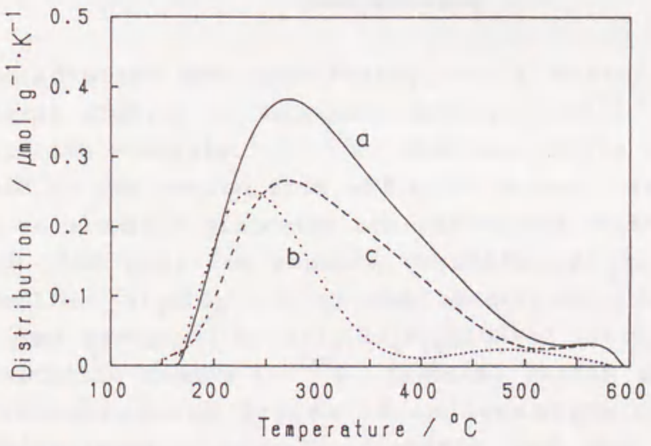

Fig. 3-21. TPD profiles of 2,6-DMP for various CVD SiO_2(12wt%)/Al_2O_3 catalysts.
Symbols as those in Fig. 3-6.

3-3 Structural Properties of Silica Deposited on Alumina

Abstract

A supported type of silica-alumina catalyst prepared by depositing silica on an alumina was characterized by solid-state magic-angle spinning (MAS) NMR measurement. The ^{29}Si MAS NMR of silica deposited on the alumina surface revealed microstructures of silica. At silica loadings lower than 12 wt%, at which both Brønsted and Lewis acid sites existed, uncovered alumina surface was exposed. At silica loadings about 12 wt%, at which Lewis acid sites disappeared and only Brønsted acid sites existed, the highly dispersed silica, forming a silica bilayer, exhibited high catalytic activities and strong Brønsted acidity. Further silica layering decreased both the catalytic activities and the acidity.

Introduction

Solid-state NMR spectroscopy is a useful technique for structural studies of inorganic materials.[1-7] In NMR studies for silicate minerals,[1,2] ^{29}Si chemical shifts in silicates are observed in the region from -60 to -120 ppm. The ^{29}Si chemical shifts in aluminum silicates are restricted to the range between -80 and -100 ppm: for example, kyanite, Al_2SiO_5, -82.9 ppm; sillimanite, Al_2SiO_5, -87.1 ppm; kaolinite, $Al_4[Si_4O_{10}](OH)_8$, -91.5 ppm; pyrophyllite, $Al_4[Si_4O_{10}](OH)_2$, -95.0 ppm. The most characteristic trends in ^{29}Si chemical shifts of silicates are that an increasing degree of condensation of the silicate tetrahedra leads to high-field shifts, and that substitution of the Si ions in silicate tetrahedra by Al ions leads to low-field shifts. For various zeolites,[3] a similar tendency is also observed. In addition to crystal materials, solid-state NMR is also sensitive to non-crystalline materials which are not

identified by the diffraction methods, and reveals microstructures of amorphous solids such as aluminosilicates[4-6] and zirconium phosphate gel.[7]

The catalytic and acidic properties of silica-alumina prepared depositing silica on an alumina surface (CVD SiO_2/Al_2O_3) were clarified in the previous sections. In this section, the structural properties of silica deposited on alumina is dealt. In order to clarify the microstructure of the silica deposited on an alumina surface of CVD SiO_2/Al_2O_3 catalyst with silica loading, the author applied ^{29}Si MAS NMR to the deposited silica.

Experimental

Catalysts. An alumina supplied by Dia Catalyst & Chemicals Ltd., DC-2282, which had a specific surface area of 203 m^2/g, a pore volume of 0.72 ml/g, and a granule size of 24-60 mesh, was used as a support. A CVD SiO_2/Al_2O_3 catalyst was prepared by contacting a tetraethoxysilane vapor with the alumina support in a CVD reactor (Fig. 1-3). The details in CVD procedure were described in the previous sections.

A silica gel supplied by Fuji Davison Co. Ltd., ID type gel, was used for a ^{29}Si MAS NMR measurement.

NMR measurements. Magic-angle spinning (MAS) NMR spectra were recorded on a Bruker AM-400 multinuclear spectrometer, while $Al(H_2O)_6^{3+}$ and tetramethylsilane (TMS) were used as external standards for ^{27}Al and ^{29}Si NMR, respectively. The ^{27}Al MAS NMR was measured at 104.3 MHz at a spinning rate of 4 kHz. Residence times of 0.1 s were allowed between pulse sequences with 0.3 μs, which corresponded to 5° tip, and 5000 free induction decays (FID) were accumulated per sample. The ^{29}Si MAS NMR was measured at 79.50 MHz at a spinning rate of 3 kHz. 10000 FID were accumulated with radio-frequency pulses of 2.3 μs and residence times of 5.0 s.

Results and Discussion

^{27}Al and ^{29}Si NMR spectra of catalyst

Figure 3-22 shows a spectrum of ^{27}Al MAS NMR for the present support of alumina itself. The alumina had two resonances at 68 and 9 ppm with several spinning side bands. The resonances at 68 and 9 ppm correspond to 4- and 6-coordinated aluminum, respectively. The area ratio of 6- to 4-coordinated aluminum was ca. 2, which is consistent with the corresponding value of a spinel type of alumina such as γ-alumina.[8] For samples of silica-deposited alumina, however, the ^{27}Al NMR spectra were the same as those of the alumina support, regardless of silica loading. The results indicate that the coordination number of surface aluminum atoms was unchanged by the deposition of silica.

Figure 3-23 shows the changes in ^{29}Si chemical shifts of the deposited silica for CVD SiO_2/Al_2O_3 catalysts prepared at 240 °C in air. At a silica loading of 2.2 wt%, a broad chemical shift was observed between -70 and -110 ppm. The broad peak may be dominated by a resonance at -85 ppm with some small chemical shifts. The intensities of the chemical shifts at higher-field increased with increasing silica loading. At a silica loading of 12 wt%, two chemical shifts at -91 and -101 ppm predominated, and the chemical shift at -85 ppm was concealed. At a silica loading of 22 wt%, another chemical shift at -110 ppm was observed in addition to the chemical shifts at -91 and -102 ppm. Moreover, no chemical shift due to 6-coordinated silicon[9] was observed between -200 and -220 ppm. The ^{29}Si chemical shifts appeared at each about 10 ppm intervals between -80 and -110 ppm. This suggests that no less than 4 different types of 4-coordinated silicon species were formed on alumina surface.

Figure 3-24 shows the spectra of ^{29}Si NMR of CVD SiO_2/Al_2O_3 catalysts prepared at 300 °C in nitrogen. The intensity of ^{29}Si chemical shift was varied with silica loading in the same manner as observed with the catalyst prepared at 240 °C in air. The major difference between the two series is the chemical shift at

-110 ppm. The CVD catalyst prepared at 300 ^{o}C in nitrogen exhibited this shift, even at a silica loading of 11 wt% (Fig. 3-24b). While the corresponding shift was not observed with the catalyst prepared at 240 ^{o}C in air (Fig. 3-23c). This is attributed to the catalytic activities, and is discussed below.

Relation between catalytic efficiency and ^{29}Si chemical shift

As shown in Figs. 3-9 and 3-10 for the cracking of cumene and the isomerization of 1-butene, respectively, the catalytic activities varied with silica loading, giving maximum activities at silica loadings of 16 and 12 wt% for cumene cracking and 1-butene isomerization, respectively. Interestingly, both catalytic activities were influenced by the conditions of catalyst preparation, in particular by CVD temperature. The catalysts prepared at 240 ^{o}C in air were more active than those prepared at 300 ^{o}C in nitrogen at the same silica loading, although a comparable rate of silica deposition was attained both at 300 ^{o}C in nitrogen and at 240 ^{o}C in air. A similar tendency in catalytic activity has been observed for the dehydration of 2-butanol. The dehydration activity was maximized at a silica loading of 23 wt%, and correlated with the amount of protonic acid, as determined in aqueous solution. Furthermore, other CVD catalysts, which were prepared at 240 ^{o}C by repetitive deposition carried out in nitrogen followed intervals of oxidation at 240 ^{o}C in air, were as active as those prepared at 240 ^{o}C in air (Fig. 3-10). Thus, the catalytic activity is influenced by the preparation conditions, in particular by CVD temperature.

As shown in Fig. 3-11, a cis/trans ratio of the produced 2-butene was varied with silica loading for 1-butene isomerization. For the CVD catalysts prepared at 240 ^{o}C in air, the cis/trans ratio decreased with increasing silica loading up to a silica loading of 12 wt%, and became constant above this loading. At this loading where a trend of change in the cis/trans ratio was altered, the maximum catalytic activity for 1-butene isomerization was obtained, as shown in Fig. 3-10. The fact and

TPD results showed that the type of acid sites varied with silica loading below 12 wt%, and that the number of acid sites decreased with further silica deposition. The activity drop above this critical loading is caused by a decrease in the number of acid sites. For the catalysts prepared at 300 ^{o}C in nitrogen, however, the cis/trans ratio rather monotonically decreased with increasing silica loading. This indicates that the microstructure of the deposited silica was affected by changes in CVD conditions.

Figure 3-25 shows the ^{29}Si MAS NMR spectra of a commercial silica gel. The silica gel showed a broad spectrum of chemical shift around -111 ppm with a shoulder at near -100 ppm (Fig. 3-25a). When the silica gel was calcined at 900 ^{o}C, a sharp peak was observed at -109 ppm (Fig. 3-25b), together with a decrease in specific surface area from 260 to 3 m^2/g. The ^{29}Si chemical shift at -111 ppm corresponds to the reported value of cristobalite (-109.9 ppm),[2] being assigned to a silicon coordinated to four silicate tetrahedra, which is expressed as Si(4Si). In addition, the shoulder around -100 ppm is assigned to a surface silicon attached to three silicate tetrahedra and a hydroxyl group,[10] expressed as Si(3Si,H).

As shown in Fig. 3-23, at least four types of ^{29}Si chemical shifts existed and their intensities varied with silica loading. Moreover, the catalytic activities also varied with silica loading, as illustrated in Figs. 3-9 and 3-10. Active catalysts prepared at 240 ^{o}C in air had no chemical shifts at around -110 ppm at silica loadings up to 12 wt%, while less active catalysts prepared at 300 ^{o}C in nitrogen had a chemical shift at -109 ppm (Fig. 3-24b). At higher silica loadings above 14 wt%, beyond which the catalytic activity for 1-butene isomerization lowered monotonously, the chemical shift at -110 ppm appeared, and its intensity increased with silica loading. These results indicate that the active catalyst had no Si(4Si), and that the increase in the amount of Si(4Si) caused the reduction of the catalytic activity.

An attempt has been made to prepare a silica monolayer on the same kind of alumina as the author used by CVD at 320 ^{o}C under reduced pressure.[11,12] This silica monolayer covered the entire surface of alumina when silica was deposited up to a Si density of 13 nm^{-2}, which corresponded to a silica loading of 19 wt%. It was reported there that the resulting silica monolayer on alumina lacked acidity.

The CVD SiO_2(22 wt%)/Al_2O_3 catalyst in the present study, however, included a large amount of Si(4Si) species on its surface. At least a trilayer of silica must be deposited to generate Si(4Si) species. Since the Si(4Si) existed even at a silica loading of 14 wt%, a large portion of the alumina surface probably remained exposed. For example, the silica loading of 12 wt% corresponds to a surface Si density of 6.8 nm^{-2}. At this loading, not more than one third or one fourth of the alumina surface is covered with the silica bilayer, because a surface Al density of alumina is reported to be in the range from 9.3 to 14.5 nm^{-2}.[8] Accordingly, spot depositions of silica forming a bilayer served as active acid sites. Furthermore, for the CVD SiO_2/Al_2O_3 catalysts prepared at 300 ^{o}C in nitrogen, a greater portion of alumina surface must have been exposed because Si(4Si) was detected even at a lower silica loading of 11 wt% (Fig. 3-24b). These suggests that silica aggregates to form multilayers at higher CVD temperatures.

Microstructure of deposited silica

Maciel *et al.* studied a surface of silica gel by means of cross-polarization NMR,[10] and attributed the ^{29}Si chemical shifts at -109.3, -99.8, and -90.6 to Si(4Si), Si(3Al,H), and Si(2Al,2H), respectively. For substituted silanes,[13] ^{29}Si chemical shifts increased at a extent of about 10 ppm by the replacement of a Si around silicate tetrahedra by a proton. For various zeolites,[3] a lower-field shift of about 4 - 6 ppm in the ^{29}Si NMR spectra was induced by the replacement of a Si around silicate tetrahedra by aluminum.

The assignments of the ^{29}Si chemical shifts of deposited silica are proposed and summarized in Table 3-2, according to the hypothesis that the replacements of Si by Al and proton around the silicate tetrahedra lead to an increase in the ^{29}Si chemical shift of ca. 5 and 10 ppm, respectively, on the basis of a Si(4Si) value of -110 ppm. Although various species are possible, the silicate species underlined in Table 3-2 are most probable. The microstructures of deposited silica are schematically illustrated in Fig. 3-26. At lower silica loadings, the deposited silica is mainly combined with aluminum atoms through oxygen to form Si(2Al,2H), Si(3Al,H), Si(3Al,Si), and Si(2Al,Si,H), which probably show the chemical shifts at -80, -85, -95, and -90 ppm, respectively. Since the ^{29}Si chemical shifts are affected by other factors, such as distortion of the bond angles in the silicon-oxygen tetrahedra and changes in Si-O-Si bond angles together with electrostatic bond strengths of the replaced cations,[1-3] the observed chemical shifts are broadened, as shown in Fig. 3-23a. Further silica deposition leads to multilayered silica, without forming a monolayer. When silica was deposited on the first silica layer, forming a silica bilayer, the ^{29}Si chemical shifts in the first layer were changed by the replacement of proton by Si to form Si(2Si,2Al), which show a chemical shift at -100 ppm. The resulting surface silicon atoms in the second layer such as Si(2Si,2H) and Si(3Si,H) show chemical shifts at -90 and -100 ppm, respectively. Such bilayer species exhibit high catalytic activity for cumene cracking and 1-butene isomerization. Further increases in silica loading introduce Si(4Si) species, and the resulting silica trilayer decrease the amount of acid and the catalytic activity. Although this model does not clarify the location of active Brønsted centers, strong Brønsted acid sites should be delocalized on the surface of catalysts, most likely on the boundary between the deposited silica and the support alumina.

As shown in Fig. 3-24, at a high CVD temperature such as 300 ^{o}C, silica was deposited as multilayers and aggregated readily to

form Si(4Si), owing to the faster and heavier thermal decomposition of the surface ethoxy groups of silica precursor fixed on alumina. Consequently, the deposited silica generated Brønsted acidity, and the exposed alumina surface exhibited Lewis acidity (Fig. 3-15b). At low temperature, e.g. 240 ^{o}C, in the presence of oxygen, the residual ethoxy groups of deposited silica precursor were moderately and effectively decomposed by oxygen, so that silica was highly dispersed on the alumina surface. In conclusion, the present NMR study has correlated the acid catalysis of CVD SiO_2/Al_2O_3 with the structures of the deposited silica species.

References

1. M. Mägi, E. Lippmaa, A. Samoson, G. Engelhardt, and A. R. Grimmer, *J. Phys. Chem.*, **88** (1984) 1518.
2. E. Lippmaa, M. Mägi, A. Samoson, G. Engelhardt, and A. R. Grimmer, *J. Am. Chem. Soc.*, **102** (1980) 4889.
3. J. M. Thomas and J. Klinowski, *Adv. Catal.*, **33** (1985) 199.
4. S. Komarneni, R. Roy, C. A. Fyfe, G. J. Kennedy, and H. Strobl, *J. Am. Ceram. Soc.*, **69** (1986) C42.
5. D. Müller, P. Starke, M. Jank, K. P. Wendlandt, H. Bremer, and G. Scheler, *Z. Anorg. Allg. Chem.*, **517** (1984) 167.
6. L. B. Welsh, J. P. Gilson, and M. J. Gattuso, *Appl. Catal.*, **15** (1985) 327.
7. K. Segawa, Y. Nakajima, S. Nakata, S. Asaoka, and H. Takahashi, *J. Catal.*, **101**, (1986) 81.
8. H. Knözinger and P. Ratnasamy, *Catal. Rev. Sci. Eng.*, **17** (1978) 31.
9. I. L. Mudrakovskii, V. M. Mastikhin, V. P. Shmachkova, and N. S. Kotsarenko, *Chem. Phys. Lett.*, **120** (1985) 424.
10. G. E. Maciel, D. W. Sindorf, and V. J. Bartuska, *J. Am. Chem. Soc.*, **102** (1980) 7606.
11. M. Niwa, T. Hibino, H. Murata, N. Katada, and Y. Murakami, *J. Chem. Soc., Chem. Commun.*, **1989**, 289.
12. M. Niwa, N. Katada, and Y. Murakami, *J.Phys. Chem.*, **94** (1990) 6441.

13. T. Bein, R. F. Carver, R. D. Farlee, and G. D. Stucky, *J. Am. Chem. Soc.*, **110** (1988) 4546.

Table 3-2 Possible microstructures of deposited silica and their proposed ^{29}Si chemical shift values (ppm).

Si(4Si)[a]	-110						
Si(3Si,Al)	-105	Si(3Si,H)[a]	-100				
Si(2Si,2Al)[a]	-100	Si(2Si,Al,H)	-95	Si(2Si,2H)[a]	-90		
Si(Si,3Al)	-95	Si(Si,2Al,H)	-90	Si(Si,Al,2H)	-85	Si(Si,3H)	-80
Si(4Al)	-90						
Si(3Al,Si)[b]	-95	Si(3Al,H)[b]	-85				
Si(2Al,2Si)	-100	Si(2Al,Si,H)[b]	-90	Si(2Al,2H)[b]	-80		
Si(Al,3Si)	-105	Si(Al,2Si,H)	-95	Si(Al,Si,2H)	-85	Si(Al,3H)	-75

Underlined species are: a, most probable at higher silica loading;
b, most probable at lower silica loading.

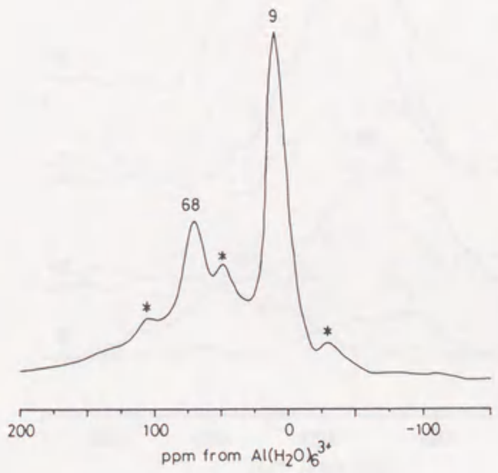

Fig. 3-22. ^{27}Al MAS NMR spectrum for alumina support.
* denotes a spinning side band.

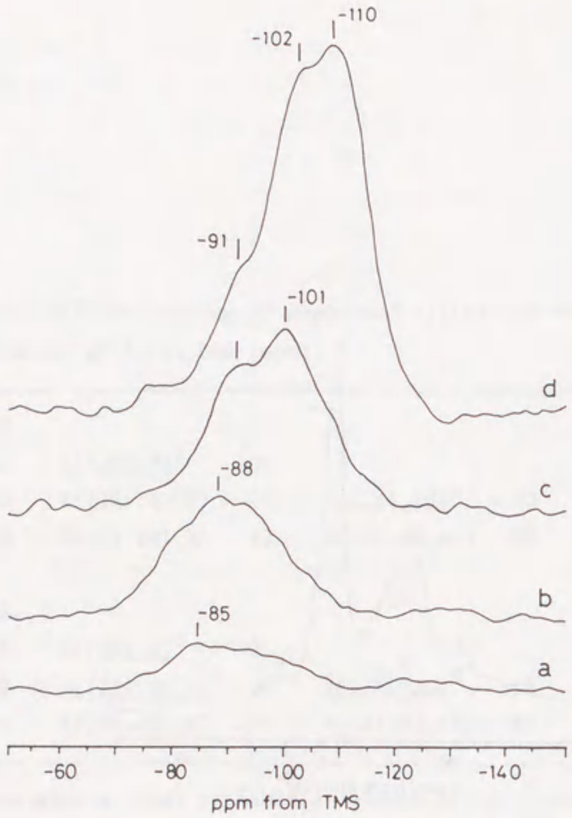

Fig. 3-23. Change in ^{29}Si chemical shifts of silica deposited on alumina.
The CVD catalysts were prepared at 240 ^{o}C in air. Silica loading: a, 2.2 wt%; b, 7.8 wt%; c, 11.8 wt%; d, 22.2 wt%.

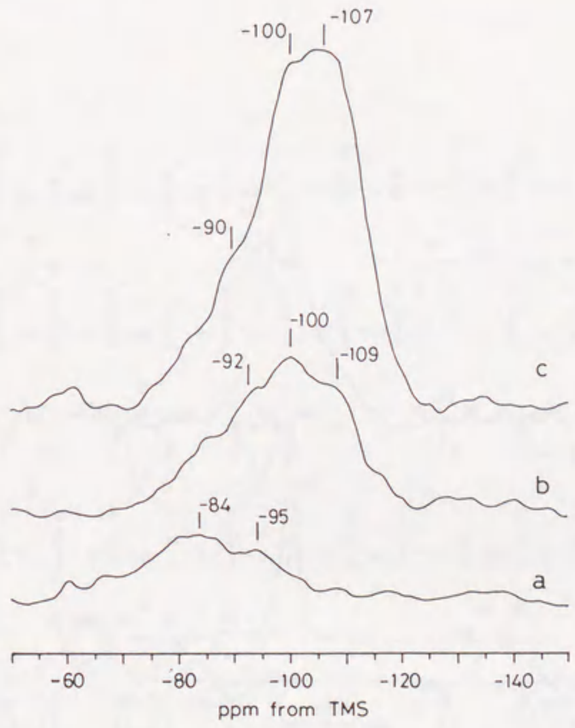

Fig. 3-24. ^{29}Si NMR spectra of CVD SiO_2/Al_2O_3 catalysts prepared at 300 ^{o}C.
Silica loading: a, 2.0 wt%; b, 10.7 wt%; c, 23.1 wt%.

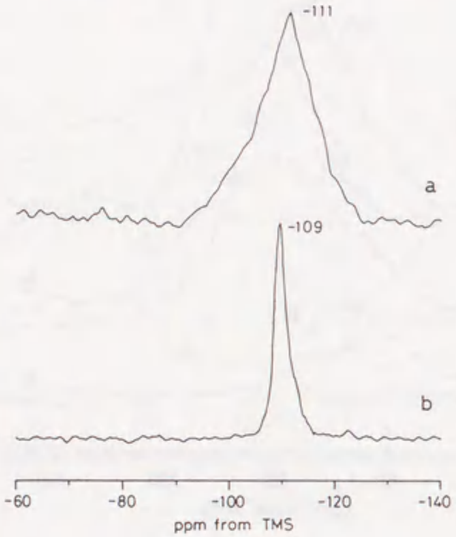

Fig. 3-25. ^{29}Si MAS NMR spectra of silica gel.
a, Silica gel without calcination;
b, calcined at 900 ^{o}C.

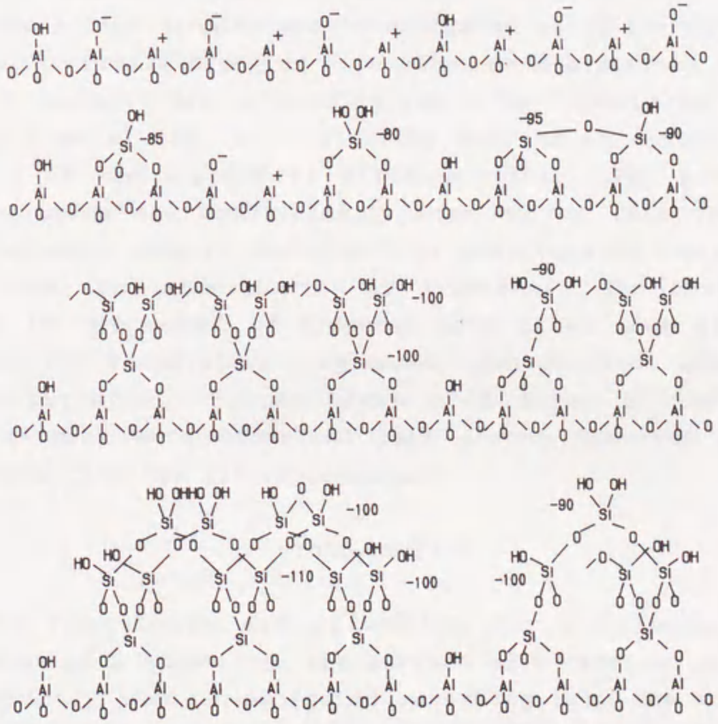

Fig. 3-26. Schematic model for microstructures of deposited silica.
Numbers denote the value predicted for chemical shifts (ppm).

3-4 Deposition of Silica on Amorphous Silica-Alumina

Abstract

The chemical vapor deposition (CVD) of silica onto an amorphous silica-alumina was investigated using tetraethoxysilane in order to create Brønsted acid sites on the surface of original silica-alumina. Silica loading could be readily controlled by the CVD time at 160 ^{o}C; the silica covered an internal wall of mesopore of the support of silica-alumina. The resulting CVD silica-alumina was catalytically more active than the original silica-alumina support for such test reactions as the cracking of cumene and the isomerization of 1-butene. The characteristic changes in the amount of Brønsted acid sites were clarified by means of the temperature-programmed desorption of adsorbed 2,6-dimethylpyridine. Strong Lewis acid sites of the original silica-alumina were converted into strong Brønsted acid sites upon depositing the silica component.

Introduction

CVD techniques are effective for attaining the high dispersion of a deposit on the surface of a catalyst support, and have recently been investigated regarding both the modification and preparation of solid acid catalysts.[1-9] A supported type of silica-alumina catalyst prepared by depositing silica on an alumina surface was described in the previous sections.[5,9] Silica was effectively deposited onto the alumina by using tetraethoxysilane at 240 ^{o}C in the presence of oxygen; silica loading was readily controlled by the deposition time. The obtained alumina-supported silica catalyst was found to have predominantly Brønsted acid sites which are transformed from the Lewis acid sites of an alumina surface. The silica-alumina

catalyst exhibited catalytic activities for several reactions such as cracking, isomerization, and dehydration.

Silica-alumina is an important catalyst for manufacturing various petrochemical products, and is commercially prepared by wet methods, such as co-precipitation and co-gelation. Although the conventional preparation methods are suitable for obtaining a "bulk" level dispersion of the binary oxide component, the respective oxide species do not disperse atomically. Thus, amorphous silica-alumina usually has both Brønsted and Lewis acid sites. In contrast to the wet methods, CVD techniques are attractive for surface modifications used to attain atomical dispersions of other oxide species on the surface of a catalyst support.

If the Lewis acid sites of amorphous silica-alumina can be converted into Brønsted acid sites by the deposition of silica, the catalytic properties must be improved. In this section, the author described various experimental results concerning the CVD of silica onto an amorphous silica-alumina support commercially produced by the co-gelation preparation method. In addition, the author described the acidic character of the CVD silica-alumina catalyst, which has been clarified by means of temperature-programmed desorption (TPD) using 2,6-dimethylpyridine as an adsorbate, together with the pore characteristics.

Experimental

Catalysts. Commercial silica-alumina (N631-L) with a specific surface area of 420 m^2/g, an alumina content of 13 wt%, and a granule size of 24-60 mesh was supplied by Nikki Chemical Co., Ltd.. A CVD silica-alumina catalyst was prepared at the prescribed temperatures by bringing tetraethoxysilane vapor together with a carrier gas into contact with the silica-alumina support in a CVD reactor made up of a Pyrex glass tube rotating in an electrical furnace inclined at 45° (Fig. 1-3);[9] the flow rates of tetraethoxysilane and the carrier gas were 2.7 and 400

mmol/h, respectively. After CVD operation, the sample was calcined at 550 °C for 3h in an air atmosphere. The silica loading was calculated by measuring the weight increase of the CVD samples after calcination.

Catalytic tests. The cracking of cumene was tested at 350 °C using a fixed-bed continuous flow apparatus under atmospheric pressure at a W/F of 28 $g.h.mol^{-1}$, where W is the weight of the catalyst and F is the molar flow rate of cumene, together with a nitrogen carrier gas (15 ml/min). The reactor effluent was analyzed by on-line GLC using a column of Bentone 34 and dinonyl phthalate (1 m).

The isomerization of 1-butene was performed in a closed circulation reactor comprising a circulation volume of 200 ml. After a catalyst (55 mg) had been evacuated at 200 °C for 1 h, the reaction was carried out at 50 °C at an initial pressure of 22 kPa. The products were analyzed by on-line GLC with a VZ-7 column (4.5 m). The isomerization activity was evaluated by the first-order rate constant during the initial reaction period.

Characterization. A BET surface area and pore characteristics were obtained by nitrogen physisorption at -196 °C. The pore volume distribution was calculated using the method of Cranston and Inkley[10] and the desorption isotherm of nitrogen. A T-plot, giving an information about micropores with radii less than 0.35 nm, was also obtained from the desorption isotherm according to the articles by Boer and co-workers.[11-13]

A TPD measurement of the adsorbed pyridine or 2,6-dimethylpyridine was performed in order to evaluate the acidic property. After a sample (10 mg) had been evacuated at 500 °C for 1 h, pyridine was injected at 200 °C; the sample was then evacuated at 200 °C for 1 h. The TPD measurement was run from 200 to 700 °C at a heating rate of 5 °C/min. The desorbed pyridine was bubbled into a conductivity cell containing 0.5 mmol/l of a sulfuric acid solution (30.0 g) together with nitrogen flow (70 ml/min); the amount of desorbed pyridine was monitored by the change in the solution conductivity.[14] The

obtained cumulative curve was differentiated to give an acid strength distribution as a function of desorption temperature.

Results and discussion

Catalyst preparation

Figure 3-27 shows the influence of the CVD temperature and time upon silica loading. In a stream of air, silica loading was increased with the CVD temperature at temperatures below 200 ^{o}C, and maximized at nearly 200 ^{o}C. Above this temperature, the silica loading decreased with the CVD temperature; above 280 ^{o}C the obtained catalyst had a color which varied from brown to black, due to coking. Thus, the optimum CVD temperature was found to be below 200 ^{o}C. At CVD temperature of 160 ^{o}C, the silica loading increased monotonously with the CVD time up to 2 h, and then leveled off. The silica loadings were 0.20 and 0.39 g/g-support for 2 and 8 h, respectively. In a stream of nitrogen, the silica loading also changed with the CVD time at 160 ^{o}C in the same manner as in the presence of oxygen. It can consequently be said that silica loading is readily controlled by the CVD time at 160 ^{o}C. No oxygen was needed for to accelerate the deposition rate at 160 ^{o}C, although oxygen was effective for the acceleration of silica deposition onto an alumina support at 240 ^{o}C.[9] Silica deposition onto silica-alumina occurred at lower temperatures (about 80 degree) compared to that for silica deposition onto an alumina support. In a stream of nitrogen above 200 ^{o}C, silica loading was almost unchanged with the CVD temperature, whereas it varied with the CVD temperature below 200 ^{o}C in a similar way as in air. This observation is presumed to be related to the deposition rate, as will be discussed later.

Physical properties

Changes in the surface area of CVD catalysts with silica loading are shown in Fig. 3-28. For CVD catalysts prepared at 160 ^{o}C, the surface area (based on the unit weight of the

original silica-alumina support) slightly decreased with an increase in silica loading up to a loading of 0.2 g/g-support; it then decreased steeply. For an alumina support which has relatively large mesopores (ranging from 4 to 20 nm in diameter),[9] the deposited silica is uniformly dispersed on the support, since the surface area (based on the unit weight of the alumina support) is almost unchanged, irrespective of the silica loading. For the present silica-alumina, the deposition of silica is considered to be affected by the pore structure of the support. Figure 3-29 shows the pore volume distribution of CVD catalysts together with the original silica-alumina support. The silica-alumina support had 0.47 ml/g of total pore volume and a maximum pore volume at a diameter of about 3.8 nm, which was smaller than that of the alumina support mentioned above. The CVD catalysts had the maximum pore volume at a diameter close to 3.8 nm, although the total pore volume was significantly decreased with silica loading. Furthermore, for CVD catalysts prepared at temperatures higher than 200 ^{o}C in air, the surface area was much smaller than those prepared at 160 ^{o}C (Fig. 3-28). This indicates that aggregated deposition occurred in the neighborhood of the entrance of the micropores of the support; it then followed by the closure of the micropores at higher temperatures in air owing to a too-fast deposition. For a catalyst prepared at 300 ^{o}C in nitrogen, however, the surface area was not so small as those prepared in air. Since oxygen results in an aggregated deposition of silica at high temperatures (above 200 ^{o}C), the surface area steeply decreased.

In order to elucidate the existence of micropores under a diameter of 0.7 nm, a T-plot was examined according to the procedure proposed by Boer *et al.*.[11-13] T-plots for CVD catalysts are shown in Fig. 3-30. A T-plot passes through the origin for a sample having no micropores, whereas it has an intercept which expresses the micropore volume for a sample having micropores.[13] Thus, an original silica-alumina support has no micropores because of the passing through the origin in

the T-plot. For a CVD catalyst with a silica loading of 0.20 g/g-support, micropores (21 ml-S.T.P., which corresponds to a micropore volume of ca. 0.01 ml/g) were generated with a small decrease in the BET surface area (Fig. 3-28b). Further silica deposition (0.39 g/g-support) led to a decrease in the micropore volume (10 ml-S.T.P.) together with a large decrease in the surface area (Figs. 3-28 and 3-30c). The deposition of silica resulted in the formation of micropores in the silica-alumina support. These results indicate that silica deposition develops on the interior wall of mesopore in such a characteristic way that the pore size decreases with silica deposition.

Acidic properties

It has been known that 2,6-dimethylpyridine (2,6-DMP) selectively adsorbs on Brønsted acid sites, but not on Lewis acid sites because of a steric hindrance of two methyl groups, whereas sterically nonhindered pyridine adsorbs on both Brønsted and Lewis acid sites.[15,16] 2,6-DMP has been used for the characterization of acid surfaces with pulse adsorption,[15] IR spectroscopy,[16] and gravimetric titration.[17] Recently, the author applied the TPD measurement of adsorbed 2,6-DMP to the elucidation of the acidic nature of an alumina-supported silica catalyst.[14] This investigation has elucidated that silica deposition creates Brønsted acid sites on the surface of alumina together with the disappearance of Lewis acid sites.

The TPD spectra of adsorbed pyridine and 2,6-DMP are illustrated in Fig. 3-31. The original silica-alumina support had a large desorption peak of pyridine and a somewhat smaller peak of 2,6-DMP than that of pyridine at peak tops of about 300 ^{o}C. Since curve b shows the acid strength distribution of Brønsted acid sites, the difference between curves a and b is a measure of Lewis acid sites. The silica-alumina support dominates Brønsted acid sites with a small amount of Lewis acid sites. This fact is also supported by the ^{31}P-NMR of trimethylphosphine adsorbed on it (Fig. 3-13).[9] In contrast,

for a CVD catalyst loaded 0.20 g/g-support of silica, it had no significant difference between two distribution curves of pyridine and 2,6-DMP. This indicates that the CVD catalyst has dominantly Brønsted acid sites. In addition, the total numbers of acid sites, represented by the amount of desorbed pyridine, were reduced, as can be seen from a comparison of curves c and a. Moreover, the amount of desorbed 2,6-DMP decreased in the low-temperature region, but increased in the high-temperature region, as can be understood from a comparison of curves d and b. This indicates that strong Brønsted acid sites, represented by the desorption of 2,6-DMP at temperatures above 500 ^{o}C, were increased together with a decrease in the total number of Brønsted acid sites.

Figure 3-32 illustrates the changes in the Brønsted acidity, measured by the desorption of 2,6-DMP, with a variation of silica loading; Table 3-3 summarizes the amounts of desorbed pyridine and 2,6-DMP. A small silica loading of 0.11 g/g-support decreased the total amounts of desorbed pyridine and 2,6-DMP. Interestingly, a further silica loading increased the total amounts, and enhanced the Brønsted acid strength. In particular, the number of strong Brønsted acid sites (expressed by the desorption of 2,6-DMP at temperatures above 400 ^{o}C) was maximized at silica loadings near 0.20 g/g-support. Above this loading, the total numbers of desorbed pyridine and 2,6-DMP monotonically decreased with increasing the silica loading. Another catalyst, such as a K^{+} ion-exchanged silica-alumina, which gave no desorption of 2,6-DMP in the temperature region above 400 ^{o}C, exhibited no catalytic activity for 1-butene isomerization.[14] The effective Brønsted acid sites for 1-butene isomerization held 2,6-DMP, even at high temperatures above 400 ^{o}C. The present TPD results indicate that strong Brønsted acid sites were generated upon depositing silica onto strong Lewis acid sites.

Catalytic activities

The catalytic activities were examined for CVD catalysts

prepared at 160 °C. Figure 3-33 shows the change in the cumene-cracking activity with process time at 350 °C. Cumene conversion was significantly improved by depositing silica on the original silica-alumina support. Figure 3-34 depicts the change in the catalytic activity for the cracking of cumene with silica loading, together with the results concerning the isomerization of 1-butene at 50 °C. Since the conversion of cumene decreased with the process time, the cracking activity was evaluated in terms of the average conversion during process times of 1 - 2 h. Cumene conversion increased with increasing silica loading, and attained a maximum at a silica loading of about 0.2 g/g-support. Above this loading, the cracking activity decreased with silica loading. For 1-butene isomerization, the initial first-order rate constant exhibited a maximum at a silica loading of about 0.2 g/g-support. This activity-pattern was similar to that for cumene conversion. Although the original silica-alumina support has essential activities for the reactions, the deposition of silica made it possible to increase the catalytic activities to twice the value for cumene cracking, and three times that for 1-butene isomerization, compared with the activity levels of the original silica-alumina support. In addition, with regard to the product distribution of 1-butene isomerization, the ratio of cis-/trans-2-butene was slightly decreased (from 0.95 to 0.83) with an increase in the silica loading, compared to the values at 1-butene conversion of 50 %.

It is worth noting that the silica loading of a 0.2 g/g-support, at which catalytic activities were maximized, is equal to the loading at which the rate of silica deposition decelerated (Fig. 3-27), the loading at which the strong Brønsted acid sites were maximized (Fig. 3-32 and Table 3-3), and the loading at which the surface area steeply decreased (Fig. 3-28). Below this critical loading, the catalytic activity for 1-butene isomerization was apparently unchanged (Fig. 3-34b). For the cracking of cumene, however, the cumene conversion increased with increasing silica loading (Fig. 3-34a). Since the pretreatment

conditions for the cracking of cumene were different from those for the isomerization of 1-butene, the surface acidities are presumed to be different from each other. On the other hand, above the critical loading, the decreasing features in both the deposition rate and the catalytic activities are in fair agreement with the decreasing pattern in strong Brønsted acidity of the CVD silica-alumina catalyst.

In view of practical usage, the present CVD catalyst was compared with an alumina-supported silica catalyst dealt with in section 3-1.[9,14] For the isomerization of 1-butene, the alumina-supported silica catalyst was active, even at a low temperature of 0 °C (Table 3-1),[14] and superior to the present CVD catalyst. This shows no discrepancy with the fact reported by Imizu and Tada.[8] In contrast, for the cracking of cumene, the present CVD silica-alumina catalyst was much preferable because even the original support was superior to the alumina-supported silica catalyst (Table 3-1).[9] It is interesting that the enhanced activities vary regarding reaction type.

Formation of active site on silica-alumina surface

Although the original silica-alumina support, itself, has Brønsted acidity, an optimal silica deposit results in an increase in the number of strong Brønsted acid sites as well as enhancements in catalytic activity. The superiority of CVD catalysts for catalytic reactions is presumably caused by an increase in the number of Brønsted acid sites for CVD catalysts. When alumina is used as a support, these features are much clearer.[5,9,14] Since an alumina surface almost comprises Lewis acid sites, Brønsted acid sites are effectively generated by the deposition of silica. The resulting alumina-supported silica shows significant catalytic activities for various reactions, whereas the alumina support showed few activities by itself. An excess of the silica deposit, however, weakened strong Brønsted acid sites.[14]

The present silica-alumina support originally had not only

strong Brønsted acid sites but also Lewis acid sites.[9] A small amount of silica loading decreased the number of strong Brønsted acid sites (Fig. 3-32b). Prior to CVD operation, a support was heated at a low temperature of 160 ^{o}C in a stream of carrier gas, so that strong Lewis acid sites could be hydrated to form hydroxyl groups. Silica deposits proceed via an ester exchange of tetraethoxysilane with the surface hydroxyl groups. During the initial stage of deposition, a silica deposit is mainly initiated on strong Brønsted acid sites, and contributes to a weakening of the acid strength. After the original Brønsted acid sites are weakened, further silica deposition induces a transformation of Lewis acid sites into Brønsted acid sites. Furthermore, an excess of silica deposits weaken Brønsted acid sites. Consequently, strong Brønsted acid sites were maximized at silica loadings close to 0.2 g/g-support, as shown in Table 3-3. Such Lewis acid sites are probably localized not on isolated alumina in the original silica-alumina, but on the boundary between silica and alumina. If Lewis acid sites exist on isolated alumina, the cis/trans ratio of produced 2-butene for 1-butene isomerization should be increased from 1 to close to about 2.5 (Fig. 3-11), which has been reported for silica overlayers deposited on alumina.[8,18] The ratio actually decreased to less than 1 for the present CVD silica-alumina. The difference in Lewis acidity of support materials results in variations of the catalytic properties for the above-mentioned reactions.

In conclusion, an enhancement of catalytic efficiency was achieved by depositing silica onto amorphous silica-alumina. This favorable nature should be attributed to an additional formation of Brønsted acid sites which are ascribable to the transformation of Lewis acid sites through the CVD process.

References

1. M. Niwa, S. Kato, T. Hattori, and Y. Murakami, *J. Chem. Soc., Faraday Trans. 1*, **80** (1984) 3135.

2. S. Sato, K. Urabe, and Y. Izumi, *J. Catal.*, **102** (1986) 99.
3. S. Sato, S. Hasebe, H. Sakurai K. Urabe, and Y. Izumi, *Appl. Catal.*, **29** (1987) 107.
4. T. Okuhara and J. M. White, *Appl. Surf. Sci.*, **29** (1987) 223.
5. S. Sato, M. Toita, Y. Q. Yu, T. Sodesawa, and F. Nozaki, *Chem. Lett.*, **1987**, 1535.
6. Y. Imizu, A. Tada, and I. Toyoshima, *Shokubai (Catalyst)*, **30** (1988) 388.
7. M. Niwa, T. Hibino, H. Murata, N. Katada, and Y. Murakami, *J. Chem. Soc., Chem. Commun.*, **1989**, 289.
8. Y. Imizu and A. Tada, *Chem. Lett.*, **1989**, 1793.
9. S. Sato, M. Toita, T. Sodesawa, and F. Nozaki, *Appl. Catal.*, **62** (1990) 73.
10. R. W. Cranston and F. A. Inkley, *Adv. Catal.*, **9** (1957) 143.
11. B. C. Lippens, B. G. Linsen, and J. H. de Bore, *J. Catal.*, **3** (1964) 32.
12. B. C. Lippens and J. H. de Bore, *J. Catal.*, **4** (1965) 319.
13. J. H. de Bore, B. G. Linsen, Th. van der Plas, and G. J. Zondervan, *J. Catal.*, **4** (1965) 649.
14. S. Sato, M. Tokumitsu, T. Sodesawa, and F. Nozaki, *Bull. Chem. Soc. Jpn.*, **64** (1991) 1005.
15. H. A. Benesi, *J. Catal.*, **28** (1973) 176.
16. A. Corma, C. Rodellas, and V. Fornes, *J. Catal.*, **88** (1984) 374.
17. L. L. Murrell, and N. C. Dispenziere, Jr., *J. Catal.*, **117** (1989) 275.
18. S. Sato, T. Sodesawa, F. Nozaki, and H. Shoji, *J. Mol. Catal.*, **66** (1991) 343.

Table 3-3. Amounts of pyridine and 2,6-dimethylpyridine desorbed from catalysts

Catalyst (loading)[a]	Adsorbate	Amount (μmol/g-support) total	400 - 500[b]	>500[b]
Support (0)	pyridine	190	44	35
	2,6-DMP	126	33	7
CVD (0.11)	pyridine	102	18	12
	2,6-DMP	84	17	5
CVD (0.20)	pyridine	130	28	25
	2,6-DMP	108	29	13
CVD (0.30)	pyridine	99	30	17
	2,6-DMP	84	26	10
CVD (0.39)	pyridine	62	14	11
	2,6-DMP	58	17	10

a, silica loading (g/g-support);
b, desorption temperature (^{o}C).

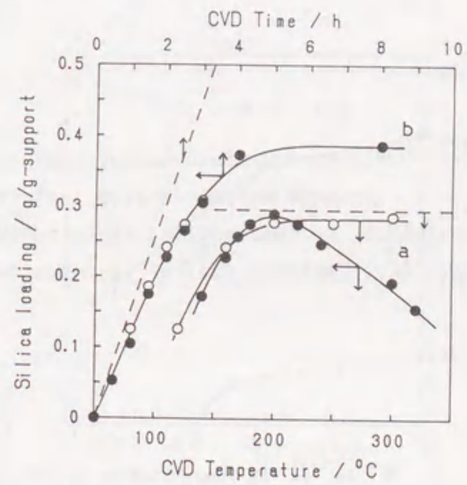

Fig. 3-27. Effect of CVD temperature and time.
a, CVD was operated for 2 h; b, CVD was operated at 160 ^{o}C;
●, CVD was operated in air; ○, in nitrogen.
Dashed line denotes the critical deposition amount limited by an amount of fed tetraethoxysilane.

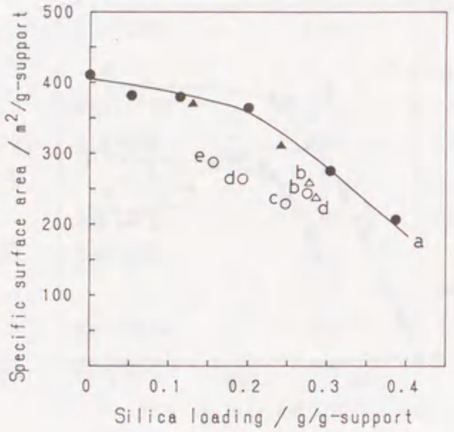

Fig. 3-28. Change in the surface area of a CVD catalyst with silica loading.

●, ○, CVD was operated in air; ▲, △, in nitrogen.
a (solid line), prepared at 160°C; b, 200 °C; c, 240 °C;
d, 300 °C; e, 320 °C.

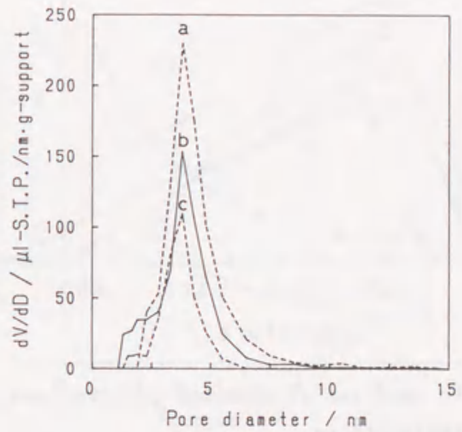

Fig. 3-29. Pore volume distribution of CVD catalysts.
a, Original silica-alumina support;
b, CVD catalyst (silica loading, 0.20 g/g-support);
c, CVD catalyst (silica loading, 0.39 g/g-support).

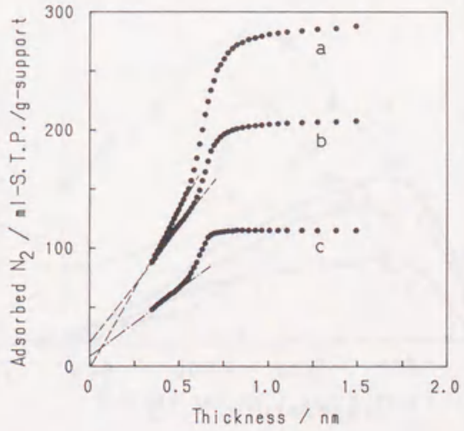

Fig. 3-30. T-plot for CVD catalysts.
Symbols as those in Fig. 3-29.

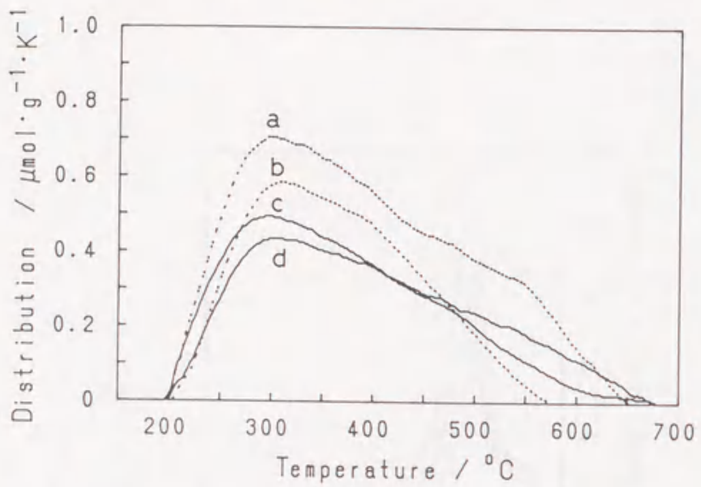

Fig. 3-31. TPD profiles of adsorbed pyridine and 2,6-dimethylpyridine.
Original silica-alumina support (dotted line):
a, pyridine; b, 2,6-DMP;
CVD catalyst (silica loading, 0.20 g/g-support):
c, pyridine; d, 2,6-DMP.

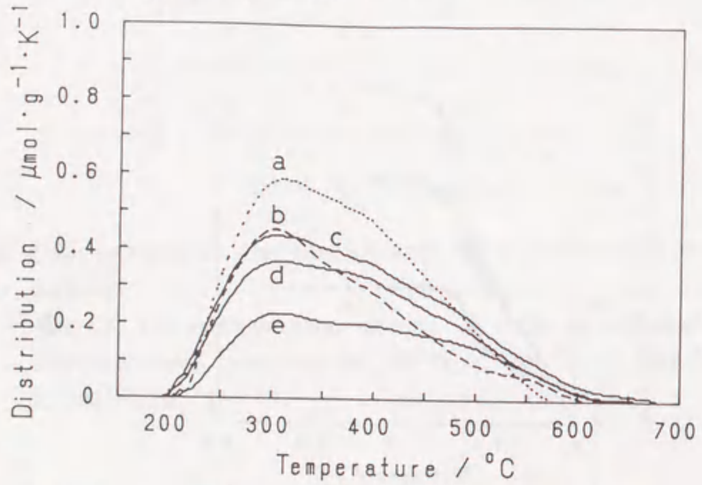

Fig. 3-32. TPD profiles of 2,6-dimethylpyridine.
a, Original silica-alumina support (dotted line);
b, CVD catalyst (dashed line): silica loading, 0.10;
c, 0.20; d, 0.30; e, 0.39 g/g-support.

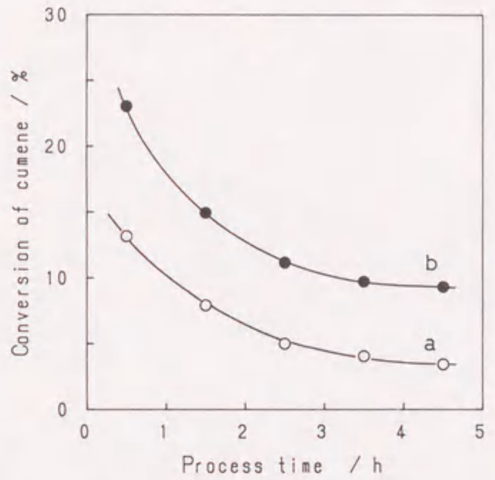

Fig. 3-33. Cumene conversion with process time.
a, Original silica-alumina support;
b, CVD catalyst (silica loading, 0.20 g/g-support).

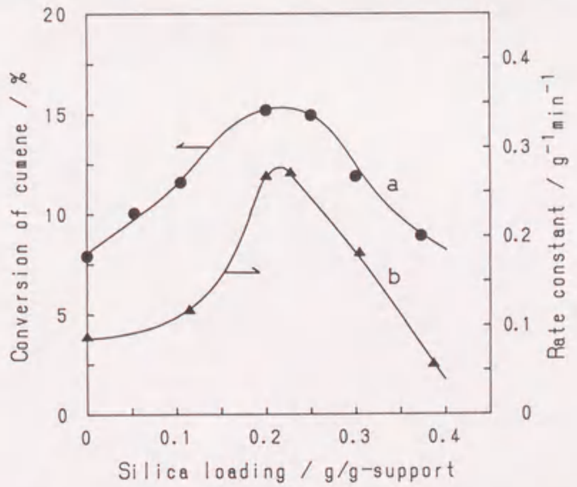

Fig. 3-34. Changes in the catalytic activities with silica loading.
a, Cumene cracking at 350 °C;
b, 1-butene isomerization at 50 °C.

Chapter 4. Silica-Supported Boron Phosphate Catalyst

Abstract

A silica-supported boron phosphate (BPO_4) catalyst was prepared by chemical vapor deposition (CVD) using mixtures of boron triethoxide and phosphoryl trimethoxide. Both the amount and the P/B ratio of deposited BPO_4 were changed with the CVD temperature and time. At the optimum CVD temperature of 300 ^{o}C, the amount of deposited BPO_4 linearly increased with the CVD time. When alkoxide mixtures with the desired P/B ratio were used as CVD sources at 300 ^{o}C, the expected P/B ratios were available. At CVD temperatures below 300 ^{o}C, neither a sufficient amount nor a desired P/B ratio was given. On the other hand, above 325 ^{o}C, the deposition was suppressed by blocking the micropore of silica, especially for long-time CVD operation, owing to the too fast deposition. Although the resulting surface compound was amorphous, it was revealed to have micro-structures of BPO_4 by means of a ^{31}P NMR measurement. The amorphous BPO_4 dispersed highly on silica exhibited a high catalytic efficiency for the isomerization of 1-butene and a simultaneous oligomerization of 1-butene in comparison with a catalyst prepared by the conventional impregnation method.

Introduction

Boron phosphate (BPO_4) is known to be a solid acid which is an effective catalyst for various organic reactions such as hydration,[1] dehydration,[2-5] alkylation,[6-8] and oligomerization.[9,10] The catalytic activities depend on the ratio P/B. In a region including excess phosphorus, BPO_4 catalysts have a large percentage of Brønsted acid sites,[2,11] and exhibit catalytic activities for such reactions as the

hydration of ethylene,[1] the dehydration of ethanol to ethylene,[2] and the oligomerization of 1-decene.[10] In contrast, in a region including excess boron, BPO_4 catalysts consist predominately of Lewis acid sites,[2,11] and show catalytic efficiencies for the dehydration of ethanol to diethyl ether,[2] the dehydration of 2-methylbutanal to isoprene,[5] the ethylation of phenol,[8] and the Beckmann rearrangement of cyclohexanone oxime.[2] Unsupported BPO_4, however, has a relatively small surface area and its catalytic activity is often poor. Whereas BPO_4 with surface areas of more than 100 m^2/g have been reported,[12,13] carefulness is required for any reproducible preparation. In addition, it is difficult to impregnate a support material with uniform BPO_4 because of its poor solubility.

In the previous chapters, several attempts have been made to prepare a supported type of solid acids such as silica-supported boria,[14] alumina-supported boria,[15] and alumina-supported silica[16,17] by means of chemical vapor deposition (CVD) using the respective metal alkoxides. The alkoxides were easily decomposed into the respective metal oxide on the surface of the support in the presence of oxygen. The highly dispersed boria catalysts, having a weak interaction with the support materials, exhibited an excellent catalytic efficiency for a vapor-phase Beckmann rearrangement of cyclohexanone oxime.[14,15] The alumina-supported silica, having a strong interaction between the silica and alumina to form composite-oxides on the surface of alumina support, showed high catalytic activities for several organic reactions such as cracking, isomerization, and dehydration,[16,17] which was comparable to those of commercial silica-alumina catalyst.

In this chapter, the author described about the deposition of binary-oxides, for a example, a silica-supported boron phosphate catalyst (CVD BPO_4/SiO_2) prepared by the simultaneous deposition of boron and phosphorus components onto a silica surface. The deposition behavior of boron phosphate was examined

by using a mixed vapor of boron triethoxide and phosphoryl trimethoxide, compared to the individual deposition of the respective oxide. In addition, both the structural and catalytic properties of the deposited boron phosphate were investigated.

Experimental

Catalysts. A CVD BPO_4/SiO_2 catalyst was prepared by bringing a mixture of boron triethoxide ($B(OEt)_3$) and phosphoryl trimethoxide ($PO(OMe)_3$) into contact with a silica (ID type gel supplied by Fuji Davison Chemical Ltd.: surface area, 145 m^2/g; pore volume, 1.0 ml/g; particle size, 0.1 - 0.6 mm) in a CVD reactor described in Fig. 1-3.[17] The mixture of alkoxides with the prescribed P/B ratio, containing 5 wt% methanol, was supplied together with air as a carrier gas (400 mmol/h) at a flow rate of 1.7 - 2.4 mmol/h. Both the BPO_4 loading and the P/B ratio in the catalyst sample were determined by the alkalimetric titration of H_3BO_3 and H_3PO_4, which were extracted from the sample with hot water. The extracted H_3PO_4 was titrated with sodium hydroxide, followed by titration of the extracted H_3BO_3, whose acidity was strengthened by addition of mannitol.

An impregnation catalyst (IMP BPO_4/SiO_2) was obtained by immersing a silica support in an aqueous solution of H_3BO_3 and H_3PO_4, drying at 110 ^oC and calcining at 300 ^oC for 2 h.

Catalytic test. Isomerization of 1-butene was carried out in a closed circulation system (reactor volume: 250 ml, catalyst: 0.2 g) with a butene initial pressure of 19 kPa at 50 ^oC. Prior to the reaction, a catalyst was heated in the reactor at 500 ^oC for 1 h under reduced pressure (0.1 Pa). The catalytic performance for the isomerization of 1-butene was evaluated by the 1st-order rate constant during the initial reaction period, and for a simultaneous side reaction of 1-butene oligomerization, forming mainly C_8 olefins by a conversion which was calculated from the pressure drop in the circulation system after the reaction had proceeded for 1 h.

Characterization. An X-ray diffractogram (XRD) was recorded using a Rigaku Geiger Flex. A ^{31}P magic angle-spinning (MAS) NMR measurement was performed at 161.98 MHz at a spinning rate of 4 kHz with a Bruker AM-400, while H_3PO_4 was used as an external standard. Time intervals of 2 s were allowed between pulse sequences with 4 μs and 500 free induction decays were accumulated for each sample. The samples were used for the measurement without any further pretreatment.

The amount of chemisorbed ammonia was measured using a static volumetric method. Prior to adsorption, 0.5 g of the catalyst was evacuated at 500 ^{o}C for 1 h. A first adsorption of ammonia was performed at the prescribed temperature at pressures of about 1.2 kPa, followed by several repetitions of adsorption until obtaining a final pressure of 6.6 kPa. The amounts of physisorbed and chemisorbed ammonia were estimated by extrapolating the given isotherm. The physisorbed ammonia was desorbed by evacuating the sample at the same temperature as in the first adsorption for 1 h; then, only the physisorbed ammonia was measured with the second adsorption. The amount of chemisorbed ammonia was evaluated by the difference between the first and second adsorption of ammonia.

Results and Discussion

Deposition of boron phosphate

Figures 4-1 and 4-2 show the effects of the CVD temperature upon BPO_4 deposition for a source P/B ratio of 1. For a CVD time of 3 h or above, the BPO_4 loading exhibited a maximum at a CVD temperature of 300 ^{o}C, while the BPO_4 loading slightly increased with increasing CVD temperature for CVD times of 1 and 2 h (Fig. 4-1). This is related to the change in surface area of the catalyst, and is discussed later. At 300 ^{o}C, the BPO_4 loading was increased monotonously with a CVD time up to a maximum of 0.96 g/g-silica for 5 h. Such a large loading could not be realized by the impregnation method. The P/B ratio in the

catalyst changed with both the CVD temperature and time (Fig. 4-2). At CVD temperatures below 300 ^{o}C, especially for a short CVD time, the P/B ratio became smaller than 1. At 300 ^{o}C and above, however, the P/B ratio nearly equaled 1. Therefore, both the sufficient deposition rate and the expected P/B ratio were attained at 300 ^{o}C.

Figure 4-3 shows a comparison of the individual deposition with a simultaneous deposition of both the boron and phosphorus components. When either $B(OEt)_3$ or $PO(OMe)_3$ was fed individually, the deposition behavior of individual oxides was similar to each other. At a CVD temperature of 325 ^{o}C, either B_2O_3 or P_2O_5 was readily deposited on SiO_2, whereas at temperatures lower than 325 ^{o}C, the individual oxides were slowly deposited. In contrast to individual deposition, the simultaneous deposition of boron and phosphorus components satisfactorily proceeded, even at 275 ^{o}C with a P/B ratio of 1. The simultaneous supply of alkoxides drastically lowered the deposition temperature, and the deposition of BPO_4 proceeded with an excess boron component at 250 ^{o}C at which the individual oxides could hardly be deposited. Although oxygen accelerated the deposition rate of individual oxide, such as B_2O_3,[14] BPO_4 was deposited on silica even at 300 ^{o}C in the absence of oxygen. Moreover, both B_2O_3/SiO_2 and P_2O_5/SiO_2 prepared by CVD using the corresponding alkoxides at 350 ^{o}C were inactive for the isomerization of 1-butene, while the BPO_4/SiO_2 prepared at 300 ^{o}C was catalytically active. These results indicate that the deposition of BPO_4 occurred on the surface of silica with an accompanying formation of boron phosphate.

Figures 4-4 and 4-5 show the effects of the P/B ratio in the CVD source upon BPO_4 deposition. At an optimum CVD temperature of 300 ^{o}C, the BPO_4 loading almost reached the maximum deposition expressed by dashed lines for each CVD time (Fig. 4-4). Furthermore, the P/B ratio in the catalyst nearly equaled the source P/B ratio, whereas an excess boron component was deposited for a short CVD time of 1 h (Fig. 4-5). Consequently, BPO_4 with

the desired P/B ratio could be deposited on a silica support at 300 ^{o}C by controlling the source P/B ratio in the range between 0.7 and 1.4.

Structure of deposited boron phosphate

Figure 4-6 shows changes in specific surface area with BPO_4 loading. For CVD BPO_4/SiO_2 catalysts prepared at 300 ^{o}C, the surface area based on the unit weight of the silica support did not change, even at a BPO_4 loading of 0.6 g/g-silica, whereas those of the impregnation catalysts linearly decreased with an increase in BPO_4 loading. Above the loading of 0.6 g/g-silica, however, it steeply decreased with an increase in BPO_4 loading. On the other hand, for CVD catalysts prepared at 350 ^{o}C, the surface area decreased with BPO_4 loading in a similar manner as those of IMP BPO_4/SiO_2 catalysts. As shown in Fig. 4-1, BPO_4 loading decreased at high CVD temperatures. This fact is speculated to be caused by concentrated deposition onto the entrance of the micropore of the support, followed by a closure of the micropore. These findings in Figs. 4-1 and 4-6 suggest that a uniform deposition of BPO_4 was attained at 300 ^{o}C, owing to an optimum deposition rate of BPO_4.

Figure 4-7 illustrates the XRD spectra of BPO_4 catalysts. An unsupported BPO_4 exhibited sharp crystalline diffraction peaks at 2θ = 24.5 ^{o}, 40.0 ^{o}, and 49.0 ^{o} attributed to a cristobalite-type structure[2] (Fig. 4-7a). An IMP BPO_4/SiO_2 catalyst also showed the same diffraction patterns as unsupported BPO_4 with low crystallinity, even after drying at 110 ^{o}C (Fig. 4-7b). None of the CVD BPO_4/SiO_2 catalysts, however, showed any diffraction peaks, indicating that the BPO_4 deposited on silica was amorphous.

The ^{31}P MAS NMR of the catalyst was measured in order to elucidate the amorphous phase of deposited BPO_4. For a P/B ratio of 1, an unsupported crystalline BPO_4 showed a sharp resonance at -29.6 ppm together with two small signals at 0.4 and -21.7 ppm (Fig. 4-8a). The chemical shift at -29.6 ppm is a characteristic

signal for a crystalline BPO_4, which is considered to be caused by a phosphate anion tetrahedrally coordinated by four boron atoms. An additional shift at 0.4 ppm may be attributed to a free phosphate anion, such as phosphoric acid. The silica-supported P_2O_5 had two characteristic chemical shifts at -43.9 and 0.3 ppm (Fig. 4-8b). The chemical shifts of P_2O_5 are quite different from those of BPO_4.

For a P/B ratio of 1.1, the ^{31}P MAS NMR spectra of BPO_4 catalysts are shown in Fig. 4-9. Both the unsupported BPO_4 and the IMP BPO_4/SiO_2 had three chemical shifts at -29.5, -21.5, and 0.4 ppm (Fig. 4-9a and b) in similar manner as for Fig. 4-8a. An increase in the phosphorus content weakened the intensity of the shift at -29.2 ppm, and strengthened that at 0.4 ppm. The CVD BPO_4/SiO_2 had two other signals at -14.3 and -7.4 ppm in addition to the above-mentioned three chemical shifts (Fig. 4-9c). Further, the chemical shift at 0.4 ppm was split into two signals at 0 and 1.1 ppm. These five chemical shifts, except for that at 1.1 ppm, each appeared at about 7.2 ppm intervals between -29.1 and 0 ppm. For chemical shifts of ^{29}Si in aluminosilicates, the most characteristic trend is that substitution of the Si ions in silicate tetrahedra by Al ions leads to low-field shifts at each 4 to 6 ppm intervals.[18] The five ^{31}P chemical sifts suggest that not less than 5 different types of phosphate tetrahedra existed on the surface of the CVD BPO_4/SiO_2 catalyst. These results indicate that amorphous composite oxides, having micro-structures of BPO_4, were highly dispersed on silica for the CVD catalyst.

Catalytic activity of CVD BPO_4/SiO_2

The catalytic activity for the isomerization of 1-butene was affected by the P/B ratio in the CVD BPO_4/SiO_2 catalyst prepared at 300 ^{o}C (Fig. 4-10). In the region of excess phosphorus, the activity was much higher than that in the region of excess boron, and the maximum activity was obtained at a P/B ratio near 1.1. The trans/cis ratio of product 2-butene ranged from 1.0 to 1.3 at

a 1-butene conversion level of 50 %, irrespective of the P/B ratio. In addition to isomerization, a small amount of butene dimers was produced with passing of the reaction time. The conversions of 1-butene to oligomers were 10 - 29 % after the reaction had proceeded for 1 h. In order to clarify the catalytic behavior for oligomerization, the reaction was performed at lower temperatures. Since the isomerization activity was suppressed, the essential oligomerization activity appeared at 0 ^{o}C (Fig. 4-11). The maximum oligomerization activity was also observed at a P/B ratio near 1.1. This result is consistent with the catalytic behavior of unsupported BPO_4 for the liquid-phase oligomerization of 1-decene.[10)]

Figure 4-12 shows a comparison of CVD BPO_4/SiO_2 with the IMP BPO_4/SiO_2 catalyst regarding catalytic activity in 1-butene isomerization. For the CVD catalyst with a P/B ratio of 1, the isomerization activity increased with BPO_4 loading, passed through a maximum and then decreased above a loading of 0.6 g/g-silica. The decrease in the activity was considered to be caused by a closure of the micropore of the support, as has been described in connection with the results of the change in the specific surface area with BPO_4 loading (Fig. 4-6). The CVD catalysts, especially for the P/B ratio of 1.1, were much more active than both the IMP BPO_4/SiO_2 catalysts and the unsupported BPO_4 (P/B = 1.1) whose rate constant for 1-butene isomerization was 89 h^{-1}.g-catalyst^{-1}. In addition, for the oligomerization activity, the CVD catalysts were also more active than both IMP BPO_4/SiO_2 and unsupported BPO_4 whose conversions were 6 - 9 % at 50 ^{o}C (Fig. 4-10).

In order to evaluate the acid amount of catalyst, the amount of chemisorbed ammonia was measured volumetrically (Table 4-1). Irrespective of the P/B ratio, the amounts of ammonia chemisorbed on CVD catalysts were almost unchanged. The changes in the catalytic activity with the P/B ratio (Figs. 4-10 and 4-11) are not attributable to the acid amount, but probably to acid type (Brønsted or Lewis acid) of catalyst.[2,11)] However, it has been

clearly demonstrated that the acid amount of the CVD BPO_4/SiO_2 catalyst is much larger than those of both IMP BPO_4/SiO_2 and unsupported BPO_4. This tentatively explains the superiority of the CVD catalyst for the reactions mentioned above.

In conclusion, amorphous boron phosphate was deposited on a silica support with the desired P/B ratio and with high dispersion by means of a CVD method. The resulting CVD BPO_4/SiO_2 catalyst was superior to the impregnation catalyst for the isomerization of 1-butene and the simultaneous side reaction of oligomerization.

References

1. R. Tartarelli, M. Giorgini, A. Lucchesi, G. Stoppato, and F. Moreli, *J. Catal.*, 17 (1970) 41.
2. J. Haber and U. Szybalska, *Faraday Discuss. Chem. Soc.*, 72 (1981) 263.
3. J. B. Moffat, *Catal. Rev. Sci. Eng.*, 18 (1978) 199.
4. S. S. Jewur and J. B. Moffat, *J. Catal.*, 57 (1979) 167.
5. J. B. Moffat and A. Schmidtmeyer, *Appl. Catal.*, 28 (1986) 161.
6. F. Nozaki and I. Kimura, *Bull. Chem. Soc. Jpn.*, 50 (1977) 614.
7. T. Sodesawa, I. Kimura, and F. Nozaki, *Bull. Chem. Soc. Jpn.*, 52 (1979) 2431.
8. J. Morey, J. M. Marinas, and J. V. Sinisterra, *React. Kinet. Catal. Lett.*, 22 (1983) 175.
9. Y. Imizu, S. Aoyama, H. Itoh, and A. Tada, *Chem. Lett.*, 1981, 1455.
10. A. Tada, H. Suzuka, and Y. Imizu, *Chem. Lett.*, 1987, 423.
11. H. Miyata and J. B. Moffat, *J. Catal.*, 62 (1980) 357.
12. H. L. Goltz and J. B. Moffat, *J. Catal.*, 22 (1971) 85.
13. J. B. Moffat and J. F. Neeleman, *J. Catal.*, 31 (1973) 274.
14. S. Sato, K. Urabe, and Y. Izumi, *J. Catal.*, 102 (1986) 99.
15. S. Sato, S. Hasebe, H. Sakurai, K. Urabe, and Y. Izumi, *Appl. Catal.*, 29 (1987) 107.
16. S. Sato, M. Toita, Y. Q. Yu, T. Sodesawa, and F. Nozaki, *Chem. Lett.*, 1987, 1535.
17. S. Sato, M. Toita, T. Sodesawa, and F. Nozaki, *Appl. Catal.*, 62 (1990)

73.
18. J. M. Thomas and J. Klimowski, *Adv. Catal.*, 33 (1985) 199.

Table 4-1. Acid amount measured by ammonia adsorption.

BPO_4 catalyst (P/B ratio)		Content wt%	Adsorbed amount (mmol/g) 150 °C[a]	300 °C[a]
CVD	(1.0)	28	-	0.12
CVD	(0.83)	27	0.34	0.13
CVD	(1.1)	29	0.39	0.13
Impregnation	(1.1)	30	0.22	0.11
Unsupported	(1.1)	100	0.08	0.04

a, adsorption temperature of ammonia.

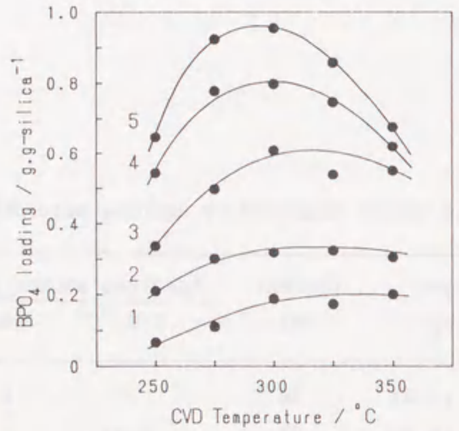

Fig. 4-1. Effect of CVD temperature and time on the BPO_4 deposition.
P/B ratio in CVD source is 1. Numbers show the CVD time (h).

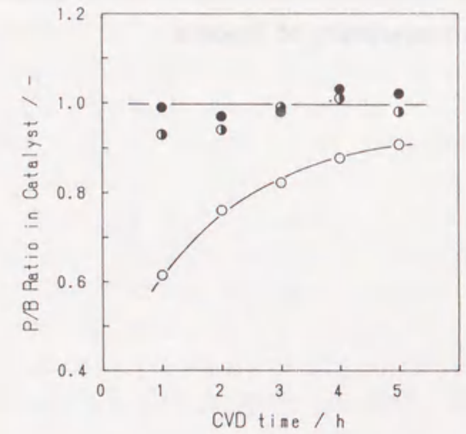

Fig. 4-2. Change in P/B ratio with CVD time.
○, prepared at 250 °C; ◑, 300 °C; ●, 350 °C.
P/B ratio in CVD source is 1.

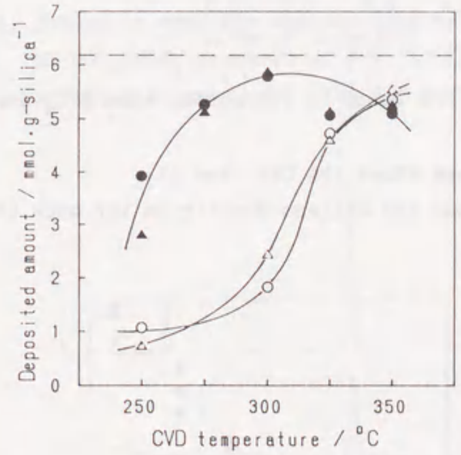

Fig. 4-3. Comparison of individual deposition with simultaneous deposition of B_2O_3 and P_2O_5.
○, B in B_2O_3/SiO_2; △, P in P_2O_5/SiO_2;
●, B; ▲, P in CVD BPO_4/SiO_2 (P/B = 1).
Dashed line shows the maximum deposition.

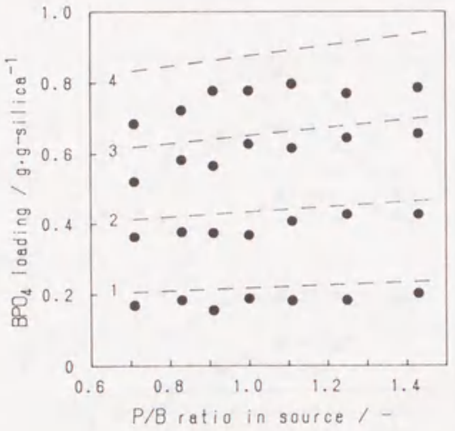

Fig. 4-4. Effect of P/B ratio in CVD source upon BPO_4 deposition at 300 °C.
Numbers in Figure shows the CVD time (h).
Dashed line shows the maximum deposition for each CVD time.

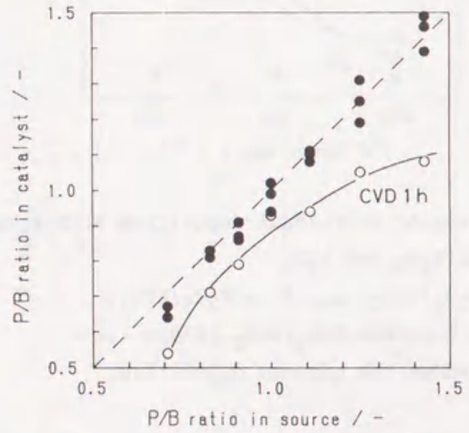

Fig. 4-5. Effect of P/B ratio in CVD source on P/B ratio in deposited BPO_4.
Dashed line shows the controlled composition of deposition.

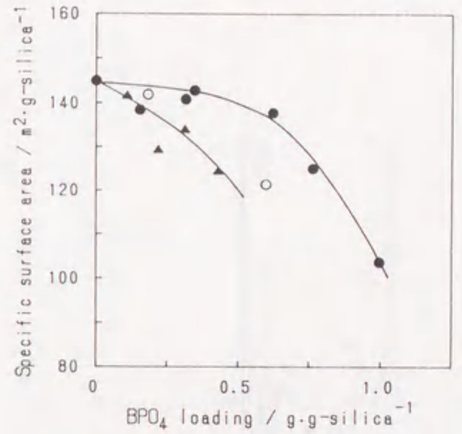

Fig. 4-6. Change in specific surface area with BPO_4 loading.
●, CVD BPO_4/SiO_2 prepared at 300 °C; ○, at 350 °C;
▲, impregnation catalyst. The P/B ratio is 1.

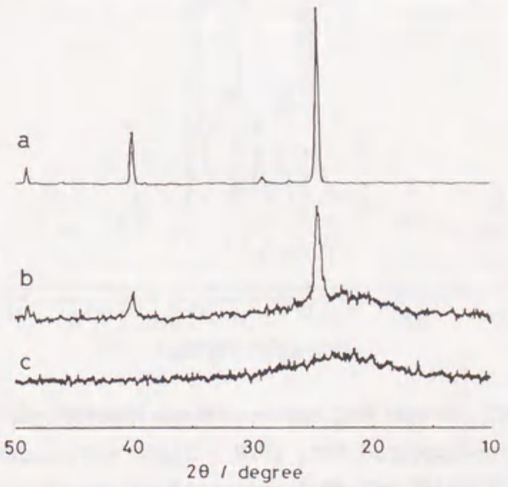

Fig. 4-7. XRD spectra of catalysts prepared under different conditions.
a, unsupported BPO_4 (P/B = 1);
b, BPO_4(36 wt%)/SiO_2 prepared by impregnation;
c, BPO_4(36 wt%)/SiO_2 prepared by CVD.

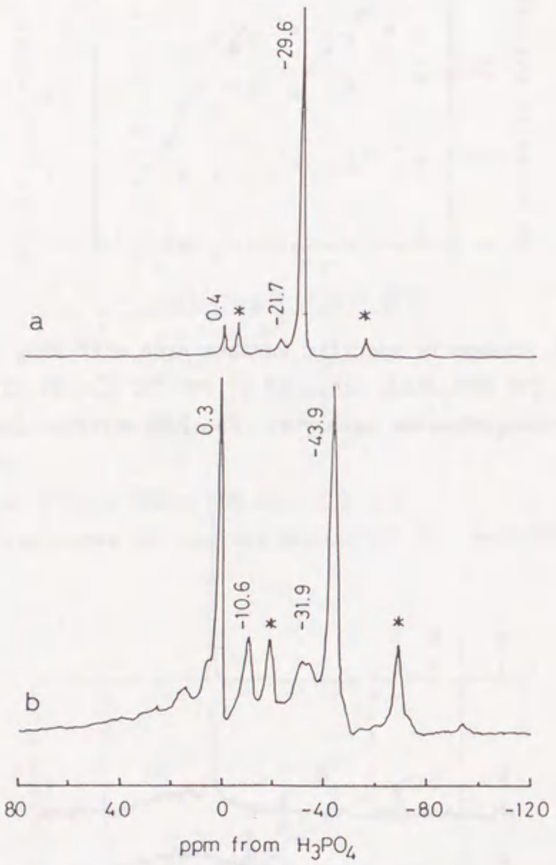

Fig. 4-8. ^{31}P MAS NMR spectra of phosphate catalysts.
a, unsupported BPO_4 (P/B = 1);
b, P_2O_5(20 wt%)/SiO_2 prepared by impregnation.
* denotes a spinning side band.

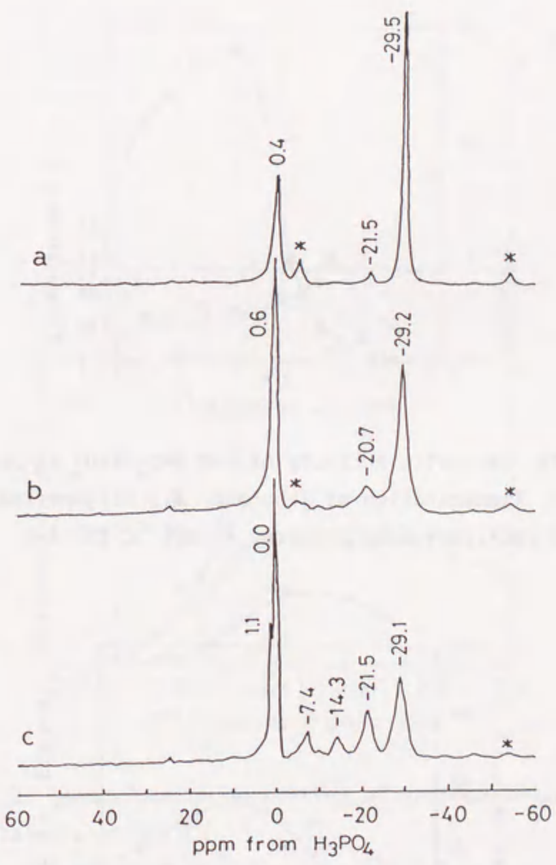

Fig. 4-9. ^{31}P MAS NMR spectra of BPO_4 (P/B = 1.1) catalysts.
a, unsupported BPO_4;
b, BPO_4(20 wt%)/SiO_2 prepared by impregnation;
c, BPO_4(36 wt%)/SiO_2 prepared by CVD.
* denotes a spinning side band.

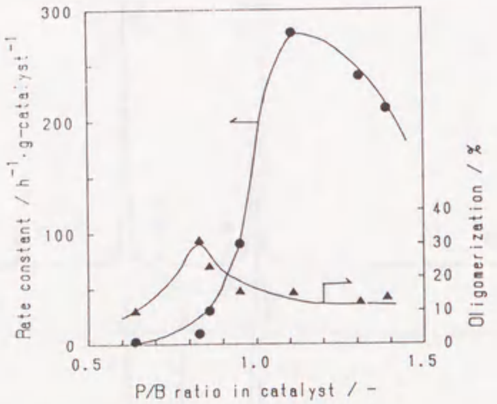

Fig. 4-10. Catalytic activity of CVD BPO_4/SiO_2 at 50 °C.
●, Isomerization of 1-butene; ▲, oligomerization.
CVD catalysts were prepared at 300 °C for 2 h.

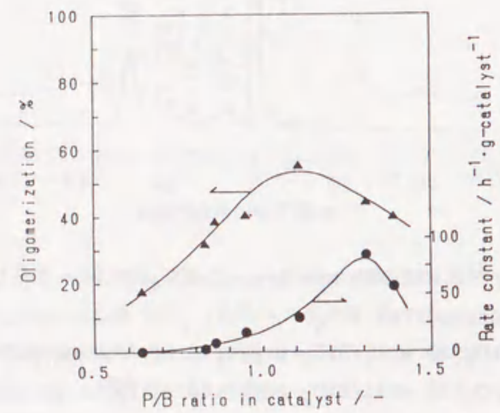

Fig. 4-11. Oligomerization activity of CVD BPO_4/SiO_2 at 0 °C.
Symbols as those in Fig. 4-10.

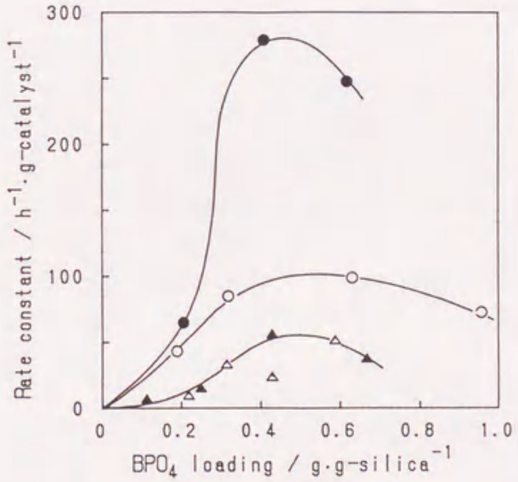

Fig. 4-12. Isomerization activities of various BPO_4/SiO_2 catalysts at 50 °C.
●, CVD catalyst of P/B = 1.1; ○, P/B = 1.
▲, Impregnation catalyst of P/B = 1.1; △, P/B = 1.

Chapter 5. Deposition Behavior of Metal Oxides

Abstract

Deposition behaviors characteristic of metal oxides in the preparation of solid acid catalysts were summarized. Effect of support material on the deposition behaviors was also discussed. Deposition of single metal oxides such as boria and silica was greatly influenced by the acidic properties of support surface. The deposition rate increased with increasing acid strength of support surface. The simultaneous supply of a mixture of alkoxides drastically lowered the temperature required for deposition of individual oxides. At an optimum CVD temperature, the amount of deposit was readily controlled by the CVD time, and a desired molar ratio of binary oxides was obtained by adjusting the molar ratio of the alkoxides. To minimize the concentration gradient for the source alkoxides and to make uniform deposition of oxides on the pore surface, deposition should be carried out at the lowest possible temperatures. In addition, for the catalyst preparation by a rotary-type CVD reactor, an appropriate rate of rotation of the support bed was effective for leveling concentration gradient for the source alkoxide vapor.

Introduction

In the previous chapters, the preparation of solid acids such as supported boria, silica, and boron phosphate catalysts has been described, and the catalytic and physical properties of the resulting catalysts were individually investigated in detail. In every case, deposit loadings were affected by CVD temperature, time, and atmosphere. An optimum CVD temperature was intrinsic for the kinds of both deposit and support.[1-8] For example, silica was effectively deposited on alumina using

tetraethoxysilane at 240 °C in the presence of oxygen.[5,6] Catalytic properties of the resulting solid acids were also greatly influenced by the CVD conditions. In addition, the catalytic properties were also affected by the type of CVD reactor employed for preparation.

In this chapter, deposition behaviors characteristic of metal oxides in the preparation of solid acid catalysts and the effect of support materials on the deposition behaviors are discussed. The effect of mixing up of support particles is also described in the experiment using a rotary-type CVD apparatus.

Experimental

Deposition. A CVD operation was performed in a fixed-bed reactor, as shown in Fig. 1-2.[3] Another CVD operation was also performed in a rotary-type reactor, as shown in Fig. 1-3.[6] The objective materials were prepared by bringing vapors of respective alkoxides, such as boron triethoxide ($B(OEt)_3$), phosphoryl trimethoxide ($PO(OMe)_3$), and silicon tetraethoxide ($Si(OEt)_4$), into contact with 24 - 60 mesh granules of the following support materials, such as alumina, silica, and silica-alumina at the prescribed temperature in a stream of carrier gas, air or nitrogen. The details of individual CVD procedure and the results of catalytic reactions and physical properties are described in the previous chapters.

Support materials. For the deposition of boria, three types of catalyst support were employed. A specific silica support (Fuji Davison Chemical, ID type gel: surface area, 281 m^2/g; pore volume, 1.35 ml/g.) was used for the preparation of boria-silica in a fixed-bed CVD reactor shown in Fig. 1-2. An alumina (JRC,[9] ALO-1: surface area, 160 m^2/g; pore volume, 0.67 ml/g.) was used as a catalyst support for the preparation of boria-alumina in the fixed-bed reactor. Another alumina (Shokubai Kasei, ACBM: surface area, 210 m^2/g; pore volume, 1.0 ml/g.) was also used for the preparation of boria-alumina using a rotary-type CVD reactor

shown in Fig. 1-3.

The following support materials were used as supports for the silica deposition using the rotary CVD reactor. An alumina (DC-2282: specific surface area, 203 m^2/g; pore volume, 0.72 ml/g.) was supplied by Dia Catalyst & Chemicals Ltd.. Amorphous silica-aluminas (N631-L: specific surface area, 420 m^2/g; alumina content, 13 wt%. N631-H: specific surface area, 360 m^2/g; alumina content, 27 wt%.) were commercially supplied by Nikki Chemical Co., Ltd.. A Na^+ ion-exchanged sample was prepared by immersing 10 g of N631-L in sodium nitrate or sodium hydroxide solution (100 ml) at room temperature for 2 h followed by filtration, washing, and drying at 100 °C for 20 h.

A silica gel (Fuji Davison Chemical Ltd., ID type: surface area, 145 m^2/g; pore volume, 1.0 ml/g) was used for the deposition of boron phosphate in the rotary CVD reactor.

Results and Discussion

Deposition behaviors of single metal oxides

Every deposit material examined in this thesis required an optimum temperature for CVD. The optimum CVD temperature is a temperature at which deposition is realized on the whole surface of support without diffusion limitation through the micropores of support. The amount of the respective metal oxide deposit increased linearly with CVD time at an optimum temperature. Therefore, the metal oxide loading was readily controlled by the CVD time. The optimum CVD temperatures are summarized in Table 5-1 for several deposits and supports examined in this thesis. The optimum CVD temperatures differ from one another depending on the combination of deposit and support material.

The preparative method of silica- and alumina-supported boria catalysts was described in chapter 2.[1-4] The influence of CVD temperature upon the boria deposition is illustrated in Fig. 5-1. The temperature dependence upon the deposition of boria onto silica is different from that onto alumina. Over silica

support, boria loading increased steeply at a temperature beyond 300 ^{o}C. In contrast, boria was deposited on alumina even at a low temperature of 225 ^{o}C. The deposition rate of boria on alumina is obviously higher than that on silica (Fig. 5-2).

The property of CVD catalyst obtained was dependent not only on the nature of the oxide deposit itself but also on the kind of support. Silica-supported boria catalyst is composed of boria and silica showing no strong interaction each other. The surface acidity was attributed to the boria deposited on silica whose acid strength is relatively weak.[1,3] On the other hand, for alumina-supported boria, there exists strong interaction between boria and alumina to generate strong Brønsted acidity at low boria contents (ca. 12 wt%).[2,10] At high boria contents, however, the interaction between boria and alumina is weakened with increasing boria deposit, and the catalytic property of the resulting alumina-supported boria resembled to that of silica-supported boria catalyst.[2,4] The acid strength of course decreased with increasing boria content.

Deposition of silica was described in chapter 3.[5,6,8] Optimum deposition temperatures were also affected by the kind of support materials such as alumina and amorphous silica-alumina for the deposition of silica. The silica deposition essentially produces binary mixed oxides of silica-alumina over the support materials. The differences in deposition behavior are influenced by the acidity of support surface and frequently pore structure.

Figure 5-3 shows the effect of acidity of support surface upon silica deposition.[11] Both the number and the strength of acid sites on an amorphous silica-alumina decreased with increasing the degree of ion-exchange of the proton of the support with sodium cation. Over the Na^{+} ion-exchanged silica-alumina, an optimum temperature of silica deposition increased with increasing the amount of Na^{+} ion-exchanged, that is with a decrease in acidity of the support surface. This corresponds with the results over several zeolites: pore-opening size of protonic zeolites is finely controlled by silica deposition at

low temperature.[12-14] The deposition of metal oxides takes place around the acidic sites; the stronger acid sites the support has, the lower the optimum deposition temperature becomes.

Figure 5-4 illustrates temperature dependence of silica deposition over some supports.[11] Silica deposition onto alumina occurred at a higher temperature by about 80 degrees compared to those onto amorphous silica-alumina supports. This is also explained by the surface acidity; strong Lewis acid sites were not exposed on the surface of the alumina preheated at 240 ^{o}C, while strong Brønsted acid sites were generated on the surface of the silica-alumina (section 3-2). In addition, for two silica-aluminas with different alumina contents, optimum CVD temperatures differ from each other. On a silica-alumina support (N631-L) which possessed strong Brønsted acid sites, silica was readily deposited at lower temperatures than on another silica-alumina support N631-H which has a large number of relatively weak Brønsted acid sites (Fig. 5-5).[6,11]

At 160 ^{o}C in a stream of nitrogen, silica loading on N631-L was changed with the CVD time in the same manner as in the presence of oxygen (Fig. 3-27).[8] No oxygen was needed to accelerate the deposition rate at a temperature lower than 200 ^{o}C. At a temperature above 200 ^{o}C, however, oxygen accelerate the deposition. Because the acceleration caused a closure of mesopore of N631-L, the silica loading did not increase with CVD temperature above 200 ^{o}C (Fig. 3-27). Oxygen was certainly effective for acceleration of silica deposition onto an alumina support at a temperature above 200 ^{o}C (Fig. 3-1).[6] Oxygen probably acts as an accelerator for the decomposition of $Si(OEt)_4$ on the surface of support above 200 ^{o}C.

Deposition of binary oxide

A silica-supported boron phosphate (BPO_4) catalyst was prepared by CVD using a mixture of boron triethoxide and phosphoryl trimethoxide as mentioned in chapter 4.[7] Both the

amount and the P/B ratio of deposited BPO_4 were changed with CVD temperature and CVD time (Figs. 4-1, 4-2, 4-4, and 4-5). At an optimum CVD temperature of 300 ^{o}C, the amount of deposited BPO_4 was linearly increased with CVD time (Fig. 4-1). The P/B ratio of the binary oxide deposit could be adjusted as desired through CVD at 300 ^{o}C using an alkoxide mixture with the same P/B ratio (Fig. 4-5). At CVD temperatures below 300 ^{o}C, neither a sufficient amount nor a desired P/B ratio was achieved.

As shown in Fig. 4-3, individual deposition of B_2O_3 and P_2O_5 was significantly different from the deposition of BPO_4. When either $B(OEt)_3$ or $PO(OMe)_3$ was fed individually, the deposition behaviors of the oxides were similar to each other. At a CVD temperature of 325 ^{o}C, both B_2O_3 and P_2O_5 were readily deposited on silica, whereas they were slowly deposited at temperatures lower than 325 ^{o}C. In contrast to individual deposition, simultaneous deposition of B_2O_3 and P_2O_5 satisfactorily proceeded to produce BPO_4 even at 275 ^{o}C. Simultaneous supply of the alkoxides drastically lowered deposition temperature; the deposition of BPO_4 proceeded with an excess boron component at 250 ^{o}C at which both B_2O_3 and P_2O_5 could hardly be deposited individually. In addition, BPO_4 was deposited on silica even in the absence of oxygen at 300 ^{o}C whereas oxygen accelerated the rate at the deposition of individual oxides.

In SiO_2-P_2O_5 system, the behavior in simultaneous deposition of silicon and phosphorus oxides onto silica is similar to that of B_2O_3-P_2O_5 system.[15] Simultaneous supply of silicon and phosphorus alkoxides also greatly lowered CVD temperature; the optimum CVD temperature was in the range between 275 and 300 ^{o}C while phosphorus oxide was individually deposited most efficiently at 325 ^{o}C.[7]

Consequently, the deposition rate of binary metal oxides is faster than that of the individual deposition of the respective oxides. At an optimum CVD temperature, the amount of the deposit was readily controlled by CVD time, and its molar ratio was adjusted as desired using a mixture of the respective alkoxides

with the same molar ratio.

Effect of rotation of CVD reactor in catalyst preparation

The deposition of boria onto silica and alumina was described in chapter 2. When boria was deposited onto silica support at relatively high CVD temperature of 400 ^{o}C in the fixed-bed reactor (Fig. 1-2),[3] much more amount of boria was deposited on the upper side than on the lower side of the support silica bed. This undesirable phenomenon was probably due to an increase in concentration gradient for alkoxide source caused by high deposition rate at a temperature higher than the optimum temperature. Since ununiformity between upper and lower beds is large at higher temperatures in the fixed-bed CVD reactor, deposition should be carried out at the lowest possible temperature.

In order to assure more uniform deposition of boria onto silica throughout the support bed, it seems efficient to mix up support granules or to fluidize support powders. Thus, the effect of rotation of CVD reactor was examined for the preparation of alumina-supported boria catalyst using a rotary-type CVD apparatus.

Table 5-2 shows the influence of rotation of CVD reactor upon the boria deposition onto alumina.[16] The rotation slightly affected the amount of boria loading and the catalytic activity of the resulting samples. The boria loading slightly increased with increasing rotation up to a rate of 120 rpm (revolutions per minute). The vapor-phase Beckmann rearrangement of cyclohexanone oxime was efficiently catalyzed by the alumina-supported boria catalysts (section 2-2). The selectivity to lactam was increased with increasing rotation up to 80 rpm. Since the rotation leveled the concentration gradient of feed through the support bed, the rotation was effective in mixing up support particles. Too fast rotation, however, induced ununiform deposition because the granules of support were rotated together with the CVD reactor to affect no agitation of support; thus a decrease in

uniformity of boria deposit decreased the lactam selectivity. Consequently, appropriate rotation is effective for leveling the concentration gradient of feed through the support bed.

Although the rotation procedure is effective for agitation of support particularly at high CVD temperatures at which the concentration gradient of source alkoxide was large, there still remains a problem of diffusion of reactant in the pore of support. Deposition is limited by diffusion in the pore of support at high temperatures even in a region A labeled in Fig. 1-1. At high temperatures, concentrated deposition occurred near the entrance of pore because of diffusion limitation of the reactant alkoxide. This has been discussed in sections 3-1, 3-4, and chapter 4.

In the catalyst preparation through CVD process, it is noted that deposition should be carried out at the lowest possible temperatures even in a rotary-type CVD reactor in order to minimize the concentration gradient for the source alkoxide and to make uniform deposition on the surface of pores.

References

1. S. Sato, H. Sakurai, K. Urabe, and Y. Izumi, *Chem. Lett.*, **1985**, 277.
2. H. Sakurai, S. Sato, K. Urabe, and Y. Izumi, *Chem. Lett.*, **1985**, 1783.
3. S. Sato, K. Urabe, and Y. Izumi, *J. Catal.*, **102** (1986) 99.
4. S. Sato, S. Hasebe, H. Sakurai, K. Urabe, and Y. Izumi, *Appl. Catal.*, **29** (1987) 107.
5. S. Sato, M. Toita, Y. Q. Yu, T. Sodesawa, and F. Nozaki, *Chem. Lett.*, **1987**, 1535.
6. S. Sato, M. Toita, T. Sodesawa, and F. Nozaki, *Appl. Catal.*, **62** (1990) 73.
7. S. Sato, M. Hasegawa, T. Sodesawa, and F. Nozaki, *Bull. Chem. Soc. Jpn.*, **64** (1991) 516.
8. S. Sato, M. Hiratsuka, T. Sodesawa, and F. Nozaki, *Bull. Chem. Soc. Jpn.*, **64** (1991) 2214.
9. A reference catalyst of The Catalysis Society of Japan (JRC).
10. Y. Izumi and T. Shiba, *Bull. Chem. Soc. Jpn.*, **37** (1964) 1797.
11. M. Hiratsuka, S. Sato, T. Sodesawa, and F. Nozaki, *Proc. 62nd. Catal. Soc. Jpn.*, (1988) 3D204, 324.
12. M. Niwa, S. Kato, T. Hattori, and Y. Murakami, *J. Chem. Soc. Faraday Trans. 1*, **80** (1984) 3145.
13. M. Niwa and Y. Murakami, *Nippon Kagaku Kaishi*, **1989**, 410.
14. H. Itoh, S. Okamoto, and A. Furuta, *Nippon Kagaku Kaishi*, **1989**, 420.
15. T. Urahata, S. Sato, T. Sodesawa, and F. Nozaki, *Proc. 66th. Catal. Soc. Jpn.*, (1990) 4L201, 62.
16. S. Hasebe, S.Sato, K. Urabe, and Y. Izumi, unpublished results.

Table 5-1. Optimum temperature for deposition of various materials.

Deposit	Optimum CVD temperature on various supports (°C)		
	Silica	Alumina	Silica-Alumina
Boria	350[a]	250[b]	-
Silica	-	240[a]	160[b]

CVD was performed under air flow conditions.

[a] Oxygen acted as an accelerator of deposition.

[b] Oxygen did not act as an accelerator of deposition.

Table 5-2. Effect of rotation in the CVD catalyst preparation of B_2O_3/Al_2O_3.

Revolution (rpm)	B_2O_3 content (wt%)	Conversion of oxime (%)	Selectivity to lactam (mol%)
0	18.5	100	85.2
40	19.5	100	92.8
80	20.6	100	95.4
120	21.1	100	90.4

CVD was operated in a rotary reactor (Fig. 1-3). $B(OEt)_3$ vapor (3.5 mmol/h) and air (115 ml/min) was brought into contact with an alumina (ACBM) support at 250 °C for 3 h. The Beckmann rearrangement of cyclohexanone oxime: 300 °C; WHSV, 0.81 h^{-1} based on the oxime; oxime:benzene:N_2 = 1:13:16.

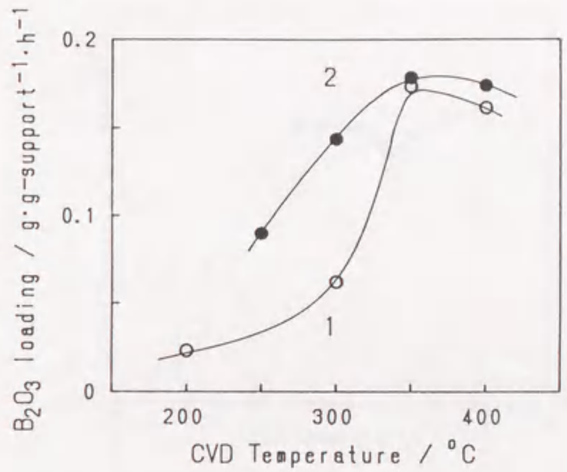

Fig. 5-1. Effect of CVD temperature upon the deposition of boria.
Flow rate of $B(OEt)_3$, 3.5 mmol/h; air, 113 ml/min;
1, silica support (ID gel, 3 h); 2, alumina (ALO-1, 2 h).

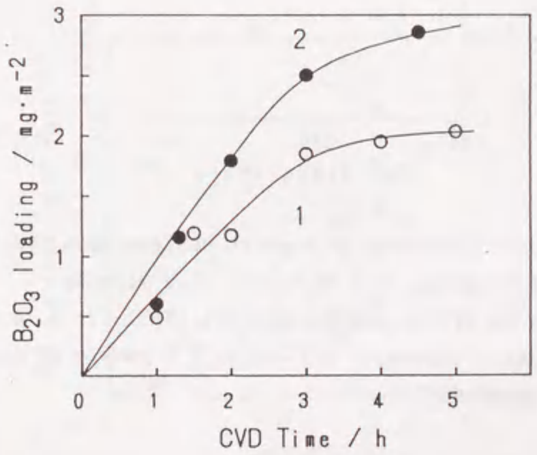

Fig. 5-2. Effect of CVD time upon the deposition of boria.
Flow rate of $B(OEt)_3$, 3.5 mmol/h; air, 113 ml/min;
1, silica support (ID gel, 350 °C); 2, alumina (ALO-1, 300 °C).

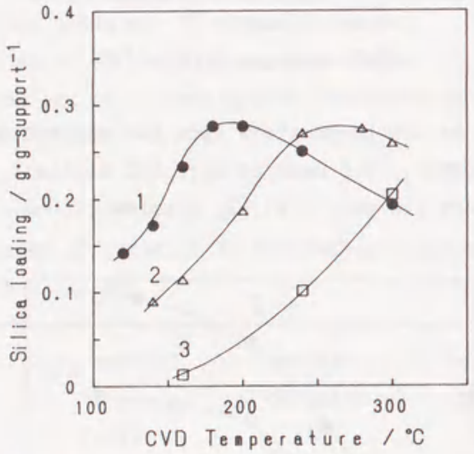

Fig. 5-3. Effect of acidity of support surface upon the deposition.
Flow rate of $Si(OEt)_4$, 0.6 ml/h; air, 113 ml/min;
1, deposited on silica-alumina support (N631-L); 2, 0.18 mmol/g of sodium cation-exchanged N631-L; 3, 2.1 mmol/g of sodium cation-exchanged N631-L.

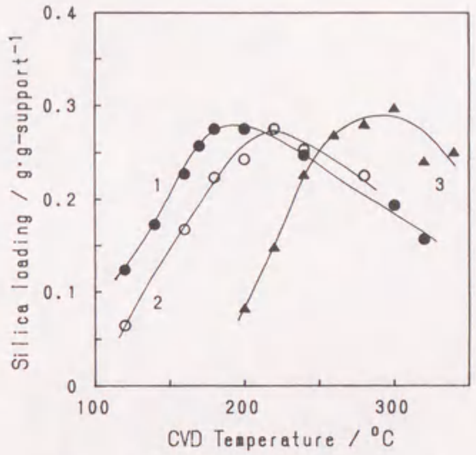

Fig. 5-4. Effect of CVD temperature upon the deposition of silica.
Flow rate of $Si(OEt)_4$, 0.6 ml/h; air, 113 ml/min;
1, deposited on silica-alumina support (N631-L) for 2 h;
2, N631-H; 3,alumina support (ALO-4).

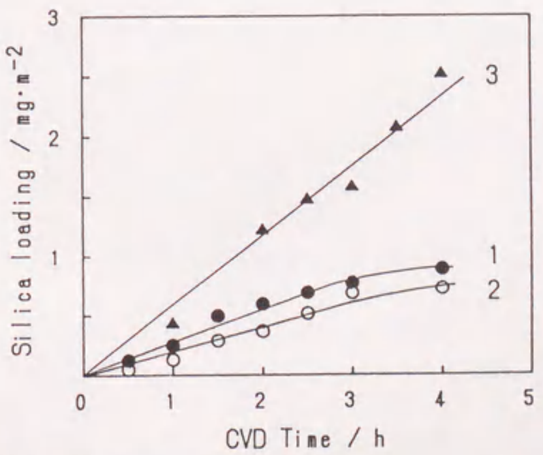

Fig. 5-5. Effect of CVD time upon the deposition of silica.
Flow rate of $Si(OEt)_4$, 0.6 ml/h; air, 113 ml/min;
1, deposited on silica-alumina support (N631-L) at 160 °C;
2, N631-H at 160 °C; 3,alumina support (ALO-4) at 240 °C.

6. Summary and General Conclusion

The author has investigated the preparation of solid acids using CVD technique and the catalytic properties of the resulting solid acids, then clarified the relation between their catalytic and acidic properties. Various types of metal oxides deposited on support materials were found to be effective for many kinds of catalytic reactions. The main results are summarized as follows.

In section 2-1, a CVD method was introduced to catalyst preparation which involved the deposition of triethylborate onto silica in air to produce a silica-supported boria (CVD B_2O_3/SiO_2). The resulting CVD B_2O_3/SiO_2 showed high catalytic efficiency for the vapor-phase Beckmann rearrangement of cyclohexanone oxime even at 250 ^{o}C (conversion of oxime: 98 %, selectivity to ε-caprolactam: 96 mol%, at a boria content of 34 wt%). The CVD catalyst was more active and selective at any boria contents than the boria-silica obtained by the ordinary impregnation method using boric acid. The number of acid sites whose acid strengths exceeded 80 kJ/mol in terms of the differential heat of adsorption of ammonia were 0.7 and 0.4 mmol/g for the most active CVD catalyst and the most active impregnation catalyst, respectively. The CVD effected uniform deposition of boria on silica, and produced a solid acid with relatively uniform distribution of acid strength.

In section 2-2, alumina-supported boria (CVD B_2O_3/Al_2O_3) catalysts were prepared by CVD technique using triethylborate in the presence of oxygen under atmospheric pressure. Both acidic and catalytic properties of the resulting CVD B_2O_3/Al_2O_3 greatly changed with boria content. At boria contents less than 12 wt%, both boria-alumina ($H_o \geq -8.2$) obtained by CVD and impregnation methods showed almost the same catalytic activity for the isomerization of m-xylene. In contrast to the case of low boria content, the CVD B_2O_3/Al_2O_3 ($H_o \geq -3.0$) exhibited higher

catalytic efficiency, e.g. for the vapor-phase Beckmann rearrangement of cyclohexanone oxime at boria contents higher than 15 wt%. In particular, at a boria content of 25 wt%, the complete oxime conversion (100 %) and high lactam selectivity (95 - 98 mol%) were obtained at 300 ^{o}C. The CVD B_2O_3/Al_2O_3 excelled the counterpart obtained by means of the conventional impregnation method in selectivity for the lactam. The results of microscopic observation and surface area measurement suggested that the high lactam selectivity of the CVD catalyst was probably due to uniform dispersion of boria onto alumina which was effected by a procedure of CVD.

In section 3-1, a supported type of silica-alumina was prepared by depositing silica on alumina surface through CVD process using tetraethoxysilane. Silica loading was affected by CVD temperature, time, and reaction atmosphere. Silica was effectively and uniformly deposited on alumina at 240 ^{o}C in the presence of oxygen. The resulting silica-alumina (CVD SiO_2/Al_2O_3) was active for several types of organic reactions such as 2-butanol dehydration, m-xylene isomerization, 1-butene isomerization, cumene cracking, and n-heptane cracking. The catalytic activities of CVD SiO_2/Al_2O_3 varied with silica loading, attaining the maximum conversions for the respective reactions at different silica loadings. They were comparable to those of commercial silica-alumina catalysts; particularly, for the isomerization of 1-butene, the catalytic activity of CVD SiO_2/Al_2O_3 was four times higher than that of the commercial silica-alumina. In addition, the catalytic activities of the CVD SiO_2/Al_2O_3 prepared under different conditions differed from each other even at the same silica content.

In section 3-2, acidic properties of CVD SiO_2/Al_2O_3 were characterized by several measurements, such as solid-state magic-angle spinning (MAS) NMR measurement and temperature-programmed desorption (TPD) of adsorbed dimethylpyridine. The ^{31}P MAS NMR of trimethylphosphine chemisorbed on the catalyst elucidated the change in acid property (Brønsted or Lewis type) with silica

loading. The Lewis acid sites on the alumina surface were converted into Brønsted acid sites by the deposition of silica. At lower silica loadings, both Brønsted and Lewis acid sites existed. Above 12 wt% silica loading, the Lewis acid sites disappeared and only Brønsted acid sites were observed. Furthermore, a temperature-programmed desorption of adsorbed dimethylpyridine clarified the characteristic changes in acid type, acid strength, and acid amount of the CVD SiO_2/Al_2O_3 catalyst. The Lewis acid sites of the support alumina changed into Brønsted acid sites together with a change in acid strength with increasing silica deposition. The catalytic activities of CVD SiO_2/Al_2O_3 were correlated with the amount of Brønsted acid sites generated by silica deposition.

In section 3-3, a structural character of CVD SiO_2/Al_2O_3 was investigated with solid-state MAS NMR measurements. The ^{29}Si MAS NMR of silica deposited on the alumina surface revealed the microstructures of silica. At silica loadings lower than 12 wt%, at which both Brønsted and Lewis acid sites existed, uncovered alumina surface was exposed. At silica loadings about 12 wt%, at which Lewis acid sites disappeared and only Brønsted acid sites existed, the highly dispersed silica, forming a silica bilayer, exhibited high catalytic activities and strong Brønsted acidity. Further silica layering, however, decreased both the catalytic activities and the acidity.

In section 3-4, the CVD of silica onto an amorphous silica-alumina was investigated using tetraethoxysilane in order to create Brønsted acid sites on the surface of original silica-alumina. Silica loading could be readily controlled by CVD time at 160 ^{o}C; silica covered internal walls of mesopores of the support of silica-alumina. The resulting CVD silica-alumina was catalytically more active than the original silica-alumina support for such test reactions as the cracking of cumene and the isomerization of 1-butene. The characteristic changes in the amount of Brønsted acid sites were clarified by means of the temperature-programmed desorption of adsorbed 2,6-

dimethylpyridine. The strong Lewis acid sites of the original silica-alumina were converted into strong Brønsted acid sites through deposition of silica.

In chapter 4, an attempt was made to prepare surface composite compounds by depositing binary mixed components onto inert supports. As a representative example, boron phosphate (BPO_4) was deposited on a silica support using a mixture of boron triethoxide and phosphoryl trimethoxide giving a silica-supported BPO_4 catalyst. Both the amount and the P/B ratio of BPO_4 deposited were changed with CVD temperature and CVD time. At an optimum CVD temperature of 300 ^{o}C, the amount of deposited BPO_4 linearly increased with CVD time. The P/B ratio of the binary oxide deposit could be adjusted as desired through CVD at 300 ^{o}C using an alkoxide mixture with the same P/B ratio. At CVD temperatures below 300 ^{o}C, neither a sufficient amount nor a desired P/B ratio was given. At higher temperatures above 325 ^{o}C, however, the deposition was suppressed by blocking the micropores of silica, especially for long-time CVD operation, owing to rapid deposition. Although the resulting surface compound was amorphous, it was revealed that the compound showed micro-structures of BPO_4 through a ^{31}P MAS NMR measurement. The amorphous BPO_4 highly dispersed on silica exhibited high catalytic efficiency for the isomerization of 1-butene and the simultaneous oligomerization of 1-butene in comparison with both unsupported BPO_4 and supported BPO_4 prepared by the conventional impregnation method.

In chapter 5, deposition behaviors characteristic of metal oxides in the preparation of solid acid catalysts were discussed. Effect of support material on the deposition behaviors was also described. Deposition of single metal oxides such as boria and silica was greatly influenced by the acidic properties of support surface. The deposition rate increased with increasing acid strength of support surface. The simultaneous supply of a mixture of alkoxides drastically lowered the temperature required for deposition of individual oxides. At an optimum CVD

temperature, the amount of deposit was readily controlled by CVD time, and a desired molar ratio of binary oxides was obtained by adjusting the molar ratio of the alkoxides. In order to minimize the concentration gradient for the source alkoxides and to make uniform deposition on the pore surface, deposition should be carried out at the lowest possible temperatures. In addition, for the catalyst preparation using a rotary-type CVD reactor, an appropriate rate of rotation of the CVD reactor was also effective for leveling the concentration gradient for the source alkoxide vapor.

In consideration of the results mentioned above, the following are adduced as the general conclusion.

(1) A supported type of solid acid catalyst was readily prepared by depositing either single metal oxide or binary metal oxides on an appropriate support by means of CVD technique using metal alkoxide or a mixture of metal alkoxides. The metal oxide deposited uniformly covered the internal walls of the mesopores of support material.

(2) Deposition should be carried out at the lowest possible temperatures in order to minimize the concentration gradient for the source alkoxide and to make uniform deposition on the pore surface. A rotary-type CVD reactor in which support granules could be agitated by rotation was designed and found to be effective for leveling the concentration gradient for the CVD source alkoxide vapor.

(3) Deposition of metal oxides such as boria and silica was greatly influenced by acidic property of support materials. Optimum CVD temperature decreased with increasing acid strength of support. At an optimum CVD temperature, metal oxide loading was readily controlled by CVD time. Oxygen addition is also effective for acceleration of deposition rate at temperatures higher than 200 ^{o}C.

(4) Deposition rate of binary mixed metal oxides is faster than that for individual deposition of the respective oxides. At

an optimum CVD temperature, the amount of deposit was readily controlled by CVD time, and a desired molar ratio of binary oxides was obtained by adjusting the molar ratio of the alkoxides.

(5) A CVD process was particularly efficient for such sparingly soluble species as boria and boron phosphate being supported. Such deposits highly dispersed on the surface of support produced relatively uniform distribution of acid strength. The resulting CVD catalysts were more active than the counterparts obtained from the conventional impregnation method for such reactions as vapor-phase Beckmann rearrangement of cyclohexanone oxime and isomerization of olefin.

(6) Deposition of silica on alumina or amorphous silica-alumina surface to produce the surface composite oxide induced the conversion of Lewis acid sites on the alumina into Brønsted acid sites together with a change in acid strength. The deposition of silica enhanced catalytic activities of the resulting silica-alumina for several types of reactions such as dehydration, isomerization, and cracking. The catalytic activities were well correlated with the number of Brønsted acid sites generated by silica deposition.

(7) For the most active alumina-supported silica catalyst, a silica bilayer highly dispersed on alumina exhibited strong Brønsted acidity and high catalytic activities. Further silica layering decreased both acidity and catalytic activity. Alumina surface uncovered with silica, on the other hand, was exposed to show Lewis acidity at low silica loading.

The author has demonstrated several preparative examples of solid acid catalysts with the aid of CVD technique. There still, however, remain some unsettled problems concerning the deposition sites of support surface, the mechanism of the generation of acid sites through CVD process, and the detailed mechanism of the oxide deposition from an alkoxide in the presence of oxygen; which sites or what kind of hydroxyl groups of alumina surface

are responsible for the deposition of silica?, and how are the strong Brønsted acid sites formed in the process of the CVD of silica on alumina? or where do the newly generated protons locate?

It is important for understanding the catalysis by solid acids to clarify the relation between the catalytic property and the surface states of acid sites. Thus the solid acids prepared through CVD process may be designated as model acid catalysts for studying the fundamental concept of acid catalysis, if the surface structures of the deposits are thoroughly investigated.

CVD technique has many advantages as a method for catalyst preparation together with high reproducibility, as mentioned above. The author is confident that CVD technique will be of great use as a potential and practical catalyst preparation method in future, if high productivity can be realized. Catalytic and physical properties of the resulting CVD catalysts, however, depend on physical and chemical properties of support materials. Particularly, surface area and pore structure of support definitely affect deposition behavior and catalytic performance of the CVD catalysts.

The studies of which this thesis consisted have been presented in the following publication list.

List of Publications

	Location in this thesis
1. Vapor-phase Beckmann Rearrangement of Cyclohexanone Oxime over Boria-Hydroxyapatite Catalyst. Y. Izumi, S. Sato, and K. Urabe *Chem. Lett.*, **1983**, 1649.	Chapter 1
2. Vapor-Phase Beckmann Rearrangement of Cyclohexanone Oxime over Silica-Boria Catalyst Prepared by Chemical Vapor Deposition Method. S. Sato, H. Sakurai, K. Urabe, and Y. Izumi *Chem. Lett.*, **1985**, 277.	Section 2-1 Chapter 5
3. Catalytic Behavior of Boria-Alumina Prepared by Chemical Vapor Deposition Technique. H. Sakurai, S. Sato, K. Urabe, and Y. Izumi *Chem. Lett.*, **1985**, 1783.	Section 2-2 Chapter 5
4. Vapor-Phase Beckmann Rearrangement over Silica-Supported Boria Catalyst Prepared by Vapor Decomposition Method. S. Sato, K. Urabe, and Y. Izumi *J. Catal.*, **102** (1986) 99.	Chapter 1 Section 2-1 Chapter 5
5. Vapor-Phase Beckmann Rearrangement over Alumina-Supported Boria Catalyst Prepared by Vapor Decomposition Method. S. Sato, S. Hasebe, H. Sakurai, K. Urabe, and Y. Izumi *Appl. Catal.*, **29** (1987) 107.	Section 2-2 Chapter 5

6. Catalytic Properties of Silica-Alumina Prepared by Chemical Vapor Deposition. S. Sato, M. Toita, Y. Q. Yu, T. Sodesawa, and F. Nozaki *Chem. Lett.*, **1987**, 1535.	Section 3-1 Chapter 5
7. Catalytic and Acidic Properties of Silica-Alumina Prepared by Chemical Vapor Deposition. S. Sato, M. Toita, T. Sodesawa, and F. Nozaki *Appl. Catal.*, **62** (1990) 73.	Chapter 1 Section 3-1, 3-2 Chapter 5
8. Silica-Supported Boron Phosphate Catalyst Prepared by Chemical Vapor Deposition. S. Sato, M. Hasegawa, T. Sodesawa, and F. Nozaki *Bull. Chem. Soc. Jpn.*, **64** (1991) 516.	Chapter 4 Chapter 5
9. Temperature-Programmed Desorption of Dimethylpyridine Adsorbed on Silica-Alumina Prepared by Chemical Vapor Deposition. S. Sato, M. Tokumitsu, T. Sodesawa, and F. Nozaki *Bull. Chem. Soc. Jpn.*, **64** (1991) 1005.	Section 3-1, 3-2
10. Solid-State NMR of Silica-Alumina Prepared by Chemical Vapor Deposition. S. Sato, T. Sodesawa, F. Nozaki, and H. Shoji *J. Mol. Catal.*, **66** (1991) 343.	Section 3-1, 3-2, 3-3
11. Additional Formation of Brønsted Acid Sites on Silica-Alumina by Depositing Silica Component. S. Sato, M. Hiratsuka, T. Sodesawa, and F. Nozaki *Bull. Chem. Soc. Jpn.*, **64** (1991) 2214.	Section 3-4, Chapter 5